Sedimentary Geology 257–260 (2012) 1–30

Contents lists available at SciVerse ScienceDirect

Sedimentary Geology

journal homepage: www.elsevier.com/locate/sedgeo

Review

Simplified process modeling of river avulsion and alluvial architecture: Connecting models and field data

Elizabeth A. Hajek [a,*], Matthew A. Wolinsky [b]

[a] Dept. of Geosciences, The Pennsylvania State University, United States
[b] Shell Bellaire Technology Center, Houston, United States

ARTICLE INFO

Article history:
Received 3 February 2011
Received in revised form 21 August 2011
Accepted 7 September 2011
Available online 16 September 2011

Editor: G.J. Weltje

Keywords:
Avulsion
Alluvial architecture
Cellular models
paleomorphodynamics

ABSTRACT

Modeling is an invaluable tool for studying sedimentary basin filling and for understanding depositional processes with long recurrence intervals, including channel avulsion. Simplified modeling approaches, such as cellular models and process-analogue experiments, are particularly useful for efficiently exploring alternative hypotheses and evaluating first-order controls on river avulsion and alluvial architecture. Here we review the history and current state of the art in simplified avulsion and alluvial architecture models, with a particular focus on how results and insights from these models can be incorporated into field and subsurface studies, and vice versa. Simplified avulsion and alluvial architecture models have proliferated in the past decade, providing a wide variety of models to serve as a basis for future coupled field-modeling studies. We compare features of leading models and discuss avenues for effectively pairing model capabilities with hypotheses and field data. Outstanding questions highlighted by recent modeling efforts include 1) What thresholds control avulsion initiation in different systems? 2) How do floodplain processes and topography influence avulsion dynamics and alluvial architecture? 3) What factors determine where avulsion channels stabilize? Answering these questions will require targeted modeling efforts coupled to data from ancient systems. Hence our model comparison emphasizes features that can be used to choose or design fit-for-purpose models, and we outline how quantitative data useful for model selection and validation can be obtained from modern systems and ancient deposits. Matching model goals with targeted questions, and model parameters and predictions with quantitative field data, will help tighten communication between field- and model-oriented sedimentary geologists, facilitating advances in our understanding of river avulsion and alluvial architecture.

1. Introduction

Sedimentary geologists are often required to interpret deposits which are only an incomplete record of Earth-surface processes acting on geologic timescales. Consequently field studies of ancient deposits rely heavily on insights from research on active sedimentary processes via modern systems, physical experiments, and numerical models. At the scale of an event, observations from modern systems and sediment-transport laws at reach and flume scale are useful for interpreting and predicting sedimentation and erosion (Parker, E-book; Dietrich et al., 2003; Paola et al., 2009). Likewise, at the scale of a stratigraphic sequence or basin fill, sedimentation patterns can be explained by relationships between sediment transport, basin subsidence, and mass extraction (Strong et al., 2005; Fedele and Paola, 2007; Duller et al., 2010; also Muto and Steel, 2000; Kim et al., 2006a; Wolinsky, 2009). Between these scales emergent processes arise and produce self-organized patterns of autogenic variability which are poorly understood and difficult to predict (Werner, 1999, 2003; Murray, 2003; Jerolmack and Paola, 2010; Kleinhans, 2010). The archetype example of emergent dynamics in depositional fluvial landscapes is river avulsion: the process whereby flow escapes its channel and carves a new path (or reoccupies an abandoned path) on the adjacent floodplain (Slingerland and Smith, 2004).

Avulsion is a threshold process inherent to channelized depositional systems where channels aggrade or prograde faster than surrounding non-channelized regions. Preferential storage of incoming sediment in localized fluvial landforms, such as alluvial ridges, eventually pushes a system to a threshold of instability, e.g. as an aggrading channel becomes "perched" above the surrounding floodplain. This drives intermittent avulsions that form new channels, redistributing flow and sediment through the system - a process of episodic storage and release analogous to how earthquakes store and release strain energy (e.g. Sammis and Smith, 1999; Sheets et al., 2002; Jerolmack and Paola, 2007; Martin et al., 2009; Reitz et al., 2010).

Like earthquakes, avulsions can have catastrophic consequences for nearby populations, but are very difficult to predict (e.g. Sinha, 2009; Chakraborty et al., 2010). Avulsion is also an important influence on stratigraphic architecture in sedimentary basins filled by

* Corresponding author.
E-mail address: hajek@psu.edu (E.A. Hajek).

0037-0738/$ – see front matter © 2011 Published by Elsevier B.V.
doi:10.1016/j.sedgeo.2011.09.005

channelized depositional systems (e.g. Allen, 1978; Leeder, 1978; Mackey and Bridge, 1995). The convolution of avulsion dynamics with time-varying accommodation and sediment supply determines the size, shape, and distribution of channel sandstone bodies in alluvial basins. These properties are notoriously difficult to predict, but are critical for developing and managing subsurface reservoirs of hydrocarbons, groundwater, or sequestered CO_2 (e.g. Koltermann and Gorelick, 1996; Karssenberg et al., 2001).

The wide range of scales spanned by avulsion processes and products makes understanding avulsions a fundamentally interdisciplinary endeavor. While recent examples of river avulsion can be mined for data, long recurrence intervals (O[kyr] for large Holocene sand-bed rivers; Jerolmack and Mohrig, 2007) mean that globally examples are few. Hence a robust understanding of where these fit within the full statistical spectrum of avulsive behaviors requires more information, which must come from ancient deposits. Similarly, our ability to interpret process from the stratigraphic record is limited by poor age control, preservation biases, and technical-logistical challenges in collecting suitable data from outcrops and subsurface deposits. Modeling is often necessary to bridge these gaps, allowing geoscientists to predict the products resulting from a known process (e.g. Camporeale et al., 2005), or to constrain the processes which generated a known product (e.g. Burgess et al., 2006). The advent of open source model-data repositories such as the Community Surface Dynamics Modeling System (CSDMS, Syvitski, 2010, http://csdms.colorado.edu/) provides an unprecedented opportunity for applying diverse modeling tools in sedimentary geology.

Simplified process models can be used to explore poorly understood processes and to identify which variables and conditions most strongly influence a complicated system (e.g. Murray, 2003). In this way, simplified avulsion models are well suited for developing testable hypotheses that can be evaluated with field data, providing common ground for collaborations between field-oriented stratigraphers and theory-oriented modelers. Here we review simplified (cellular and flume-tank) models of river avulsion and alluvial architecture, with an emphasis on connecting model parameters and results with data from natural systems. We provide some background and context for simplified avulsion modeling, review model process formulations and rules, discuss key outcomes and outstanding questions from avulsion and alluvial architecture models, provide examples of quantitative field measurements useful for model comparisons, and offer suggestions about directions for future work. For general information on numerical and experimental modeling of fluvial processes and stratigraphy we refer readers to existing review papers (Paola, 2000; Coulthard et al., 2007; Bridge, 2008; Paola et al., 2009; Kleinhans, 2010).

2. Modeling purpose and approaches

Modeling occurs both in response to and as a driver of field and laboratory data collection. In some instances models are created to generate hypotheses which must then be tested with field data. Other times models are developed to explain observations. This give-and-take between theoretical and field geologists is critical and, when effective, can facilitate important scientific advances. While the relationship between modeling and observation, process and product, is arguably fairly tight in fields like civil engineering and geomorphology, it is more distant in stratigraphic studies. This results in part from our limited understanding of long-timescale sedimentary dynamics, and is further confounded by the challenges of obtaining quantitative spatial and temporal data from the stratigraphic record.

Field stratigraphers and modelers can be further disconnected by misunderstandings surrounding the purposes and capabilities of various models, and the limitations and possibilities associated with different types of data. For example simplified models of sedimentary processes are often criticized for not reproducing the rich detail observable in the stratigraphic record. However, while models with more bells and whistles can generate more detailed predictions, they can also be difficult or impossible to validate; detail can be a "bug" as well as a "feature". This is especially true in applied stratigraphic problems (e.g. outcrop interpretation, reservoir modeling), where limited data typically precludes a unique solution, and more details can make a model appear more *plausible* while actually making it less *probable* (e.g. Welsh et al., 2005; Bratvold and Begg, 2008; also see Tversky and Kahneman, 1983).

A number of different strategies can be employed when modeling sedimentary systems – all of which have their own advantages and limitations. While cellular and experimental landscape modeling is a cottage industry full of specialists, for non-modelers it is helpful to understand how the various approaches affect strategies to 1) incorporate models into field studies and interpretations of field data, 2) collect data at an analogous or comparable scale to that of a model, and 3) communicate data and results to modelers.

It has been said that "All models are wrong but some are useful" (Box, 1979) – a sentiment which seems essentially correct. So then how can field stratigraphers ascertain which models are useful? And what, exactly, is a "simplified" model (given that "unsimplified model" is an oxymoron)? To those of a practical bent, discussion of philosophical approaches to modeling can seem moot, but these issues are inescapable.

2.1. Model goals and strategies

Models of sedimentary systems are used in a wide array of applications, and within a particular discipline model design tends to reflect the "typical problem type". For example an engineering model may aim to reproduce specific natural conditions in as much detail as possible to facilitate precise prediction or design (e.g. for stream restoration; Soar and Thorne, 2001; Kang et al., 2010), whereas a basin-filling model may be designed to more broadly explore sedimentary-system response to different forcing scenarios (e.g. Blum and Törnqvist, 2000; Burgess et al., 2006; Kim et al., 2006a). In geomorphic pattern-formation problems, rule-based exploratory models may help identify the essential smaller-scale processes that drive emergent system dynamics (Murray, 2003). For energy-industry reservoir problems where the primary goal is probabilistic subsurface prediction, process-based approaches are commonly abandoned entirely, in favor of structure-imitating geostatistical models (Koltermann and Gorelick, 1996; although the wisdom of this is debatable, Bridge, 2008).

Independent of application or discipline, issues of scale and emergence arise in all models of sedimentary systems. Self-organization and emergent structures are major themes arising from process-oriented numerical and physical models of sedimentary systems (Werner, 1999; Murray, 2003; Paola et al., 2009; Kleinhans, 2010). Are emergent entities such as landforms "real", or simply reified abstractions? Similarly, issues of discrete hierarchy vs. continuous ("fractal") scaling consistently recur in stratigraphy (e.g. Kelly, 2006; Jerolmack and Sadler, 2007; Schlager, 2010). These deep philosophical questions are interesting, but if "all models are wrong", then nothing in our models is "really real". From a scientific perspective then, the more pressing question is essentially empirical: How useful is a particular model for increasing our understanding or prediction accuracy?

The hierarchical modeling approach of Werner (1999, 2003) takes a more pragmatic approach to these issues, based on the empirical observation that complex systems typically display dynamical asymmetry, such that the fast dynamics of fine-scale elements (e.g. sand grains or turbulent eddies) becomes "slaved" to larger-scale more slowly evolving emergent elements (e.g. bedforms). In simple cases hierarchical models may be formally derived from "fundamental equations" via multiscale perturbation (Fowler, 1997), e.g. quasi-steady approximations of catalytic reaction rates (Segel and Slemrod, 1989) or river hydrodynamics (where flow is slaved to bed morphology, Parker, E-book Ch13). However useful hierarchical models can

also be constructed based on empirically-observed separation of timescales (Werner, 2003; Murray, 2007; Liang et al., 2009).

The hierarchical approach has most commonly been used for exploratory models (sensu Murray, 2003), but hierarchical models can also be used for prediction. Most questions in sedimentary geology are at scales >1 order of magnitude larger than the scale of individual events. As computing power increases many of these questions could in principal be addressed with detailed "full physics" models, but in practice error accumulation can limit prediction horizons to a few orders of magnitude beyond the scale of model calibration. This holds for simplified models as well, but the hierarchical approach can be used to bootstrap across scales, using a sequence of models which each operate within this prediction horizon. If properly targeted, fit-for-purpose hierarchical models can even give more accurate predictions than bottom-up models (Werner, 2003; Murray, 2007). Hence when designing or choosing a model for a particular application, the desired prediction scale influences which modeling strategies are most appropriate.

2.2. Sedimentary scales: process and product

In this review we group sedimentary processes and their resultant products into three relative scales (Table 1). Event Scale includes modern processes that produce landforms and event beds; examples include bar formation and growth within a river channel, levee building, crevassing, splay deposition, and overbank flooding. These processes are typically short lived (days to decades) and result from stochastic environmental forcing (e.g. weather). Studies of event-scale processes are usually conducted in civil engineering and geomorphology disciplines, and typically use fluid flow and topography data from modern systems or rigorously scaled experiments (or even full-scale experiments, e.g. Wilcock, 2009).

Architecture Scale processes dictate how landscapes form and evolve. These processes are often internally generated (autogenic) and dominate over intervals of 10^3-10^4 years, timescales over which external forcing (e.g. climate, sediment supply/base-level rise rates) may be quasi-steady. Architecture-scale processes, including meandering, avulsion, and coupled channel-floodplain-landscape evolution, typically fall under the purview of geomorphologists and stratigraphers. These processes produce reservoir scale features such as channel-belt, multi-story, and amalgamated sandstones. Field data about architecture-scale processes typically come from ancient outcrops, hi-res shallow seismic data, or stratigraphy of extant (Holocene to Pleistocene) systems. Stratigraphic morphometrics characterizing architecture-scale data include intra-channel sand-body architecture and heterogeneities, channel trajectories (Sylvester et al., 2011), and channel-belt sandstone stacking patterns within fluvial successions.

Over longer timescales (100 kyr – 1 Myr) Basin Scale processes such as variable allogenic forcing and mass balance (supply vs. accommodation) become important. Under changing basin boundary conditions these processes dictate where sediment will be deposited within a basin, which influences shoreline and channel-system migration, and the distribution of depositional environments. This is the scale of sequence stratigraphy and petroleum exploration; consequently, field data for understanding these processes come primarily from seismic, outcrop, and well datasets that span substantial portions of a basin.

Avulsion is considered architecture scale here, but the term "avulsion" has no precisely agreed upon definition in the literature, and can refer to a wide array of processes operating at different scales. In any river system there is always a potential for re-localization of "sheetwash" floodplain flows, resulting in scour, headward incision, and formation of a quasi-stable avulsive channel. Successful avulsion requires both reach-scale cross-channel flow potential exceeding a threshold, and availability of a more favorable downstream path at landscape-scale (in other words the concept of "gradient advantage" is necessarily a multiscale phenomenon). In this paper we subdivide the avulsion process into three phases:

1) Initiation = onset of channelized flow outside the parent channel (e.g. via crevasse formation)
2) Finding (Flowpath Selection) = distributed flow on the floodplain adjacent to the parent channel which "tests" alternative flow-paths, seeking gradient advantage (e.g. Hoyal and Sheets, 2009; Reitz et al., 2010)
3) Stabilization = flow recollects into a quasi-stable daughter channel, commonly accompanied by incision

In this context a "failed avulsion" is an avulsion that never reaches the stabilization phase, and a "progradational avulsion" (Slingerland and Smith, 2004) is an avulsion with a spatio-temporally extended finding phase accompanied by significant deposition via an anastomosed floodplain channel network. Processes that produce deposits and unconformities readily identified in the stratigraphic record are common in the finding and stabilization phases of avulsion.

2.3. Early alluvial architecture models

Simplified avulsion models have typically been used to address fundamental questions such as: What factors influence avulsion initiation and flow-path selection? What is the "baseline" autogenic architecture of an alluvial basin under constant forcing? How does alluvial architecture change in response to changing basin boundary conditions? The pioneering work of Leeder (1978), Allen (1978), and Bridge and Leeder (1979) (collectively termed "LAB" models by Bryant et al., 1995) revealed the importance of channel avulsion in alluvial-basin filling. These exploratory models were used to evaluate how the interplay of avulsion and subsidence (or basin aggradation) affect stratigraphic architecture. These models build 2D strike

Table 1
Stratigraphic scales and processes.

Strat-Level	Event	Architecture	Basin
Timescale	0.1 yr – 10 yr	1 kyr – 10 kyr	100 kyr – Myr
Forcing	Stochastic (e.g. Weather)	Steady / Autogenic (e.g. Climate)	Allogenic (e.g. Climate Change)
Process	Morphodynamics	Landscape evolution	Mass balance (e.g. supply/accommodation), Migration of depositional environments or depositional centers (e.g. progradation, compensation)
Product	Event Beds, Landforms	Sand bodies, Landscape topography	Sedimentary Sequence
Modeling strategy	Fluid dynamics, Scaled experiments	Simplified / Hierarchical Cellular/Geometric/Hybrid, Process analogue experiments	Mass-conserving geometric, Diffusive Cellular, Subsiding analogue experiments

Comparison of sedimentary processes and products at different scales. Timescales and modeling strategies are only suggestive, as in reality there is significant overlap.

Table 2
Survey of simplified avulsion models.

Model	Hydrodynamics			Morphodynamics				
	Flow routing	Flow dynamics	Water surface	Sediment transport	Overbank	Avulsion initiation	Mass balance	Sediment storage
Murray–Paola (MP)	dispersive	steady	no	bedload	≈process	self-org.	yes	bar , ≈splay
CAESAR	dispersive	≈transient	≈	≈bedload	≈process	self-org.	yes	chan. , overbank
Mackey–Bridge (MB)	steepest	steady	no	bedload	geometric	S_c	no	none
Jerolmack–Paola (JP)	steepest	steady	no	bedload	geometric	H_c	≈	ch.-belt
Karssenberg–Bridge (KB)	dispersive	steady	no	bedload	≈geometric	S_c & H_c	≈	ch.-belt
Dalman–Weltje (DW)	dispersive	steady	no	≈bedload	geometric	≈ S_c & H_c	≈	ch.-belt
Sun	dispersive	steady	no	bedload	≈none	S_c & H_c	yes	ch.-belt
Seybold	dispersive	≈steady	yes	≈suspended	process	self-org.	yes	chan., levee, floodpl.
Delft3D	dispersive	transient	yes	bedload + suspended	process	self-org.	yes	bar, chan., levee, floodpl.
DIONISOS	dispersive	steady	no	bedload	not resolved	not resolved	yes	undifferentiated
Non-Cohesive Delta Exp's (SAFL)	dispersive	≈steady	≈no	bedload	≈process	self-org.	yes	bedform, bar, chan., ≈splay
Cohesive Delta Exp's (EM)	dispersive	≈steady	yes	bedload + suspended	process	self-org.	yes	chan., bar, levee, floodpl.

Comparison of a representative sample of state of the art simplified avulsion models. For full details see original references. Abbreviations following names in Model column are used in the text to refer to models. Note that for models that do not resolve channels the Flow routing column describes routing within the active channel network, but some models use different schemes for avulsion routing and/or floodplain flow. The Sediment storage column refers only to landforms included in the model mass balance. Notes column index: 1) Quasi-1D flow routing (3-nbr). Original model purely intra-channel, but dynamic vegetation version has ≈process overbank. 2) Water-surface defined locally so no backwater effects. Original model pure bedload, but reach-scale version also suspended and can simulate overbank deposition. However simulations to date have not produced leveed channels ab initio. 3) Quasi-1D flow routing (5-nbr). Incorporates sub-grid channels by tracking high (levee-top) and low (channel-bottom) cell elevations. 4) Overbank deposition geometric, but floodplain erosion by flow routing. 5) Includes quasi-process rule for dynamic channel-belt widening. 6) Avulsion initiation threshold incorporates sub-grid crevasse stability. Channels not resolved, but model output can be stochastically populated with sub-grid channels. 7) Suspended transport includes turbulent diffusion in addition to advection by mean flow. 8) User specified Pr /Δt for sub-grid "random walk" avulsions ($Pr = 0$ gives steepest-descent routing). Channels unresolved, but width effectively Δx for incision. References column index: (1) Burgess et al., 2006. (2) Coulthard et al., 2002. (3) Dalman and Weltje, 2008. (4) Edmonds and Slingerland, 2008. (5) Edmonds et al., 2009. (6) Edmonds and Slingerland, 2010. (7) Granjeon and Joseph, 1999. (8) Jerolmack and Mohrig, 2007. (9) Jerolmack and Paola, 2007. (10) Karssenberg and Bridge, 2008. (11) Lesser et al., 2004. (12) Mackey and Bridge, 1992. (13) Mackey and Bridge, 1995. (14) Martin et al., 2009. (15) Murray and Paola, 1994. (16) Murray and Paola, 2003. (17) Seybold et al., 2009. (18) Sheets et al., 2002. (19) Sheets et al., 2007. (20) Sømme et al., 2009a. (21) Straub et al., 2009. (22) Sun et al., 2002. (23) Van De Wiel et al., 2007.

stratigraphy using rules to predict deposition and channel avulsion in response to a specified subsidence (aggradation) scenario. Avulsion frequency is either taken as a specified constant (Allen, 1978; Leeder, 1978) or drawn from a distribution (Bridge and Leeder, 1979), and channels relocate to a new position with the model domain at each avulsion time step. New channel locations are either chosen randomly (Leeder, 1978), randomly with some topographic avoidance of pre-existing channel locations (Allen, 1978), or defined as the topographic minimum of the basin cross-section (Bridge and Leeder, 1979).

Despite these subtle differences, each model predicts essentially the same response: 2D channel density and interconnectedness in a strike section should be high when subsidence and basin aggradation rates are low and vice versa. Additionally the Bridge and Leeder (1979) model predicts that rivers will preferentially occupy areas of highest subsidence (this is largely a consequence of channels relocating to the lowest spot in the basin during each avulsion). The ideas developed with these models led to other conceptual models about how base level might control alluvial architecture (e.g. Shanley and McCabe, 1993; Wright and Marriott, 1993; Shanley and McCabe, 1994; Marriott, 1999) and have been used to correlate outcrop and subsurface data (e.g. Rogers, 1998; Leleu et al., 2009).

Importantly, these models yielded testable hypotheses which enabled field and laboratory studies to incorporate and build on their results. Quantitative measures such as number of channel-belt sandstones, area-density of sandstone, and interconnectedness of sandstone bodies could be used to compare stratigraphy in different basins to test the hypotheses (e.g. Sheets et al., 2002; Strong et al., 2005). In some basins these hypotheses seemed to hold, but in others the opposite effect was noted (e.g. Willis, 1993; Törnqvist, 1994). This is not surprising considering how simply avulsion processes were represented in the original LAB models. These models treated avulsion frequency as an independent variable and assumed that with each avulsion, a channel relocates to a new cross-stream position everywhere downstream of the avulsion location (e.g. "nodal" or "random" avulsions of Leeder, 1978), and did not attempt to model avulsion initiation or account for partial or failed avulsions.

Later advances from field studies and physical experiments suggested that sedimentation rates control avulsion frequency (Ashmore, 1991; Törnqvist, 1994; Bryant et al., 1995). Heller and Paola (1996) added sedimentation-rate-dependent avulsion frequency to a model similar to the Leeder, 1978 model, and also explored how avulsion type might affect alluvial architecture. Heller and Paola considered the nodal and random avulsions of Leeder (1978) to be "regional", and proposed that avulsions can also be "local", rejoining the parent channel some distance downstream of the avulsion location. (Note that we will use Heller and Paola's definitions of regional and local throughout this review.) Their study highlighted the potential influence of flow routing and sediment dynamics on avulsion and alluvial basin filling, effects which cellular models are well suited to exploring.

Early models focused primarily on understanding how alluvial architecture responds to changing basin boundary conditions in a generic fluvial system. Recently it has become clear that autogenic dynamics in sedimentary systems occur over much longer timescales than previously presumed, and can produce stratigraphic patterns rivaling those generated by changes in sea level or tectonics (Kim et al., 2006b; Kim and Paola, 2007; Sheets et al., 2007; Van de Wiel and Couthard, 2010; Hajek et al., 2010; Jerolmack and Paola, 2010). Moreover, the details of how boundary conditions influence autogenic dynamics is unknown, and variations in avulsion sub-phase (initiation, finding, stabilization) behavior under different basin-scale forcing regimes may be an important factor in the diversity of alluvial architecture observed in different systems. For these reasons, recent models have focused on incorporating more realistic process formulations in order to better understand complexities associated with avulsion dynamics over the full range of variability observed in natural systems.

3. Comparing simplified avulsion models: Event-scale formulations

Investigating sediment routing and river avulsion across alluvial landscapes requires models that keep track of evolving sedimentary environments (e.g. channel vs. floodplain) and topography over spatial

Channels			Stratigraphic scale		Systems	Notes	References			
Resolved	Confinement	Width	Short	Long						
yes	erosional	self-org.	Event	Architecture	fluvial (≈coarse)	1	15	16		
yes	≈erosional	self-org.	Event	Architecture	fluvial-fan	2	2	23		
no	sub-grid channel	specified	Architecture		fluvial		12	13		
no	sub-grid ch.-belt	fixed τ^*	Architecture		fluvial	3	9			
no	sub-grid channel	empirical hyd.-geom. ($B \sim S^a Q_w^b$)	Architecture	Basin	fluvial	4 5	10			
≈no	sub-grid ch.-belt		Architecture	Basin	fluvial-deltaic	5 6	3			
no	sub-grid ch.-belt	fixed τ^*	Architecture	Basin	fluvial-deltaic		22			
yes	constructional	self-org.	Architecture		cohesive deltas		17			
yes	constructional	self-org.	Event	Architecture	fluvial-deltaic (≈cohesive)	7	4	6	11	
no	erosional	not resolved	Basin	Geodynamic	fluvial-deltaic	8	1	7	20	
yes	erosional	self-org.	Event	Basin	fan-deltas (coarse)		8	18	19	21
yes	constructional	self-org.	Event	Basin	cohesive deltas (muddy)		5	14		

domains of O[10^2] channel widths. Basin stratigraphy and alluvial architecture can be studied with models that record this evolution over timescales of O[10^3] events (e.g. floods). Regardless of specific model goals or details, simplified avulsion models have a few common properties since all modelers face the same decisions of how to represent processes of flow routing, sediment transport and deposition, and avulsion (via cellular rules or experimental protocols), and of how to represent the resulting depositional products, including landforms and architectural elements.

First, flows must be routed through 3D terrain. Then sediment deposition and erosion must be defined at each timestep, i.e. via morphodynamic flux laws, geometric rules, or hybrid approaches (Wolinsky, 2009). Many models also include avulsion rules, for example allowing channels to relocate only when some deterministic or stochastic threshold is met. Initial and boundary conditions (e.g. sediment supply and accommodation) are also required to determine a unique model prediction (or quasi-stationary mean for stochastic models). Simplified models formulate these processes in different ways, and when evaluating a model's suitability for field-validation studies or hypothesis generation, it is worth considering how these parameterizations may impact data requirements and/or results. Table 2 compares a representative sample of simplified avulsion models, along with a cellular landscape model that doesn't specifically resolve avulsions (DIONISOS), and a "full-physics" hydrodynamic model (Delft3D).

We emphasize that none of these approaches is inherently better than any other; what matters is whether the chosen method captures the essential processes needed to address the particular question. Hence as we compare model formulations, we will do so in the context of event-scale processes and observations in natural systems, illustrating with data from modern systems where appropriate. For the sake of brevity, we focus on first-order similarities and differences between models, referring readers to the original references (see Table 2) for full details. Where appropriate we will summarize natural and model processes with simplified equations, using the variables in Table 3.

Table 3
Symbols.

Symbol		Variable	Units	Symbol	Variable	Units	
	x	planview position	m	Sediment transport			
	t	time	s	q_s	sediment flux	m^2/s	
	η	bed elevation	m	Q_s	sediment load	m^3/s	
	h	sediment thickness	m	τ^*	Shields stress	1	*Bed*
	Sediment			K_s	diffusive transport coefficient	1	
	d	bed-material grain size	m	κ_s	fluvial diffusivity	m^2/s	
	R	submerged specific gravity	1	C	depth-averaged concentration	1	*Suspended*
	Hydrodynamics			c_b	near-bed concentration	1	
	q_w	water flux	m^2/s	w_s	settling velocity	m/s	
Normal flow	Q_w	bankfull discharge	m^3/s	u_c	entrainment threshold	m/s	
	U	depth-averaged velocity	m/s	e	entrainment coefficient	1	
	B	channel width	m	κ	eddy diffusivity (depth-averaged)	m^2/s	
	H	flow depth	m	Reference scales			
	τ	shear stress (kinematic)	$(m/s)^2$	Δx	cell size	m	*Cellular*
	S	bed slope	1	ΔA	cell area	m^2	
	C_d	drag coefficient	1	ℓ	link length	m	
	g	gravitational acceleration	m/s^2	L_w	backwater length	m	*Process*
Backwater	**Fr**	Froude number	1	L_s	settling length	m	
	η_w	water-surface elevation	m	L_d	diffusion length	m	
	S_w	water-surface slope	1	λ	overbank decay length	m	
	K_w	hydraulic conductivity (diffusive-wave)	m/s	B_{cb}	channel-belt width	m	
	Mass balance			T	avulsion period	s	
	ΔQ	flux difference	m^3/s	L	length	m	*Landform*
	c_0	deposit concenration (1 - porosity)	1	B	width	m	
	f	sediment capture ratio	1	H	thickness	m	
	P	precipitation (runoff)	m/s	V	volume	m^3	
	A	drainage area	m^2	T	response time	s	

Overview of variables used in the text, including symbol, description, and MKS units (1 = dimensionless). Variables are grouped into categories roughly corresponding to sections of the text where they are introduced. Note that "x" is a generic planview coordinate, and can be in either the downstream or cross-stream direction, as determined by context.

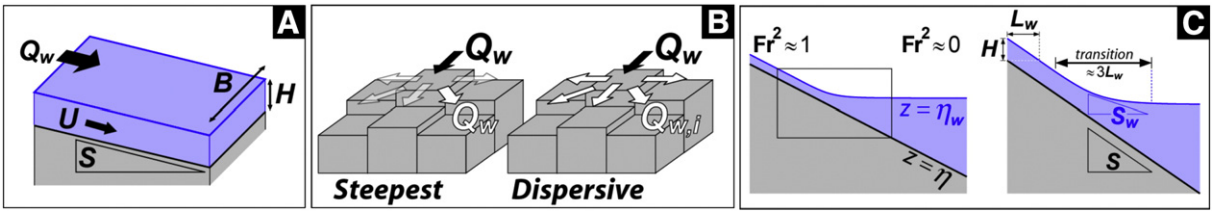

Fig. 1. Hydrodynamics concepts. Schematic diagrams illustrating key hydrodynamics concepts and variables. A) Normal flow. B) Cellular flow routing approaches. C) Backwater and low-Froude flows. In steep upland rivers the water surface typically parallels the bed, but in gently-sloping lowland rivers the water surface commonly diverges from the surface topography (left). In the backwater transition zone the influence of base level is felt upstream (right).

3.1. Hydrodynamics

Hydrodynamics, the physics of flowing water and the forces which drive it, influences fluvial geomorphology and stratigraphy primarily via two mechanisms: flow routing (which determines landscape channel paths and network geometry), and turbulent shear stress (which determines local sediment transport). The fundamental physics of turbulent fluid flow is governed by the Navier–Stokes equations, but while technological advances have recently made some bed-to-reach scale problems amenable to direct numerical simulations (Kang et al., 2010) or field-scale experiments (Wilcock, 2009), almost all fluvial hydrodynamics models are "simplified" in various ways. This is true of all models in Table 2, and will likely be the case for the foreseeable future (certainly for models at landscape/architecture scale).

3.1.1. Reach hydrodynamics: Normal flow

At its simplest, river hydrodynamics can be treated as approximately steady in time and uniform in space, which is often sufficient for geologic applications. The resulting "normal flow" equations give relationships between flow and geometry variables at reach-scale (Fig. 1A). For a shallow water flow we have

$$q_w = UH \tag{1}$$

where q_w = water flux (m^2/s), H = flow depth (m), and U = depth-averaged downstream velocity (m/s). When integrated over the channel cross-section this gives

$$Q_w = Bq_w \tag{2}$$

where Q_w = bankfull discharge (m^3/s) and B = bankfull width (m).

For normal flow the fluid momentum balance reduces to

$$\tau = gHS \tag{3}$$

where τ = *kinematic* shear stress (= stress / fluid density; $(m/s)^2$), S = slope (along flowpath; m/m), and g = gravitational acceleration ($\approx 9.8\ m/s^2$). In turbulent shallow-water flows stress is related to velocity by

$$\tau = C_d U^2 \tag{4}$$

where the drag coefficient C_d is dimensionless.

3.1.2. Topographic routing of channelized flows

Normal flow applies to a single river reach (or model cell), but flow routing determines the distribution of water and flow at landscape scale. For simplicity we specified the normal flow Eqs. (1)–(4) in scalar form, but flow shear stress τ, flux q_w, and discharge Q_w are actually vectors aligned with the downstream velocity U. In the case of normal flow, velocity is oriented in the direction of the bed slope S, i.e. water flows downhill. Hence many cellular avulsion models base flow routing on topography, using either steepest descent or dispersive approaches (Fig. 1B).

Both approaches compute the downstream slope between a cell and each of its 8-neighbors, $S = \max\{(z_{cell} - z_{nbr})/\ell, 0\}$, where $\ell = \Delta x$ for 4-neighbors and $\sqrt{2}\Delta x$ for diagonal neighbors. In the steepest descent method all discharge in a cell flows to the neighbor with maximum slope, such that flow entering at the upstream inflow point is routed through a one-cell wide path extending across the entire model domain. Hence in steepest-descent avulsion models at any time there is a single active channel with spatially constant discharge (e.g. Mackey and Bridge, 1995; Jerolmack and Paola, 2007). Modeling anastomosed or distributary channel systems therefore requires a dispersive flow routing approach. Dispersive routing was first developed to model sheetflow on upland hillslopes (Freeman, 1991) and multi-thread flow in braided river channels (Murray and Paola, 1994), but it has since been used in a variety of simplified avulsion models, where it allows anastomosed (Fig. 2A) and distributary (Fig. 2B) channel networks to develop.

Dispersive routing techniques vary in the details of how flow is distributed among downstream neighbors, but all enforce flow continuity, i.e. conservation of water. Issues of mass balance will arise throughout this review in many different forms, but in all cases a quantitative statement of mass balance requires two things: a well-defined control volume (a map-view polygon in the case of surface fluxes), and the flux difference (a.k.a. net flux divergence) across it

$$\Delta Q = Q_{out} - Q_{in} \tag{5}$$

For cellular flow routing we have

$$\Delta Q_w / \Delta A = P \tag{6a}$$

where ΔA is the planview area of a single-cell control volume, and P is precipitation (net runoff). Precipitation is commonly ignored in architecture-scale models (both cellular and experimental), but can be important in hydrological applications (e.g. CAESAR, Coulthard et al., 2002) or basin-scale models (e.g. DIONISOS, Granjeon and Joseph, 1999).

Partitioning of flow is accounted for in the flux difference

$$\Delta Q_w = \sum_{nbrs} Q_{w,i} \mathrm{out}[i] \tag{6b}$$

where for a particular cell the vector out[i] is defined over its neighbors (nbrs), taking values of 1 for effluxes, −1 for influxes, and 0 for unconnected (e.g. upslope) neighbors. The method of assignment varies between models, and depends on grid topology (e.g. 4 vs. 8 neighborhood on a rectangular grid) and routing scheme (e.g. quasi-1D vs. 2D dispersive, Fig. 2).

For topographic-based dispersive routing, flow is partitioned among downstream neighbors based on slope

$$Q_{w,i} \propto S_i^m \tag{6c}$$

where the exponent m (>0) is constant for a given model. Many models use $m = 1/2$ (Murray and Paola, 1994; Sun et al., 2002; Murray and Paola, 2003; Karssenberg and Bridge, 2008), based on the normal flow Eqs. (1)–(4), which imply $q_w \propto \sqrt{S}$. However other models use $m \approx 1$

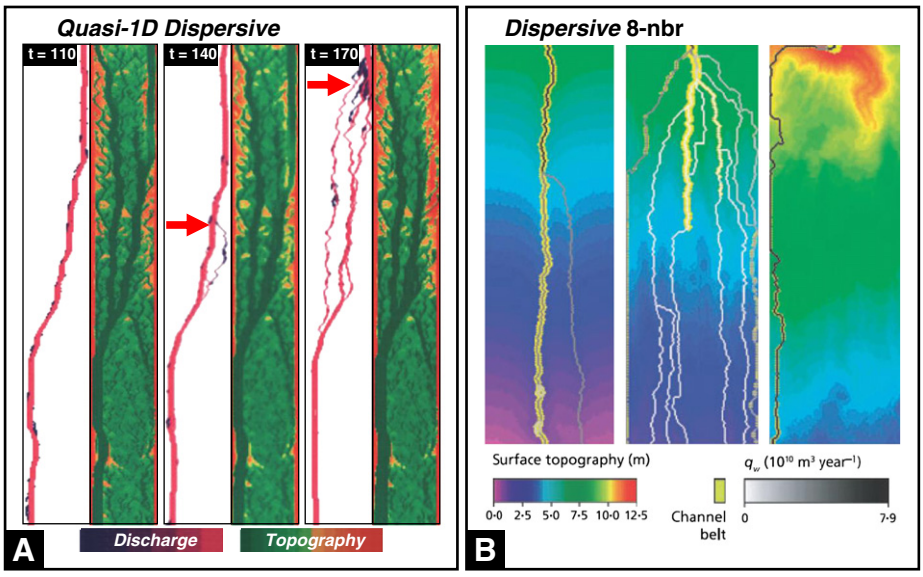

Fig. 2. Topographic Flow Routing. Examples of flow routing based on topography. A) The Murray and Paola (2003) channel-resolving cellular model of bedload-dominated vegetated streams uses a quasi-1D approach, only routing flow to cells in the next row. Red arrows show self-organized avulsions. B) The Karssenberg and Bridge (2008) channel-belt model of lowland rivers uses an isotropic approach, routing flow to all adjacent cells with a lower elevation (note horizontal and upward-sloping sections in flowpaths, vs. panel A).

(Coulthard et al., 2002; Dalman and Weltje, 2008), which may be more accurate for divergent sheetflow (Freeman, 1991).

We note that (6) captures the essence of topography-driven flow routing in simplified avulsion models, but also glosses over subtle differences between models. In particular, CAESAR (Coulthard et al., 2002, 2007; Van De Wiel, 2007) uses a hydrology-oriented approach which can offer greater flexibility (at the cost of increased computational expense). Similarly, flow routing dynamics observed in noncohesive delta experiments (e.g. Sheets et al., 2002, 2007; also see NCED, DB03, XES99) is largely comparable to that seen in topography-based channel-resolving cellular models (e.g. Murray and Paola, 1994). However, while normal flow and purely topographic flow routing are commonly sufficient, other hydrodynamic processes can significantly affect avulsion and alluvial architecture, and may need to be considered as well.

3.1.3. Backwater Effects: Routing low-Fr Channel and Overbank Flows

As in any physical system, flowing water must obey Newton's 2nd Law: $F = ma$. Under conditions of steady uniform flow this reduces to the normal-flow momentum balance (3), but for general shallow water flows we have

$$\underbrace{H\frac{dU}{dt}}_{\text{net momentum}} = \underbrace{gHS_w}_{\text{pressure+gravity}} - \underbrace{\tau}_{\text{bottom drag}} \tag{7a}$$

Physically this means that imbalances between slope and shear stress are associated with convective acceleration

$$\frac{dU}{dt} = \underbrace{\frac{\partial U}{\partial t}}_{\text{transient}} + \underbrace{U\frac{\partial U}{\partial x}}_{\text{advective}} \tag{7b}$$

Furthermore, in non-uniform flows, downstream changes in flow depth are no longer negligible, and the water-surface slope

$$S_w = -\frac{\partial \eta_w}{\partial x}, \eta_w = \eta + H \tag{7c, d}$$

can differ significantly from the topographic slope (Fig. 1C).

The most sophisticated architecture-scale models, such as Delft3D (Lesser et al., 2004) use the full shallow water Eq. (7). Inclusion of convective acceleration effects allows these models to simulate phenomenon such as quasi-steady jets (e.g. Fig. 3A) or transient flood waves. However full shallow-water models, especially transient simulations, are much more computationally intensive than cellular approaches. Computer power is increasing rapidly, and shallow-water models have already been extended to architecture-scale simulations on millennial timescales (van der Wegen et al., 2008). However shallow-water models are also quite useful for constraining detailed avulsion mechanics (e.g. Edmonds and Slingerland, 2008, 2010), and in the near-term they are likely to be most effective as part of an integrated hierarchical modeling strategy.

Under conditions of steady flow and negligible runoff, (7a) reduces to the backwater equation

$$\left(1-\mathbf{Fr}^2\right)\frac{\partial H}{\partial x} = S - C_d\mathbf{Fr}^2 \tag{8a}$$

where the dimensionless Froude number

$$\mathbf{Fr} = U/\sqrt{gH} \tag{8b}$$

is a critical parameter which determines whether or not downstream boundary conditions such as base level can influence upstream hydrodynamics (Parker, E-book Ch5).

Combining (8) with observations from modern rivers (Fig. 4A) suggests that channelized flows largely separate into two end-members. In steep gravel-bed rivers $\mathbf{Fr}^2 = \mathrm{O}[1]$, and (8a) reduces to normal flow, with $\tau \approx gHS$ and $H \approx const$. On the other hand, in low-slope sand-bed rivers $\mathbf{Fr}^2 << 1$, and (8a) reduces to $\tau \approx gHS_w$, with $S_w \neq S$ in general. The difference between these end-members can be seen in the characteristic backwater curve that occurs where normal flow enters standing water (Fig. 1C).

Far upstream we have $\mathbf{Fr}^2 \approx 1$, $S_w \approx S$, and normal flow with depth H determined by local topography and the upstream discharge boundary condition. Far downstream we have $\mathbf{Fr}^2 \approx S_w \approx 0$, with water-surface elevation η_w determined by the downstream base level boundary condition. In between is a transition zone, with $\mathbf{Fr}^2 \ll 1$ and $S_w \ll S$, where the flow "feels" the influence of both upstream discharge *and* downstream base level. The width of this transition zone scales with the backwater length (Fig. 1C)

$$L_w = H/S \tag{9}$$

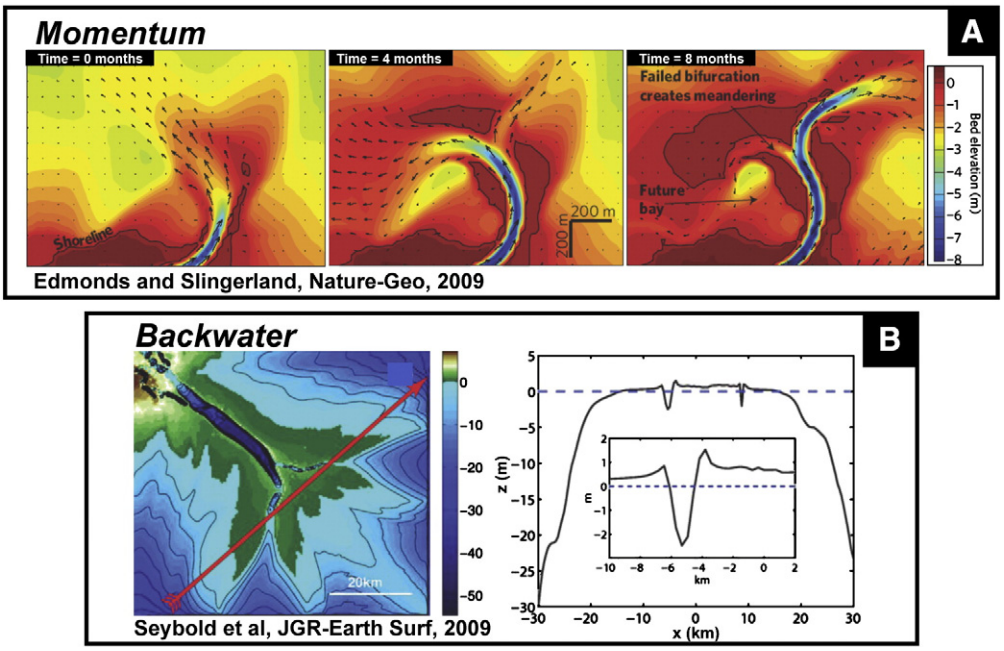

Fig. 3. Hydrodynamic flow routing. Examples of flow routing incorporating hydrodynamic effects. A) Formation of river-mouth jets in this Delft3D simulation illustrates advection of momentum (and also turbulent diffusion of momentum between the jet and basin waters). B) The model of Seybold et al. (2009) includes an explicit water surface, allowing simulation of overbank flows and self-organized levees.

which is defined in terms of the upstream "normal flow" depth and slope.

For channelized flows the backwater curve of Fig. 1C might represent a sand-bed river entering the sea, e.g. a large coastal delta, where L_w may determine the nodal avulsion point (and hence the delta length; Jerolmack and Swenson, 2007). However water-surface effects are ubiquitous in overbank flows, which are initiated when the water surface slopes away from the channel (even though the banks may slope toward the channel). In this context Fig. 1C might represent flood flow between levee crest and inundated floodplain, where L_w may influence crevasse initiation and stability (by modulating cross-channel S_w and hence shear stress; Aalto et al., 2003).

Models based on the shallow water equations (e.g. Delft3D) are of course able to properly handle low-**Fr** flows, but only at significant computational expense. However under low-**Fr** conditions the shallow water equations reduce to the diffusive wave equation (e.g. Lal, 2008)

$$\frac{\partial H}{\partial t} = -\frac{\partial q_w}{\partial x} \tag{10a}$$

$$q_w = K_w H S_w \tag{10b}$$

$$K_w = \sqrt{(g/C_d)H/S_w} \tag{10c}$$

which provides a more efficient alternative for landscape-scale applications. Surprisingly, while diffusive-wave flow routing is relatively common in large-scale engineering applications (e.g. Lal et al., 2005), it has received almost no attention in the context of simplified avulsion modeling. The cellular model of Seybold et al. (2009) is a notable exception, and uses a quasi-steady cellular approximation of (10) with constant hydraulic conductivity K_w to model large low-slope deltas such as the Mississippi (Fig. 3B).

Also worth mentioning are recent cohesive-delta experiments (Edmonds et al., 2009; Hoyal and Sheets, 2009) which manifest concurrent strongly channelized and diffuse overbank flows, and are able to capture many effects of water-surface variations on flow routing (see also Martin et al., 2009 and Wolinsky et al., 2010a supplementary movie). These experiments are unable to capture strong backwater effects though, due to high-**Fr** flows (which are largely unavoidable in experiments, Paola et al., 2009; see also Fig. 4A). However the relative importance of backwater effects for avulsion and alluvial architecture is still unknown, and remains an open research question.

3.2. Morphodynamics

While topography strongly influences hydrodynamics, flow in turn sculpts topography, driving sediment transport, erosion, and deposition. Hence morphodynamics, the coevolution of flow hydrodynamics and surface morphology, is an integral component of essentially all fluvial processes (Parker, E-book; Paola et al., 2009; Kleinhans, 2010). Simplified avulsion and alluvial architecture models represent morphodynamics with a variety of approaches, from relatively detailed models that explicitly simulate continuous topographic evolution via sediment exchange between bed and flow, to relatively coarse models that simulate only aggregate deposition and topographic change over an entire avulsion cycle. Morphodynamic feedbacks occur over a wide range of scales, including local processes of sediment transport and bed change "at a point" during a single flow event, and self-organization of landforms associated with coherent patterns of flow and deposition persisting over the course of many events (Werner, 1999; Kleinhans, 2010).

For example in fluvial landscapes, channels regulate many aspects of system dynamics and morphology. While channels are the most conspicuous fluvial landform, even casual observation of fluvial landscapes reveals an interconnected suite of landforms, including intra-channel bedforms and bars, channel-fringing levees, crevasse splays, channel belts, and alluvial ridges, and landscape-scale alluvial plains and incised valleys. Moreover, while these are modern surface features, ancient fluvial deposits primarily consist of architectural elements which are essentially landform homologues (albeit establishing unequivocal correspondences can be difficult or impossible). Hence landforms are an ideal target for both modeling and data collection, providing common ground for calibration and validation. Consequently, our discussion of model morphodynamics will naturally incorporate connections to the resulting landforms and their morphology.

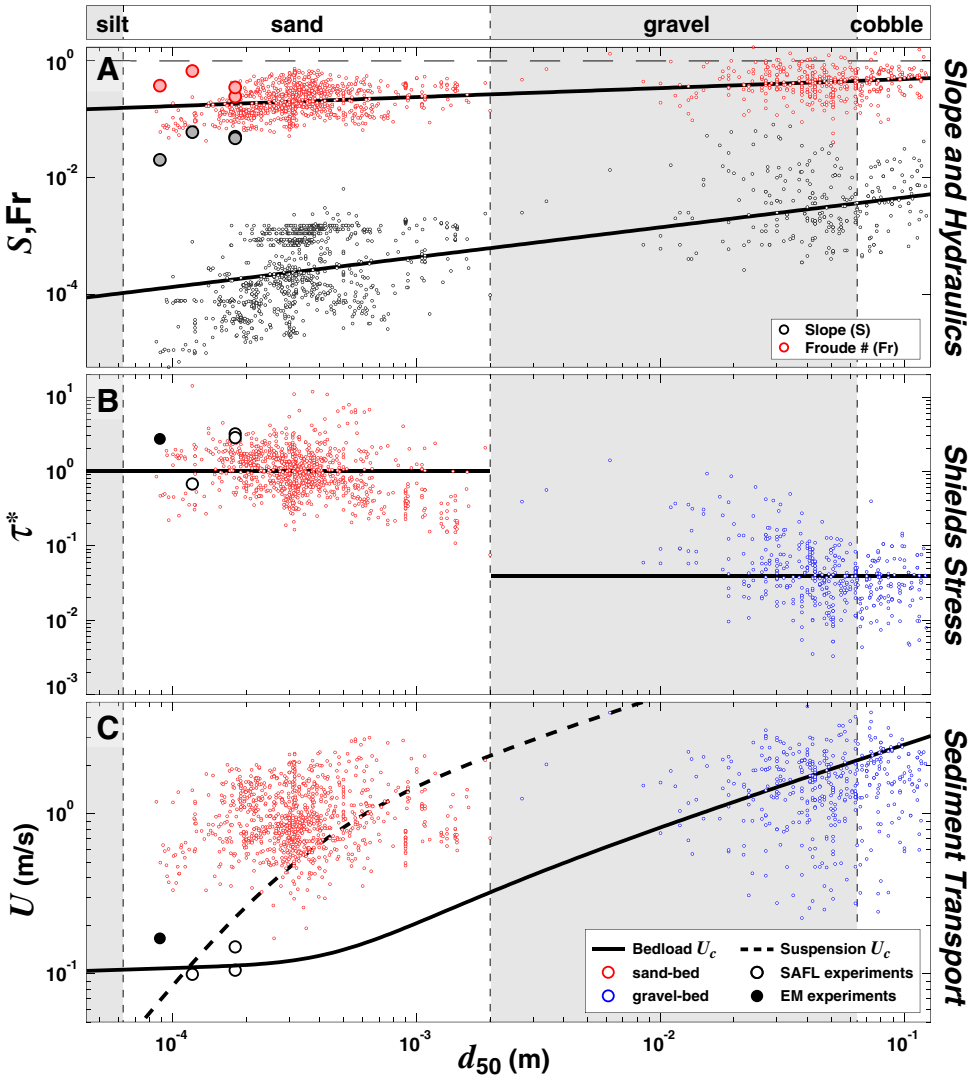

Fig. 4. Reach-scale fluvial morphodynamics. Illustration of reach-scale morphodynamics using a composite database of modern alluvial rivers and flume experiments. All variables show significant variation with bed-material grain size, with a striking separation between gravel- and sand-bed alluvial rivers. Process-analogue experiments are generally sand-bed, but at reach scale they show many similarities to gravel-bed systems, as they are aimed at reproducing architecture-scale phenomenon and so are not fully scaled (in contrast to engineering scale-model "prototype" experiments). A) Dimensionless slope S and Froude number Fr both increase significantly as bed-material coarsens from sand to gravel. B) Dimensionless Shields stress τ^* varies by an order of magnitude between sand- and gravel-bed streams. C) Depth-averaged downstream velocity U in gravel- and sand-bed rivers typically falls near the threshold for transport of bed-material as bedload (Brownlie, 1981) and suspended load (Ferguson and Church, 2004), respectively, reflecting morphodynamic self-organization of reach hydraulic geometry. (Data taken from Brownlie, 1981; Church and Rood, 1983; Soar and Thorne, 2001; Parker, E-book; Jerolmack and Mohrig, 2007; Straub et al., 2009; Edmonds et al., 2009).

3.2.1. Channel-resolving vs. channel-belt models

A fundamental distinction among cellular avulsion models is how the grid resolution Δx compares to the width of channels B and channel belts B_{cb}. In channel-resolving models $\Delta x < B$, allowing intra-channel and channel-forming processes to be modeled explicitly (MP, CAESAR, Seybold, Delft3D). On the other hand, channel-belt models assume $\Delta x > B_{cb}$, and only attempt to model the aggregate effects of channel and channel-belt processes occurring within a cell (Sun, JP, DW). A few intermediate-resolution channel-belt models assume $B < \Delta x < B_{cb}$, attempting to resolve channel belts while still treating individual channels as sub-grid (MB,KB).

Channel-resolving models apply flow-routing rules such as (6b) to all cells, and patterns of dry vs. sheetflow vs. channelized flow emerge via self-organization. In contrast, channel-belt models only distribute flow among the "active channel network", a subset of cells that is initially specified and thereafter evolves according to avulsion rules (discussed in Section 3.2.5). These models assume each active cell contains a single channel belt, but basin-scale models such as DIONISOS assume $\Delta x >> B_{cb}$, and resolve neither channel belts nor avulsions. Like channel-resolving models, DIONISOS applies dispersive flow routing to all cells, but here as a heuristic averaging over many channel-belts per cell, and many avulsions per timestep.

In natural systems, and in channel-resolving models (including experiments), an additional distinction arises from the mechanism by which channelized flows are confined. In coarse grained bedload-dominated systems, channels are purely erosional features, confined due to incision (e.g. gravel alluvial fans; SAFL and MP models in Table 2; Fig. 2A). However in systems with significant suspended load, while channels may begin as erosional features, overbank deposition builds levees which provide constructional confinement for at least the upper portions of bankfull flows (e.g. most lowland rivers; Delft3D, Seybold, and EM models in Table 2; Fig. 3).

In comparing simplified avulsion models, it is useful to consider what factors set the width of channels and channel-belts, in both

natural systems and models. For a reach with given discharge and slope, we can combine the normal flow Eqs. (1)–(4) to yield

$$\tau^{3/2} B = \left(g\sqrt{C_d}\right) Q_w S \tag{11}$$

In the case of a flume, where width B is fixed and known, (11) sets the shear stress τ. In natural alluvial channels B is not fixed, but self organizes in response to discharge, slope, and shear stress. However, observations from modern alluvial rivers show that for a given bed, with characteristic grain size d, the dimensionless Shields stress

$$\tau^* = \tau / Rgd \tag{12}$$

is relatively fixed, with $\tau^* \approx 0.04$ for gravel-bed channels and $\tau^* \approx 1.0$ for sand-bed channels (e.g. Fig. 4B, where d = bed-material d_{50}; see also Paola, 2000; Parker, E-book Ch3). Hence for natural alluvial channels τ is fixed and known (for given d), and (11) sets the width B as a function of discharge Q_w and slope S.

While channel-belt models do not resolve channels, they must still estimate B in order to compute sediment transport in sub-grid channels. Some models directly use (11) with constant τ^* (e.g. Sun, JP), while others use qualitatively similar empirical power-laws $B \propto Q_w^a S^b$ (e.g. KB, DW). The processes that set channel width in channel-resolving models are understood only qualitatively, but simplified models consistently point to bank strength (possibly dynamically varying) as a critical factor, with stronger banks resulting in narrower channels (e.g. cohesive vs. non-cohesive process-analogue experiments, Hoyal and Sheets, 2009; vegetated vs. non-vegetated experiments and cellular models, Tal and Paola, 2007; Murray and Paola, 2003). However a mechanistic quantitative theory of channel width has been elusive even in event-scale modeling (e.g. van der Wegen et al., 2008; ASCE Task Committee on Hydraulics, Bank Mechanics, and Modeling of River Width Adjustment, 1998a, 1998b).

For channel belts, while morphometric analysis of modern rivers has yielded some empirical constraints on width (Bridge and Tye, 2000), process-based understanding is generally lacking. Channel-resolving cellular models incorporating lateral erosion could potentially give insight into controls on channel-belt width (e.g. Murray and Paola, 2003; Coulthard et al., 2007), but this has not been investigated to date. However in the particular case of unconfined meander belts, Camporeale et al. (2005) obtained relatively tight constraints on B_{cb} using quasi-1D simplified models (Fig. 5). They showed that for an initially straight channel, sinuosity and channel-belt width grow over short timescales, but are limited by cutoffs over long timescales, eventually reaching a statistical steady state. Camporeale et al. (2005) argued from theoretical considerations that the equilibrium B_{cb} scales with the hydrodynamic lengthscale H/C_d (as do meander wavelength and radius of curvature), and showed that this gives excellent predictions in natural examples (e.g. Fig. 5, where B_{cb} corresponds to the "saturated oxbow fringe"). Their transient results also provide some support for heuristic B_{cb} growth rules that give an exponential approach to equilibrium, such as used in the KB and DW models. However we note that variability in bank erodibility, e.g. due to lateral confinement (Howard, 1996; Nicoll and Hickin, 2010) or substrate heterogeneity (Sun et al., 1996; Gouw and Berendsen, 2007), can significantly affect channel-belt width.

3.2.2. Sediment mass balance

Conservation of water determines accumulation of runoff (6a) and constrains flow partitioning (6b), but it is conservation of sediment which directly drives surface evolution, through changes in bed sediment thickness h. Quantitative statements of sediment mass balance between flow and bed, commonly referred to as Exner equations, are expressed in different ways depending on the application (Paola and Voller, 2005; Parker, E-book Ch4, Wolinsky, 2009). For cellular models the Exner equation takes the form

$$c_0 \frac{\Delta h}{\Delta t} = -\frac{\Delta Q_s}{\Delta A} \tag{13}$$

where c_0 is bed sediment concentration, Q_s is the (volumetric) sediment load carried by the flow, and the sediment flux difference ΔQ_s is defined analogously to ΔQ_w (6b). Note that it is gradients in transport that drive aggradation / degradation rather than transport itself, e.g. a graded river with constant Q_s will have no net deposition or

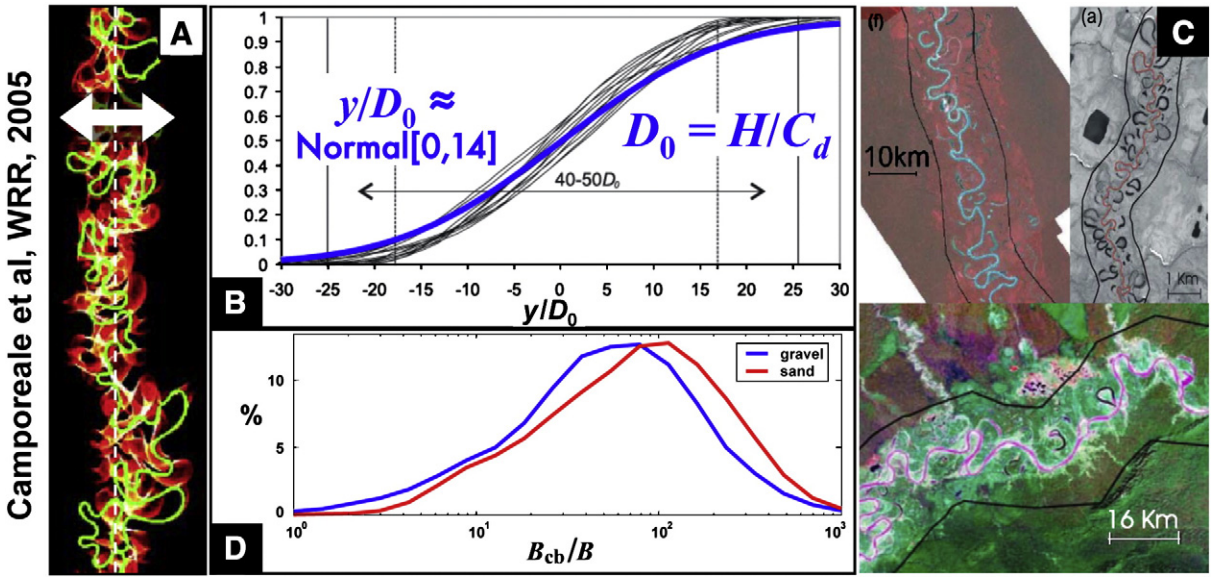

Fig. 5. Event-scale processes and landforms – Channel belts. Prediction of channel-belt width in unconfined meandering rivers (after Camporeale et al., 2005). A) Channel occupation history in a meandering simulation using the simplified process-based model of Camporeale et al. (2005). B) Distributions of lateral channel position y over a wide range of simulations collapse onto a single curve when normalized by the hydrodynamic length scale $D_0 = H/C_d$. Over long timescales cutoff dynamics constrains the channel to a fairly well-defined belt (dashed lines contain 90% of channel paths). C) Predictions of channel-belt width using the 90% confidence interval, $B_{cb} \approx 50\, D_0$, work very well on modern rivers, capturing the "oxbow fringe" (see Camporeale et al., 2005 for more validation examples). D) Predicted distribution of relative channel-belt width, B_{cb} / B, based on the alluvial reach database using $B_{cb} = 50\, D_0$.

erosion. Experimental models also conserve sediment mass, and can be analyzed with continuous analogues of (13) (e.g. Kim et al., 2006a).

Sediment discharge Q_s is the integral of sediment flux q_s across the flow width, $Q_s = \mathsf{B}q_s$. In channel-resolving models $\mathsf{B} = \Delta x$, the cell size, while in models with sub-grid channels $\mathsf{B} = B$, the channel width. (Note that throughout this paper we will use sans-serif nonitalic letters to indicate generic dimensions such as B, which can vary depending on context.)

In morphodynamic systems flow Q_w drives sediment transport Q_s. Process-based formulations of bed evolution use morphodynamic flux laws to relate local flow and transport (Sections 3.2.3 and 3.2.4), and compute deposition Δh at a point using the Exner Eq. (13) directly (Wolinsky, 2009). Alternatively, geometric formulations of bed evolution specify Δh directly, with rules that describe a spatially extended deposit (e.g. overbank deposition exponentially decaying away from the channel; Mackey and Bridge, 1995). Process-based formulations necessarily conserve mass, but geometric formulations need not (although they can, if based on the Exner equation; Wolinsky, 2009).

In channel-resolving experimental and cellular models process-based deposition (or erosion) occurs everywhere, so these models conserve mass (Table 2; this is also true for DIONISOS). Most channel-belt models only compute Q_s and apply (13) in "active" cells, using geometric rules for overbank deposition away from channels, and hence only approximately conserve mass (Table 2). Two exceptions are MB, which is purely geometric (hence not mass conserving), and Sun, which includes only channel-belt deposition (so conserves mass).

3.2.3. Channelized sediment transport

Net sediment load Q_s consists of a range of grain sizes, where each size can move in one of two transport modes. Bedload moves in frequent contact with the bed (e.g. via rolling or saltation), while suspended load is carried by the flow. For a given grain size d, transport mode is determined by relative magnitudes of flow velocity U, bedload-entrainment velocity (given by the Shields curve), and sediment settling velocity w_s (Fig. 4C; Parker, E-book). Observations of modern rivers show that gravel-bed channels cluster around the bedload threshold (relative to bed-material d_{50}), while sand-bed channels cluster around the suspension threshold (Fig. 4C). Hence in sand-bed rivers the total bed-material load typically includes both bedload and suspended fractions, while in gravel-bed rivers bed-material load is entirely bedload.

Event-scale models for bed-material load are usually flux laws $q_s = f[\tau]$ that relate flow strength to carrying capacity, where q_s is either bedload (gravel-bed rivers; Parker, E-book Ch7) or total bed-material load (sand-bed rivers; Parker, E-book Ch12). Engineering models commonly use flux laws directly (at least for bedload, e.g. Delft3D,CAESAR), but avulsion models typically use simplified formulations based on sub-grid hydraulic geometry (in Table 2 DW is the only exception). For example, combining (11) with the definition $Q_s = Bq_s$ gives the well-known "alluvial diffusion" transport law (e.g. Paola, 2000)

$$Q_s = K_s Q_w S \tag{14a}$$

$$K_s = \left(g\sqrt{C_d}\right) q_s / \tau^{3/2} \tag{14b}$$

In alluvial rivers shear stress τ is approximately a function of bed-material d_{50} (as outlined in Section 3.2.1), and hence so is bed-material flux, $q_s = f[\tau]$. Consequently, for a given river the diffusive transport coefficient is approximately constant, with $K_s \approx 0.07$ for gravel-bed channels and $K_s \approx 0.6$ for sand-bed channels (for details see Marr et al., 2000). Many simplified avulsion models use (14a) to model bed-material transport (Sun, JP, KB), although qualitatively similar empirical power-laws $Q_s \propto Q_w^a S^b$ are also common (MP, DIONISOS). Noncohesive experiments are typically bedload dominated (e.g. SAFL; Fig. 4C), and exhibit bed-scale behavior broadly similar to that of channel-resolving noncohesive bedload-dominated cellular models (e.g. MP non-vegetated).

In a river with depth-averaged suspended-sediment concentration C, advection of suspended sediment by the mean flow produces a sediment flux $q_s = Cq_w$. Suspended-load models track changes in C due to entrainment of bed sediment into suspension and settling of suspended sediment onto the bed. Downstream changes in C are commonly summarized by the suspended-sediment conservation equation

$$\frac{\partial q_s}{\partial x} = w_s(e - c_b) \tag{15}$$

where c_b is the bed-sediment concentration, and e is a dimensionless sediment-entrainment coefficient (e.g. Parker, E-book Ch10 + 21). In net depositional or bypassing flows typically $c_b \approx \mathrm{O}[C]$ but more concentrated (e.g. Parker, E-book Ch21), while for net-erosional flows typically $c_b \approx c_0 >> C$ (e.g. Sanford and Maa, 2001).

Models for entrainment of sediment into suspension are essentially of the form $e = f[U/u_c]$, where u_c is a sediment-dependent critical entrainment velocity (Garcia and Parker, 1991; for noncohesive sediment $u_c \approx w_s$). Physically, e gives the equilibrium concentration, $c_{b,\mathrm{eq}}$, eventually achieved by a steady uniform flow over a homogeneous bed (after which q_s remains constant at $q_{s,\mathrm{eq}} \approx eq_w$). For channelized sand transport, the "pickup length" over which this equilibrium is reached is typically negligible, so (15) can be approximated by a carrying-capacity flux law $q_s = f[\tau]$ (Parker, E-book Ch 21).

Suspended mud transport differs from sand transport in two ways: slow settling rates w_s ensure lag effects are never negligible, while cohesion effects result in entrainment thresholds $u_c \gg w_s$ (e.g. Sanford and Maa, 2001). Recent modeling studies show that these two effects can significantly impact fluvial morphodynamics, avulsion, and stratigraphy (Hoyal and Sheets, 2009; Edmonds and Slingerland,

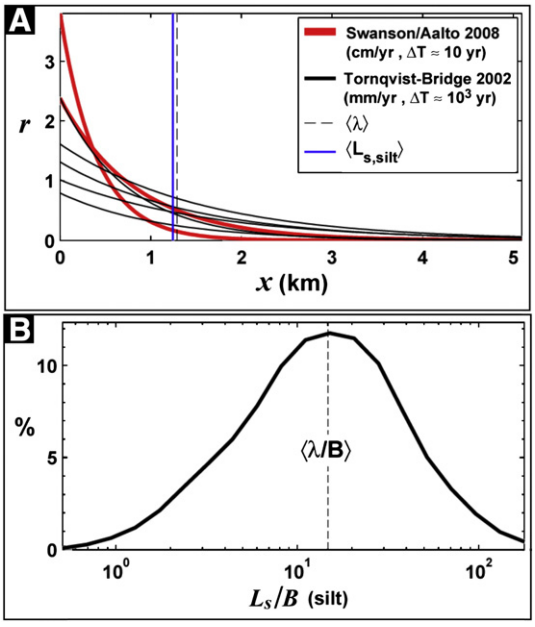

Fig. 6. Event-scale processes and landforms – Muddy overbank deposition. Lengthscale λ of exponential decay of muddy overbank deposition rates r. A) Deposition profiles $r[x]$ based on λ values measured over modern (red) and Holocene (black) timescales. B) Estimated distribution of relative decay scale λ/B in modern rivers based on the settling length $L_s = q_w/w_s$, using water flux q_w from the alluvial reach database and settling velocity w_s corresponding to silt. (The reach database has only d_{50}, but predictions based on L_s[silt] agree well with average measured λ values; vertical lines in panel A).

2010; EM/Delft3D models in Table 2). The cellular model of Seybold et al. (2009) essentially incorporates these effects via the heuristic transport rule

$$\frac{\partial q_s}{\partial x} = \alpha(q_w - q_c) \tag{16}$$

where α and q_c are constants. This rule is roughly equivalent to the more physically-based (15), assuming $e \propto q_w$ and net erosional conditions with $c_b \approx c_0 =$ constant. Interestingly, the results of Seybold et al. (2009) show many broad qualitative similarities to those of Hoyal and Sheets (2009) and Edmonds and Slingerland (2010), even though their model does not really include bed-material load.

3.2.4. Overbank and floodplain processes

The morphodynamics of overbank and floodplain processes are poorly understood relative to those in channels, particularly on landscape/architecture scales. Consequently, most alluvial architecture models parameterize these processes with geometric rules (e.g. Fig. 6). However exploratory modeling studies show that the details of these rules can significantly impact avulsion flowpath selection, and hence alluvial architecture (e.g. Jerolmack and Paola, 2007; discussed further in Sections 4.3 and 4.4). Hence a process-based understanding is essential to know when different geometric rules are appropriate, and to develop new rules from process-based models and event-to-Holocene-scale field measurements of modern systems (in a hierarchical-modeling context).

In the context of landscape-scale avulsion and alluvial architecture, floodplains are commonly an afterthought, conceived of as "background overbank deposition" between alluvial ridges. However research over the past 20 years clearly shows that floodplain morphodynamics encompasses much more than simply deposition by diffuse overbank flows. Relict channels, abandoned by cutoff (e.g. oxbow lakes, Fig. 5) or avulsion (e.g. Reitz et al., 2010), are well known floodplain features, but active channels are also common. Channelized floodplain flows can be fueled by local runoff (e.g. Mertes, 1997), or sourced from the main river via crevasses, e.g. erosional channels on subaerial splays (Fig. 7) and constructional tie-channels prograding into floodplain lakes (Rowland et al., 2009). In large (±tropical) systems, dispersal of flood sediment via floodplain channels vs. diffuse overbank flows is a significant component of event-scale sediment budgets (e.g. Dunne et al., 1998; Day et al., 2008).

Erosional floodplain channels seeded by spontaneous channelization of overbank sheetflows occur in many channel-resolving simplified models (e.g. MP03, Fig. 2A; SAFL, Fig. 6C; Seybold et al., 2009). The alluvial architecture model of Karssenberg and Bridge (2008) includes a hillslope erosion module, separate from their main channel-belt module, which computes "local" flow-accumulation and floodplain erosion via steepest-descent routing (6a,b) and a heuristic erosion rule, $\partial q_s/\partial x \propto q_w S$, similar to (16). Comparable detachment-limited erosion rules produce self-organized channel networks in upland landscape models (e.g. Howard, 1994), but it is unclear if this happens in the KB model.

Most channel-belt models simulate overbank washload (≈mud) deposition with geometric rules of the general schematic form

$$\frac{\partial h}{\partial t} = \underbrace{r_0}_{\text{background}} + \underbrace{(r_{cb} - r_0)\exp[-x/\lambda]}_{\text{channel distance}} + \underbrace{\beta(\eta_{cb} - \eta)}_{\text{floodwater depth}} \tag{17}$$

where η is the elevation of a floodplain cell and x is the distance to the nearest channel belt, which has channel-top elevation η_{cb}, channel depth H_{cb}, and aggradation rate r_{cb}. The three terms represent end-member deposition patterns which are, respectively, spatially uniform

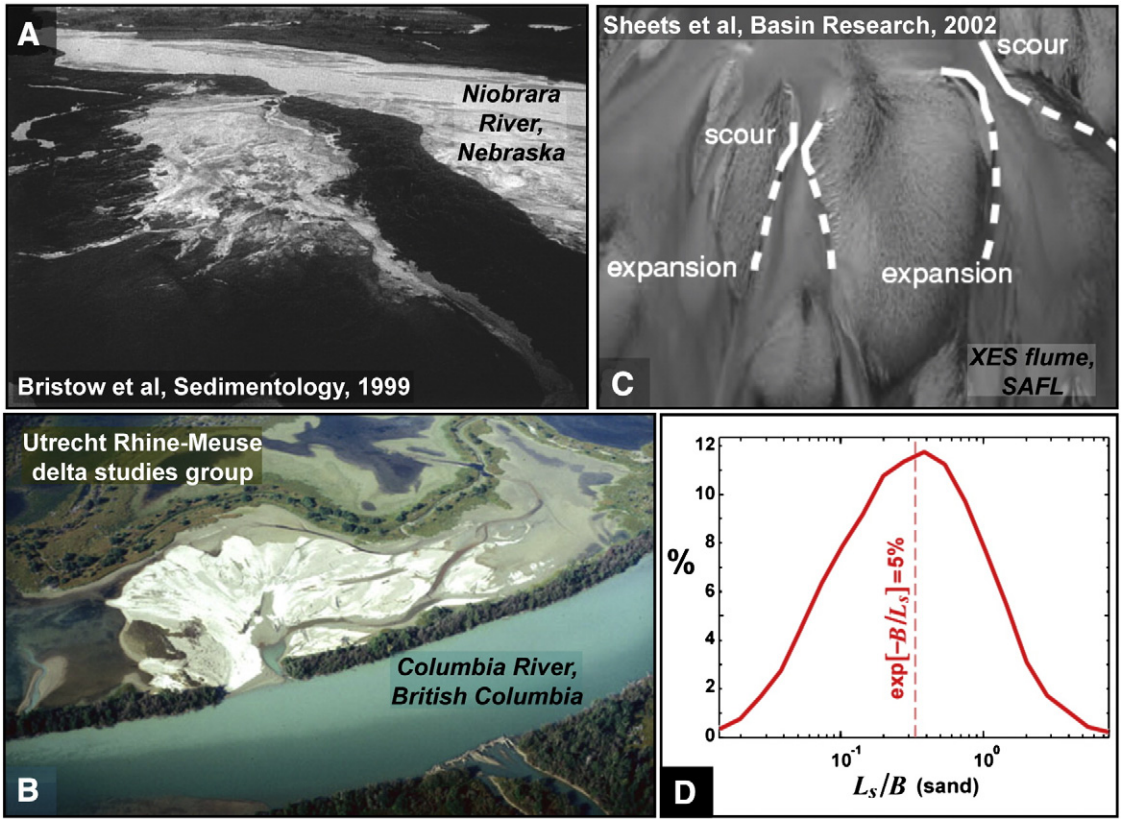

Fig. 7. Event-scale processes and landforms – Sandy overbank deposition. Examples of crevasse splays in modern rivers (A,B) and flume experiments (C). Estimated distribution of relative lengthscale for "sheetflow" splay deposits in modern sand-bed rivers based on the settling length L_s corresponding to bankfull flow and bed-material d_{50} in, using the alluvial reach database. On average the predicted length is O[B], consistent with observations that splays deposited by unchannelized flows have lengths similar to the width of the channel (e.g. panels A and B; note that channelized splay deposition can reach much farther).

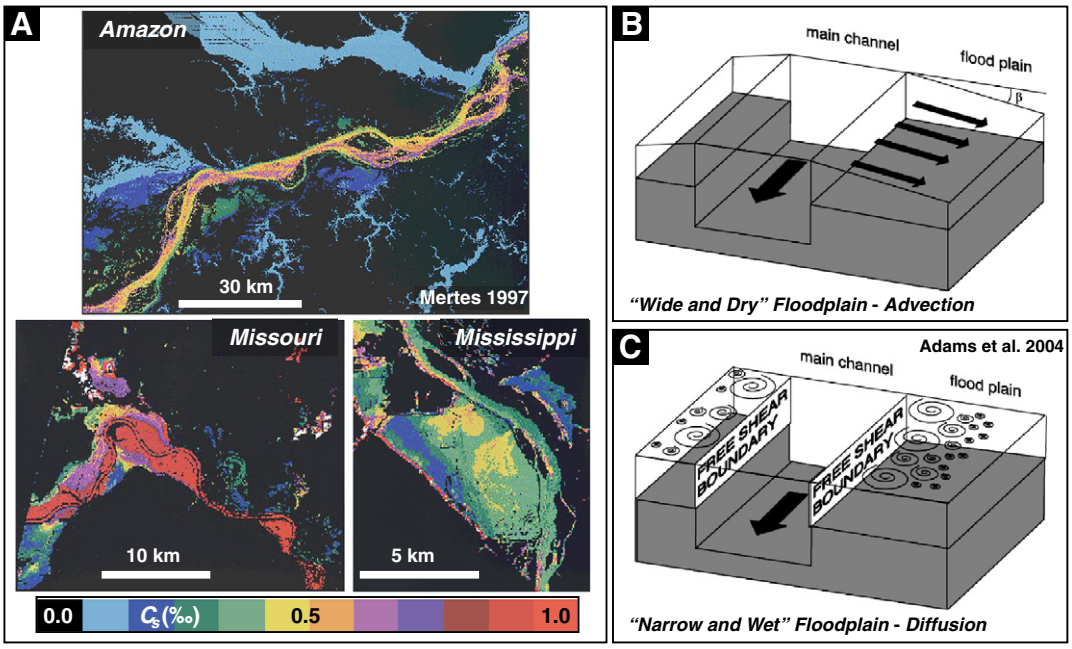

Fig. 8. Event-scale processes and landforms – Flooding style and overbank deposition. The processes and distribution of overbank deposition vary depending on the style of river-valley flooding. A) Landsat-derived images of floodwater turbidity in modern rivers (after Mertes, 1997). Note differences in degree of mixing in the different systems. Concentrations are in parts per thousand, and areas unaffected by flooding are blacked out. B) In cases where inundation is asynchronous across the floodplain, lateral water-surface slopes drive currents which advect suspended sediment away from the channel. C) In contrast, if flooding is synchronous across the width of the floodplain then overbank transport of suspended sediment must rely on the weaker process of eddy diffusion. (Panels B and C after Adams et al., 2004).

(at rate r_0), decaying away from channels (at a rate of 37% per e-folding length λ), and increasing with greater inundation, i.e. elevation below the bankfull channel high-water surface (where β = concentration / time). Eq. (17) guarantees that deposition converges to r_{cb} at the channel belt, and in implementations is only applied when $r_{cb}>0$ and $\eta<\eta_{cb}$. Existing cellular avulsion models use either distance-dependent deposition (MB,KB,DW) or depth-dependent deposition (JP), but not both (although geomorphic models typically do, e.g. Howard, 1992, 1996, which also couple the two).

Eq. (17) is fundamentally a heuristic rule, but it is inspired by observations and theoretical arguments. Measurements of floodplain deposition in extant systems over modern (multidecadal) and Holocene (millennial) timescales consistently find rates that decay away from the channel in approximately exponential fashion (Fig. 6; the discrepancy in rates between the two scales suggests accumulation of hiatuses, as is typical in intermittent sedimentary systems, e.g. Jerolmack and Sadler, 2007). Event- and Holocene-scale floodplain deposition measurements also give some evidence for background and depth-dependent terms (e.g. Walling and He, 1998; Törnqvist and Bridge, 2002).

Process-based arguments for the terms in (17) take various forms, depending on the underlying conceptual models for sediment transport and flooding. For depth-dependent sedimentation the underlying conceptual model is essentially "rapid" inundation of the floodplain by "energetic" floodwaters, such that sediment is maintained in a uniformly mixed suspension, followed by a period of standing water during which sediment settles out. In this case we expect $\beta \approx$ floodwater turbidity / (flood duration + return period). Observations of floodwater turbidity patterns in modern systems (Fig. 8A) indicate that this well-mixed end-member does occur (approximately, e.g. Missouri River; Mertes, 1997, upper left in Fig. 8A), but is perhaps atypical.

For distance-dependent sedimentation two distinct mechanisms are commonly cited, based on the dominant process of suspended sediment transport–advection vs. diffusion (Adams et al., 2004, Fig. 8B,C)–each of which can yield exponential decay of overbank sedimentation rates. If inundation occurs asynchronously across the floodplain, or if the floodplain is unconfined, there will tend to be lateral water surface slopes which drive net currents directed away from the channel (Fig. 8B). In this case overbank deposition will be dominated by advective transport, and we can rearrange (15) to give

$$\frac{\partial q_s}{\partial x} = \frac{q_{s,eq} - q_s}{L_s}, L_s = \frac{q_w}{w_s} \tag{18a, b}$$

where x and q are now cross-stream oriented, and assuming a net depositional flow (i.e. $c_b \approx C$, $q_{s,eq} \approx q_w e$). The settling length L_s is simply the distance a particle is advected as it settles through the water column, i.e. $L_s = U(H/w_s) = U$(settling time). If q_w , w_s , and e are constant, then integration gives

$$q_s - q_{s,eq} \propto \exp[-x/L_s] \tag{18c}$$

which implies

$$\partial q_s/\partial x \propto \exp[-x/L_s] \tag{18d}$$

i.e. exponentially decaying deposition. A similar process, based on (16), builds levees in the Seybold model (Fig. 3B).

Alternatively, for synchronous inundation of a confined floodplain, lateral water surface slopes will be negligible (Fig. 8C). In this case, mean currents will be negligible, but mixing by turbulent eddies can still drive transport via diffusion (e.g. Adams et al., 2004). Prior to this point we have neglected lateral eddy-diffusion of momentum and suspended sediment (in Eqs. (7a) and (15), respectively), since these are negligible relative to mean-current advection in channelized flows. However these effects can become important when net currents are small, e.g. overbank deposition in inundated floodplains (Fig. 8C), or river mouth jet-plume deposition (Fig. 3A). Pizzuto (1987) showed that overbank deposition by turbulent diffusion gives

$$\frac{\partial h}{\partial t} \propto \exp\left[-\frac{x}{L_d}\right], L_d = \frac{\kappa}{w_s} \tag{19a, b}$$

where κ is the eddy diffusivity, assumed constant. For shallow-water flows $\kappa \approx \alpha u_* H$, where α is an O[10^{-1}] constant, and for channelized

flows the shear velocity is $u_* = U\sqrt{C_d}$ (Pizzuto, 1987). Hence for typical values of $\alpha \approx 10^{-1}$ and $C_d \approx 10^{-2}$, we expect a diffusion length L_d roughly 1% of the settling length L_s (18b) associated with the bankfull channel q_w.

While this is reasonable in the boundary shear zone adjacent to the channel (Fig. 8C), beyond a distance O[H] the turbulent kinetic energy k must itself propagate via eddy diffusion, and generally $u_* \propto \sqrt{k}$ (essentially the velocity standard deviation averaged over turbulence). Hence typically κ will itself decay sharply away from the channel, rather than being constant across the floodplain. Therefore, while the diffusion model (19) is often implicitly cited as justification for the heuristic rule (17), the physical connection between the two is questionable. We note that of the models in Table 2, only Delft3D explicitly simulates eddy diffusion, using either turbulence closure schemes (e.g. k-ε) or horizontal large-eddy simulation (Lesser et al., 2004; Edmonds and Slingerland, 2010).

On the subject of process-based interpretations of the empirical exponential overbank deposition rule (17), two additional observations are worth noting. First, measured decay lengths λ are similar to predicted settling lengths L_s for silt based on typical bankfull fluxes q_w (Fig. 6). Hence advection-settling of fine silt or clay in overbank flows with q_w a few % of bankfull channel fluxes could be a reasonable explanation of observations. Second, while (17) forces continuity of overbank and channel-belt deposition, this is not required by either of the process-based exponential overbank rules (18) and (19), nor by nature. For example, non-aggrading channels commonly build levees by overbank deposition, a process seen in constructional channel-resolving models (Delft3D, Seybold, EM).

Overbank sand deposition is relatively rare, as suspended sand grains tend to travel fairly low in the flow compared to slower-settling muds. However significant floodplain sand deposition occurs via "through-bank" crevasses, producing splay deposits (e.g. Bristow et al., 1999; Slingerland and Smith, 2004, Fig. 7). Subaerial splays are similar to alluvial fans (Bristow et al., 1999), while subaqueous crevasses produce delta-like landforms, similar to e.g. bayhead (Slingerland and Smith, 2004) or birdfoot (Rowland et al., 2009) deltas. While crevasse splays are commonly channelized (Fig. 7), splay deposition is primarily driven by flow expansion, with channels acting as bypass conduits (Sheets et al., 2002, 2007). For unchannelized deposition, observations from modern rivers suggest that splay lengths should be O[B] (Fig. 7), based on bankfull sand settling lengths L_s (though eddy-diffusion in channel-adjacent shear zones would predict similar lengths, e.g. Fig. 8C). Explicit splay deposition occurs in many of the channel-resolving models in Table 2 (e.g. SAFL, EM, Delft3D, CAESAR07, MP03).

In some cases, e.g. the progradational avulsions of Slingerland and Smith (2004), interaction of channelized transport and sheetflow deposition produces extensive floodplain sand deposits of stacked splays. These "avulsion deposits" are associated with long-lived anastomosed channel networks (Slingerland and Smith, 2004). In the MP03 and KB models, similar processes can lead to development of locally extensive anastomosed channel networks and sand deposition (Murray and Paola, 2003; Karssenberg and Bridge, 2008). Recent work has suggested that intermittent splay deposition may dominate construction of levees and/or floodplains in some systems, rather than relatively continuous overbank deposition (e.g. Aslan and Autin, 1999; Adams et al., 2004; Slingerland and Smith, 2004).

3.2.5. Avulsion rules

As outlined in section 2.2, "avulsion" is not a single process, but a set of processes which comprise three phases–initiation, finding, stabilization–resulting in a variety of avulsion styles. Simplified models represent avulsion processes in different ways, from channel-belt models which include explicit rules, to channel-resolving models where avulsions are self-organized (but from which we can infer implicit "rules" that govern the emergent dynamics, at least qualitatively). Some channel-belt models use specific rules for individual phases, but others use lumped "avulsion" rules (i.e. initiation implies successful avulsion, precluding the possibility of failed avulsions). Similarly, in channel-belt models using steepest descent flow routing (e.g. MB, JP) avulsion necessarily implies full diversion of flow from parent- to daughter-channel, precluding the possibility of partial avulsions (i.e. quasi-stable bifurcations).

Avulsion initiation typically results from a combination of long-term setup and a proximal trigger (Slingerland and Smith, 2004),

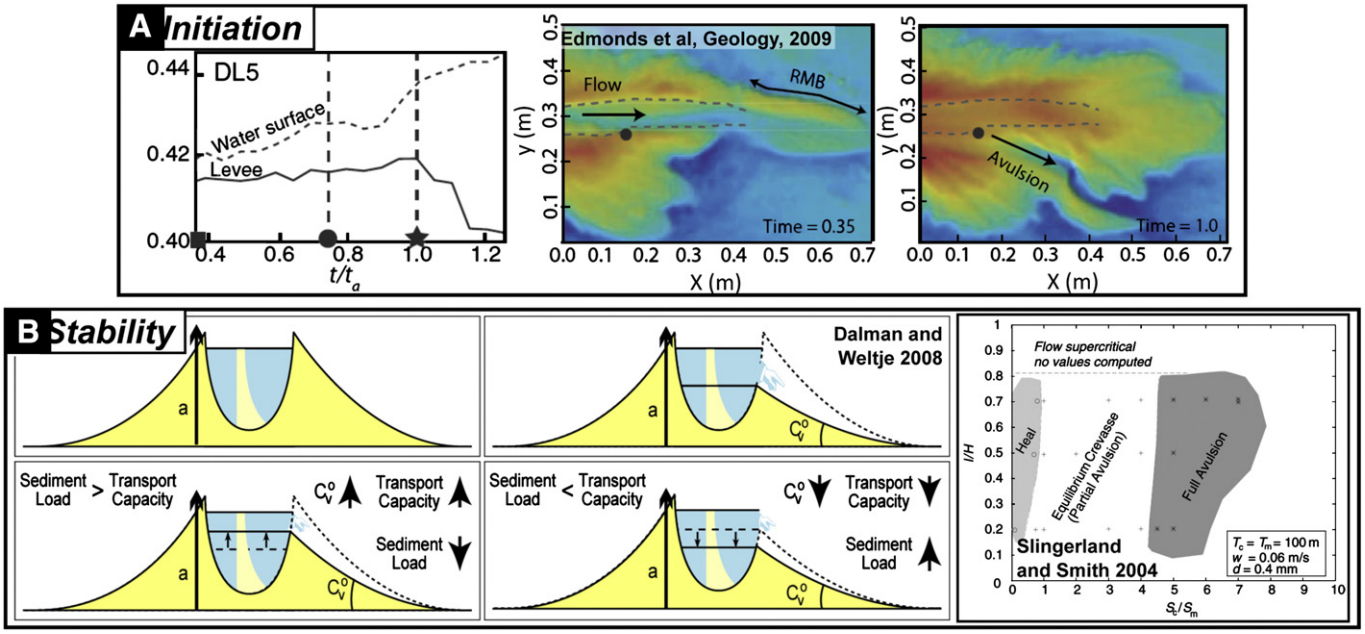

Fig. 9. Avulsion initiation rules – Crevassing. Process-based models have given significant insight into avulsion initiation by levee breaching crevasses. A) Example of crevasse initiation in the experiments of Edmonds et al. (2009). Note how rapid levee incision (crevassing, $t > 1$) is preceded by a gradual increase in the water-surface driven by channel backfilling (i.e. setup due to "morphodynamic backwater"). B) Once a crevasse is initiated it will either stabilize or heal, depending on the relative transport capacity and concentration of the crevasse and channel flows (left; sub-grid crevasse-stability model of Dalman and Weltje, 2008). For a given grain size crevasse fate is primarily determined by the relative slope of the crevasse channel and the mainstem river (right, Slingerland and Smith, 1998, 2004).

e.g. persistent channel-belt aggradation combined with a large flood. Investigation of detailed avulsion initiation mechanisms is most developed for the case of levee breaches (crevassing, Fig. 9A). Crevasses commonly form where bank shear stress is especially high, e.g. meander-bend outer banks (Slingerland and Smith, 2004), although susceptibility may be more a function of cumulative stress vs. peak stress, due to time-dependent weakening (Edmonds et al., 2009). Any crevassing event is a potential trigger for large-scale avulsion, but crevassing is much more common than avulsion, because in the absence of sufficient setup crevasses will stabilize or heal without diverting significant flow (Slingerland and Smith, 2004).

Over the course of subsequent floods, evolution of an initial crevasse must eventually result in either healing, formation of a stable bifurcation, or abandonment of the parent channel (i.e. a failed, partial, or full avulsion, respectively). Detailed morphodynamic models of bifurcation stability (reviewed in Slingerland and Smith, 2004) make relatively precise predictions of the fate of a crevasse based on the initial and boundary conditions, in the form of phase diagrams (Fig. 9B). Results show that setup (formalized in the boundary conditions) is the primary control, in particular the slope ratio between the crevasse channel and the mainstem river. The specific threshold values vary somewhat depending on grain size and transport mode (Slingerland and Smith, 2004), but typically a slope ratio of <1 results in a failed avulsion, while a slope ratio >5 will lead to a full avulsion (e.g. Fig. 9B).

In addition to the theoretical insight provided by crevasse stability models, stratigraphic studies have yielded significant insight into the conditions leading to avulsion (e.g. Mohrig et al., 2000). Due to the difficulty of constraining slope ratios in outcrops, these results are primarily expressed in terms of channel super elevation: the elevation of the bankfull water surface above the "far-field" floodplain, essentially levee relief. Mohrig et al. (2000) found that estimates of normalized superelevation–the ratio of superelevation to bankfull depth–in both fluvial outcrops and recently avulsed modern rivers occupy a fairly narrow range, $\approx 1.0 \pm 0.5$ (e.g. Fig. 10 A,B). This suggests that a normalized superelevation of O[1] is a critical threshold for avulsion, i.e. in an aggrading channel, as the channel-bed elevation approaches the floodplain elevation, avulsion becomes increasingly likely. Subsequent studies of avulsions in Holocene rivers and flume experiments have found that a related measure, net inter-avulsion aggradation normalized by channel depth, also tends to be O[1] on average (Jerolmack and Mohrig, 2007; Martin et al., 2009; see also Fig. 10C). These stratigraphic results indicate that in contrast to particular avulsions at event scale, average avulsion rates over basin timescales are setup-limited rather than trigger limited.

Channel-belt models typically incorporate heuristic avulsion initiation rules inspired by these observations. The most common approach is a local threshold based on a critical slope-ratio (MB/KB), superelevation (JP), or a combination of slope and superelevation (Sun). A notable exception is the channel-belt model of Dalman and Weltje (2008), which incorporates a sub-grid crevasse stability model (Fig. 9B). The slope and superelevation used in topographic thresholds are calculated between a cell and its neighbors, but adapted to a coarse cellular framework. For example the MB and KB models compute cross-stream slope at the channel-belt edge, but downstream slope at the nearest sub-grid channel cell. In the JP model channel-belts are sub grid, but within each cell the model tracks a top and bottom elevation, associated with the levee top and channel bed. For never-channelized floodplain cells these are equal, but in channelized cells they differ by H, hence abandoned-channel cells inherit relief. To compute superelevation the JP model compares the top elevation of a channelized cell to the bottom elevations of its neighbors, i.e. relict-channel levees are "porous". To compute normalized superelevation, the JP and Sun models estimate bankfull depth H in sub-grid channels from discharge Q_w and slope S assuming normal flow and constant Shields stress (via (1)-(4),(11)-(12)).

In channel-resolving models avulsion initiation is self-organized without explicit rules, but the emergent avulsion-initiation mechanisms can be observed unfolding in "real time", allowing insights unobtainable in any other way. In the Delft3D and EM models avulsions are initiated via crevassing, and these models essentially incorporate all the morphodynamic processes underlying crevasse-stability theory, while allowing additional subtleties to be explored (e.g. Edmonds and Slingerland, 2008; Edmonds et al., 2009). In the SAFL and MP03 models, where channels are erosionally confined, the absence of levees precludes the possibility of crevassing or superelevation. Avulsions occur in these models, but are initiated by in-channel deposition (e.g. bars) which forces the flow out of the channel (Sheets et al., 2002; Murray and Paola, 2003), a mechanism described by Makaske (2001) as loss of channel-flow capacity. In the SAFL fan-delta experiments this is typically driven by channel backfilling originating at the shoreline (e.g. NCED, DB03), i.e. the setup is due to channel-bed aggradation, but via a migrating front rather than distributed deposition as in classical superelevation (a similar process occurs in the EM delta experiments, the "morphodynamic backwater" of Hoyal and Sheets, 2009). Avulsion-initiation mechanisms in the Seybold and CAESAR models are not clear from the published descriptions, but are likely similar to those in other channel-resolving models with similar confinement mechanisms (i.e. Seybold = constructional, CAESAR = erosional, Table 2).

In several channel-belt models avulsion-initiation rules include a stochastic component, based on the idea that the closer a channel comes to an avulsion-initiation threshold, the smaller the trigger required to cause avulsion (e.g. Jones and Schumm, 1999). For example the critical slope-ratio in the MB and KB models depends on a stochastic discharge, simulating the effect of flood variability, while the DW model chooses crevassing locations randomly. Self-organized

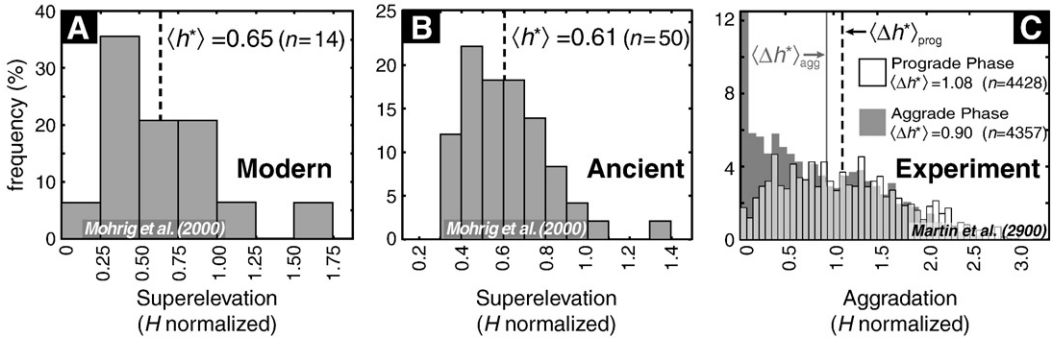

Fig. 10. Avulsion initiation rules – Superelevation. Observations from diverse systems suggest avulsions occur when a river's bed becomes superelevated O[H] above its floodplain. These include measurements of normalized superelevation in recently avulsed modern rivers (A) and ancient channels (B), as well as measurements of normalized inter-avulsion aggradation in flume experiments.

trigger-like phenomena also occur in channel-resolving models, e.g. quasi-stochastic vegetation clearing events facilitating avulsion in the MP03 model.

Once an avulsion is initiated, channel-belt models simulate the creation of daughter channels with avulsion-routing rules that effectively combine the finding and stabilization phases. While the channel-belt models of Table 2 (MB,JP,KB,DW,Sun) use different approaches to route flow through the established active channel network (Section 3.1), all essentially use steepest descent to route avulsions. Slight variations include quasi-1D routing based on cell bottom elevations in the JP model, and a stochastic random-walk component in the Sun model. Avulsive routing begins from the avulsion-initiation point in the parent channel, and extends downstream until the daughter channel either reaches the grid edge (or shoreline, e.g. Sun), a local topographic minimum (pit), or an active channel (local avulsion). The daughter channel is then added to the active channel set.

In the MB and JP models, which have a single channel, following an avulsion the parent channel is removed from the active set downstream of the avulsion point (except for local avulsions). In the other channel-belt models both the parent and daughter are retained, resulting in a bifurcation. Channel deactivation in these models occurs only when bed evolution causes a channel to locally drop below a threshold in slope S (≤ 0, Sun), velocity U (KB), or discharge Q_w (DW). In this case deactivation propagates downstream to all channel-cells whose water supply is thus cut off. The DW model includes an interesting additional twist: distributed runoff is routed through all unchannelized cells as 8-nbr dispersive sheetflow. This sheetflow does not transport any sediment, but where discharge locally exceeds a threshold a new channel is activated, essentially a hillslope sheetflow-instability channel initiation rule (cf. Montgomery and Dietrich, 1992).

In natural avulsions the transition from distributed floodplain flow in the finding phase to quasi-stable channelized flow is commonly associated with incision of order H, i.e. daughter channels begin with predominantly erosional confinement (Mohrig et al., 2000; Aslan et al., 2005; Fig. 11A). Most avulsion models do not use explicit stabilization rules, but there are a few exceptions. As noted above, within each cell the JP model tracks two elevations, where bottom = top in "virgin" floodplain cells and bottom = top − H in channelized cells (Jerolmack and Paola, 2007). Hence channelization of virgin floodplain is implicitly accompanied by incision of a channel depth. Eroded sediment is not included in the model mass balance, since it is assumed to be washload, and the JP model only applies mass balance to bed-material load (Jerolmack and Paola, 2007). Channel-resolving models have no explicit stabilization rules, but model rules do impact stabilization via effects such as self-organized confinement due to erosion of below-capacity channels (Seybold et al., 2009, Fig. 11B) or vegetation growth (Murray and Paola, 2003).

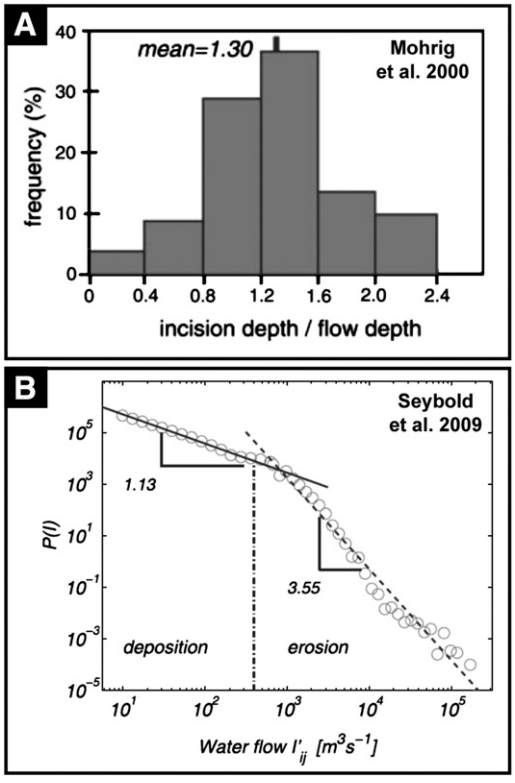

Fig. 11. Avulsion stabilization rules. Observations from ancient systems suggest that in many cases avulsion stabilization is associated with significant incision of the daughter channel into the floodplain (A). This process can simulated in channel-resolving avulsion models by incorporating cohesive-sediment erosion (B).

4. Comparing simplified avulsion models: Architecture scale predictions and unresolved questions

Taken together, simplified modeling efforts to date highlight four key questions for the next generation of model and field studies: 1) how do mass-balance effects modulate autogenic alluvial dynamics and architecture, particularly at avulsion timescales? 2) what thresholds govern avulsion in different systems? 3) how are new channel pathways established during avulsion? 4) how does floodplain sedimentation feed back into the avulsion process (and vice versa)? Answering these questions will require interdisciplinary efforts combining targeted modeling and field observations.

4.1. Mass balance at architecture scale

Mass balance, the interplay of sediment supply and accommodation, is well recognized as a first-order control on basin-scale stratigraphy. For instance mass-balance models of shoreline migration provide a simple framework for understanding the stratigraphic response to allogenic forcing such as sea level and tectonics (e.g. Jervey, 1988; Paola, 2000). However the importance of mass balance as a control on architecture-scale dynamics and stratigraphy has only recently begun to be appreciated (e.g. Strong et al., 2005; Paola et al., 2009). All architecture-resolving avulsion models in Table 2 that include at least partial mass balance (i.e. all except MB and DIONISOS) exhibit autogenic dynamics tied to intermittent sediment storage and release events within the fluvial system (e.g. Jerolmack and Paola, 2007). Whereas basin-scale factors such as subsidence create what might be termed "stable" accommodation in the subsurface, self-organized landforms on the surface produce transient accommodation. Features such as alluvial ridges represent positive, and conversely incised channels negative, perturbations to the overall accommodation defined with respect to the regional alluvial surface (e.g. the "equilibrium river profile" of Posamentier and Vail, 1988). In dynamic fluvial landscapes these landform volumes are episodically created and destroyed, commonly in association with avulsion processes. Transient storage in simplified avulsion models occurs in a variety of landforms (Table 2).

Linking accommodation to landforms may seem odd, but it is really a simple extension of the idea of using an equilibrium profile as datum for defining accommodation rather than sea level. After Muto and Steel (2000) pointed out fundamental issues with classical notions of accommodation, Kim et al. (2006b) and Wolinsky (2009) showed that to be predictive accommodation must be defined over a specified area (i.e. control volume), and must include changes in the "equilibrium profile". For example in prograding deltas maintenance of an approximately constant-slope alluvial plain requires aggradation, and in steep rivers the resulting topset sediment storage significantly impacts shoreline migration rates (Wolinsky et al., 2010b).

Mass balance strongly modulates dynamical timescales in fluvial systems. In precise terms, mass balance dictates that growth of a depositional landform with length L, width B, and height H, fed by a sediment supply Q_s, will follow

$$d(c_0 V)/dt = fQ_s \tag{20}$$

where $V = BLH$ is the net deposit volume and $f = -\Delta Q_s/Q_s$ is the net sediment capture ratio over the landform. This is essentially an Exner equation like (13), except here the control volume is not a fixed cell, but the footprint of a dynamic landform whose area $A = BL$ can evolve (e.g. a prograding delta, Wolinsky et al., 2010a, or a widening alluvial ridge). For a given landform, the time required to build up the associated deposit is

$$T \approx \frac{c_0 V}{fQ_s} \tag{21}$$

Simplified models of fluvial systems suggest this "filling time" controls timescales of response to external allogenic forcing as well as internal autogenic dynamics, including avulsion timescales (Paola et al., 2009; Reitz et al., 2010; Jerolmack and Paola, 2010, Wang et al., 2011).

For example in diffusive models of alluvial basin filling, the time for a system of length L and width B to respond to a change in boundary conditions is

$$T = \frac{L^2}{\kappa_s}, \kappa_s = \frac{K_s Q_w}{c_0 B} \tag{22a, b}$$

where κ is the fluvial diffusivity (Paola, 2000; Castelltort and Van Den Driessche, 2003). But this is simply the time to fill the sediment wedge beneath a graded alluvial plain with slope S given by (14a), i.e. (22) reduces to (21) with $H = SL$ and $f = 1$. More realistic fluvial models such as SAFL and DW suggest that the "equilibrium" alluvial-plain slope may exhibit autogenic variability associated with self-organized fluctuations in the surface wetted width, e.g. between steep sheetflow and low-slope channelized flow (Dalman and Weltje, 2008; Kim and Jerolmack, 2008). In this case the timescale of autogenic fluctuations again follows (21), but V now corresponds to the sediment wedge between the upper and lower slopes (i.e. $H = \Delta SL$).

Several lines of evidence suggest that the avulsion recurrence interval, T, is approximately the time to fill a channel, given by (21) with $B = B$ and $H = H$. This is broadly consistent with observations of O[H] superelevation and aggradation in modern, ancient, and experimental fluvial systems (Section 3.2.5, Fig. 10). Moreover, in noncohesive experiments similar to SAFL, Reitz et al. (2010) found that the channel-filling time predicted nodal avulsion periods quite well, even as the fan radius L grew during progradation. Finally, the prediction that T scales with time to fill a channel-sized volume with sediment is consistent with diverse avulsion-setup mechanisms, including both superelevation and backfilling.

4.2. Avulsion thresholds

Modeling and field studies over the last 30 years have found no consensus on the necessary and sufficient conditions for avulsion, and there is even significant disagreement on the appropriate definition of "avulsion threshold". From one perspective, arising from a civil engineering approach, "avulsion threshold" refers to the conditions under which a bifurcation or crevasse channel is stable over years to decades (e.g. Slingerland and Smith, 1998, 2004). Alternatively, in studies with a more geological emphasis, "avulsion threshold" commonly refers to the conditions that cause long-lived regional avulsions at landscape/architecture scale (e.g. Aslan et al., 2005; Jerolmack and Mohrig, 2007). While both are commonly referred to as "avulsion thresholds", the former is really a threshold for local avulsion initiation, while the latter is a threshold for a successful full regional avulsion, i.e. an avulsion which proceeds from initiation through stabilization, and where the parent channel is abandoned downstream of the avulsion point. Initiation is a necessary but not sufficient condition for avulsion in this second sense, since full avulsion also depends on regional factors influencing avulsion flowpath selection and stabilization that are relatively independent of the local conditions around a bifurcation. However imprecise language has added to confusion about the causes of avulsion in different systems and the implications for avulsion thresholds (e.g. Aslan et al., 2006; Törnqvist and Bridge, 2006).

For alluvial-architecture modeling, crevassing and bifurcation-stability thresholds are likely important for understanding intra-channel-belt processes and deposits (i.e. channel-belt, splay, and levee deposits). In contrast, formation-scale arrangements of channel-belt deposits are arguably more affected by thresholds that determine when large-scale avulsions are likely to occur–more specifically, those in which the daughter channel relocates far enough away from the parent channel that channel-belt sand bodies are separated from one another by substantial floodplain accumulations (e.g. those studied by Mohrig et al., 2000 and modeled by Jerolmack and Paola, 2007).

Field data and theory have demonstrated that both cross-valley-slope advantage and bed superelevation are reasonable proxies for channel avulsion thresholds in some systems, but neither fully explains avulsion initiation conditions for all rivers (e.g. Aslan et al., 2005; Aslan and Blum 1999; Jerolmack and Mohrig, 2007; Mohrig et al., 2000; Phillips, 2011; Tooth et al., 2007; Törnqvist and Bridge, 2002). These studies indicate that certain systems may be more sensitive to superelevation and others slope ratio (Törnqvist and Bridge, 2002). Down-channel vs. cross-channel gradient is explicitly a local measurement whereas superelevation is implicitly regional. In erosionally confined systems (those which do not produce levees; SAFL, MP, CEASAR, and dryland systems e.g. Makaske, 2001), avulsion is spurred by in-channel aggradation where bars or upstream-propagating depositional waves choke channels and divert flow out onto

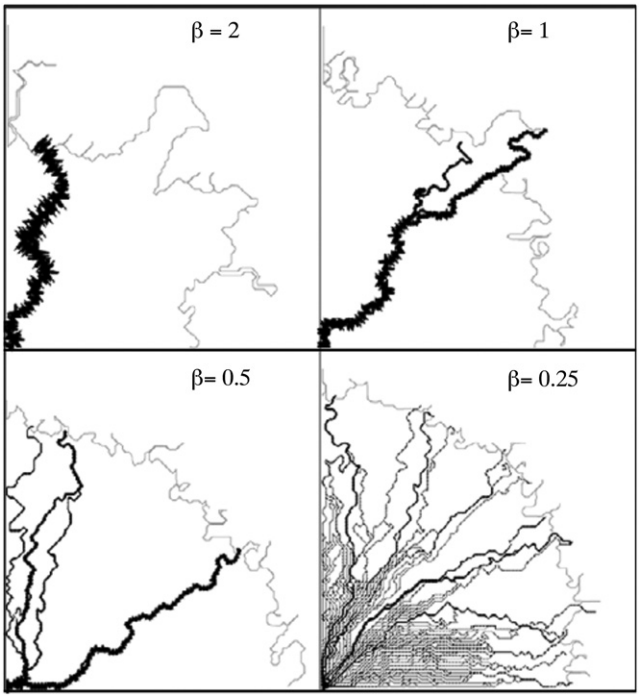

Fig. 12. Avulsion Thresholds – Implications. Avulsion thresholds strongly affect channel dynamics and planform morphology, as illustrated by simulations of the Sun fan-delta model. As the normalized superelevation threshold h_c/H (β) decreases, avulsions occur more frequently, causing an increase in the number of co-existing active channels (arrows, width $\propto B$), and a smoother shoreline (thin shaded line). (Adapted from Sun et al., 2002.).

the floodplain. In contrast to upstream or local thresholds for bifurcation stability (including cross-valley slope or local superelevation) avulsion within these model systems (SAFL, MP, CEASAR) is initiated downstream by a "morphodynamic backwater" effect. It is unclear how and to what degree far-field and local effects influence avulsion thresholds in different systems.

Sun et al. (2002) clearly show how different avulsion-initiation thresholds can significantly impact channel avulsion and, implicitly, stratigraphic architecture (Fig. 12). The lower the relative channel: floodplain aggradation needed for avulsion, the more frequently channels avulse. Furthermore, when avulsion thresholds are low, there is a tendency for more active channels across the alluvial plain or delta at any given time (e.g. Sun et al., 2002; Murray and Paola, 2003; Jerolmack and Mohrig, 2007; Karssenberg and Bridge, 2008; Reitz et al., 2010). This impacts topographic development across the alluvial plain (more avulsions lead to a rougher surface) as well as shoreline morphology in deltaic settings (fewer avulsions lead to more rugose shorelines; e.g. Edmonds and Slingerland, 2010; Wolinsky et al., 2010a, 2010b). Several important variables that may influence avulsion thresholds, including backwater effects, grain size, abundance of cohesive sediments, differences between progradational and aggradational systems, and the role of channel incision need to be further explored to constrain avulsion thresholds in different systems.

4.3. Channel flow-path selection

Once an avulsion is initiated we do not know how to predict where the new channel will go or how sediment and water will be distributed as the new channel finds a stable path. Intuitively, over long timescales, channels will be attracted to low spots across a basin; this type of compensational filling is well known in channelized systems (e.g. Straub et al., 2009). However, field data, experiments, and modeling also show that channel avulsions sometimes preferentially return to locations that were previously occupied and abandoned (Mohrig et al., 2000; Jerolmack and Paola, 2007; Stouthamer and Berendsen, 2001; Stouthamer, 2005; Sheets et al., 2007; Hajek et al., 2010; Reitz et al., 2010). Under what circumstances do channels avulse compensationally, reoccupy pre-existing flow paths, or move to random positions on the floodplain?

Heller and Paola (1996) posit that channel avulsions will commonly be rerouted back to the parent channel, particularly in tributary systems where a new flow path is likely to intersect a pre-existing tributary channel. In some cases channel reoccupation may be a stable avulsion channel configuration (e.g. Mohrig et al., 2000), or, as in the case of the 2008 Kosi River flood (Sinha, 2009; Chakraborty et al., 2010), it may be a temporary stopover during the finding phase of avulsion. Jerolmack and Paola (2007) show how topography from channel scars, for example, can "attract" channels back to certain locations over and over again leading to stratigraphic channel-belt clustering. Because of the way the JP model records channel elevations, abandoned cells tend to be regional minima, analogous to abandoned channels that become oxbow lakes. In contrast the MB model assigns alluvial-ridge height to abandoned channel cells, which means old channels tend to "repel" subsequent avulsion channels, thus encouraging compensational basin filling. As both possibilities are plausible, more work is needed to determine when alluvial ridges act to "protect" channel lows from further reoccupation.

In addition to floodplain topography, floodplain roughness may influence flow routing, particularly when the type and density of vegetation is spatially variable across alluvial plains. Furthermore, the distance that proximal-overbank deposits (e.g. levees, crevasse splays) extend away from channels may affect topographic and surface-cover roughness where there are distinct breaks between coarse-grained deposits and fine-grained overbank accumulations (e.g. Törnqvist and Bridge, 2002). Variations in substrate erodibility may also create favorable pathways for channel location. For example, reoccupation of abandoned channel locations may be more common if sandy deposits are more readily eroded than cohesive overbank mudstones (e.g. Aslan et al., 2005). Controls on temporal and spatial scales of floodplain heterogeneity are poorly understood and difficult to predict. More work is needed to weigh the relative influence of floodplain topography and various types of surface roughness on avulsion-flowpath selection.

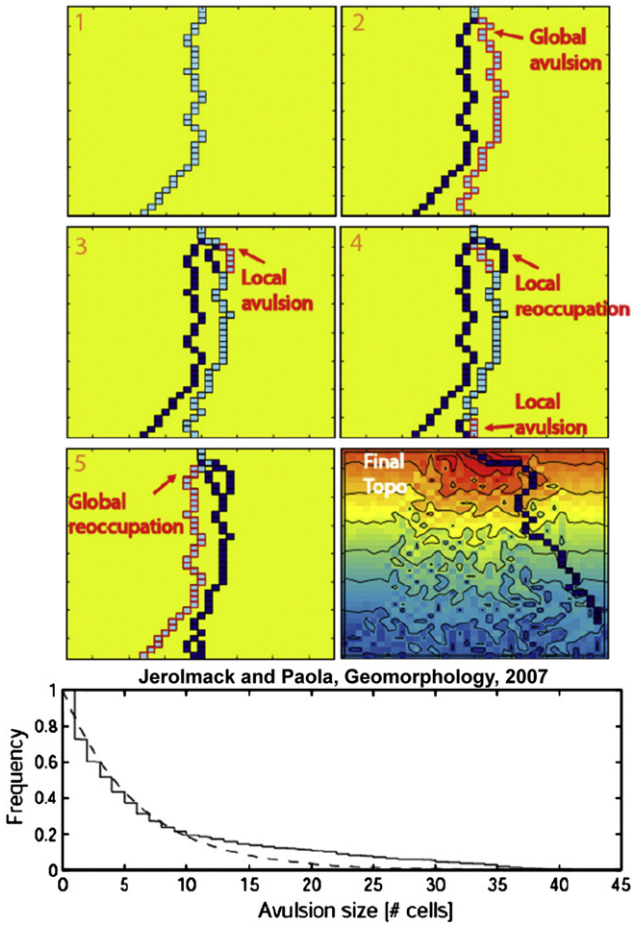

Fig. 13. Flowpath selection & avulsion lengthscales – Model results. Simulations of the JP model illustrate styles of avulsion flowpath selection (color panels) and the resulting distribution of avulsive-channel lengthscales (lower panel). Note continuous distribution of avulsion sizes across a wide range of scales (from a single cell up to the length of the model domain). Active channel path shown in light blue, avulsion flowpath outlined in red. (Adapted from Jerolmack and Paola, 2007).

Channel flowpath selection can affect the distribution of avulsion sizes in a system. Jerolmack and Paola (2007) show avulsions that range from small local avulsions to global (regional) avulsions during which the channel relocates along the entire length of the model domain (Fig. 13). Jerolmack and Swenson (2007) use backwater length to constrain the length scale of the largest avulsions in deltaic systems (i.e. regional or nodal avulsions). Their data also show a broad spectrum of channel length (avulsion) sizes (Fig. 14). The range of avulsion length scales indicates that topographic "memory" or inertia (sensu Reitz et al., 2010) strongly influences avulsion flow-path selection. This is a marked contrast with the (lateral) length scales of channel-associated landforms such as channel belts and levees/alluvial ridges, which appear to be more strongly determined by local morphodynamics (Figs. 5, 6), and are less influenced by regional topography.

For basin-scale alluvial architecture studies the specifics of how channel stabilization occurs is probably less important than predicting statistically where channels will ultimately stabilize. However, some field and modeling studies may need to consider the processes by which a channel finds and moves to its new, stable location. In general the role of the finding phase in avulsion remains poorly

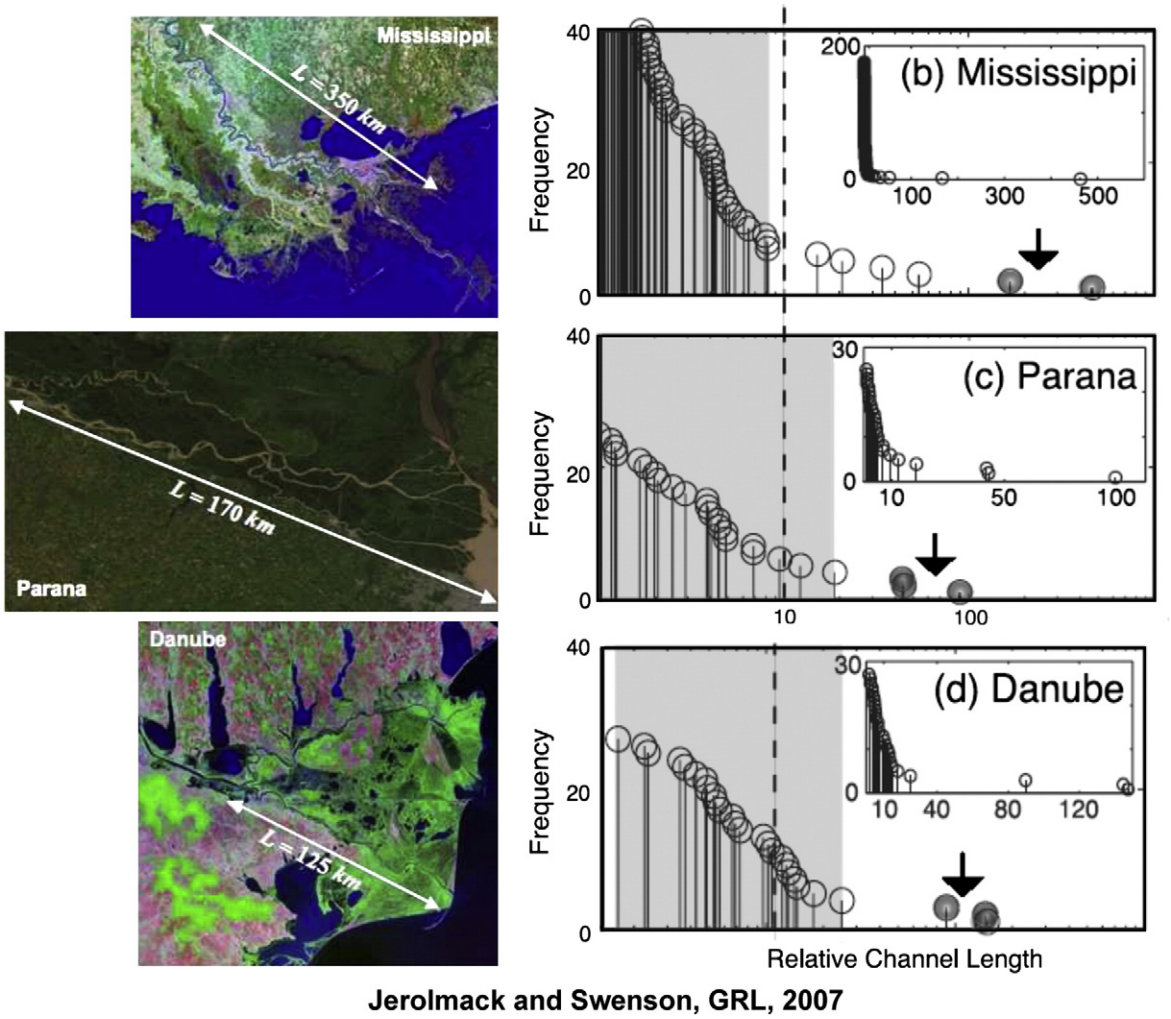

Fig. 14. Flowpath selection & avulsion lengthscales – Natural systems. Natural avulsion-influenced fluvial systems such as deltas exhibit a wide range channel lengths. Left Column: Satellite imagery of river-dominated delta distributary networks. Arrows extending from nodal avulsion point to shoreline indicate backwater length L_w. Right Column: Corresponding distributions of relative channel-length show a wide range of avulsive-channel lengths, extending from the scale of mouth-bar-driven bifurcations (dashed vertical lines) up to the backwater length (arrows, corresponding to nodal avulsion). (Adapted from Jerolmack and Swenson, 2007).

understood. Once an avulsion threshold is attained, sediment and water are redistributed across the floodplain. In the simplest cases, flow will quickly divert into and form a new stable channel (e.g. Tooth et al., 2007). In other cases, large volumes of sediment are deposited across the floodplain during a protracted finding phase (e.g. Perez-Arlucea and Smith, 1999; Aslan and Blum, 1999). Evidence from ancient deposits suggests that some systems tend to deposit significant quantities of fine sediment during the finding phase prior to avulsion (e.g. Kraus and Wells, 1999) whereas others do not (Fig. 15; Jones and Hajek, 2007). These differences may reflect systems prone to "aggradational" or "incisional" avulsions (c.f. Slingerland and Smith, 2004), respectively.

4.4. Floodplain sedimentation

Until very recently, floodplain sedimentation has been largely ignored and treated very simplistically. Most of the models discussed here use simple exponential decay to model floodplain aggradation. While this may be appropriate for some systems, the rate at which floodplain sedimentation decreases away from channels varies strongly between systems (e.g. Swanson et al., 2008, section 3.2.4 and Figs. 6A, 8A). This variation may be due in part to differences in flooding style along the continuum between "wide and dry" vs. "narrow and wet" floodplains (Fig. 8B,C), associated with relatively efficient advective sediment dispersal away from the channel vs. weaker diffusive transport.

Even in systems where floodplain-sedimentation rates generally decrease away from active channel belts, dynamic floodplain processes and vegetation can modify floodplain roughness and topography, generating spatially heterogeneous deposition patterns. Poorly constrained processes associated with floodplain lakes, tie channels, and bioturbation also sculpt floodplains in some basins (e.g. Tooth et al., 2007; Aalto et al., 2008; Day et al., 2008). Most avulsion models include the reasonable assumption that avulsion is most affected by longer-term floodplain aggradation rates (e.g. Sadler, 1981). However, if avulsion behavior is sensitive to floodplain topography, surface roughness, and substrate composition, event-scale overbank conditions might matter as much or more than long-term aggradation rates.

Jerolmack and Paola (2007) elegantly demonstrate the potential effects different floodplain-sedimentation models may have on channel avulsion and alluvial architecture. Depth-dependent and uniform overbank sedimentation rules in the JP model dramatically changed stratigraphic sand-body distributions primarily because floodplain topography was either filled in (depth-dependent) or preserved (uniform) (Fig. 16). Reitz et al. (2010) also showed how "floodplain annealing" of relict channels has important consequences for where channels avulse and relocate. Additionally, the Karssenberg and Bridge (2008) model includes floodplain erosion and highlights the

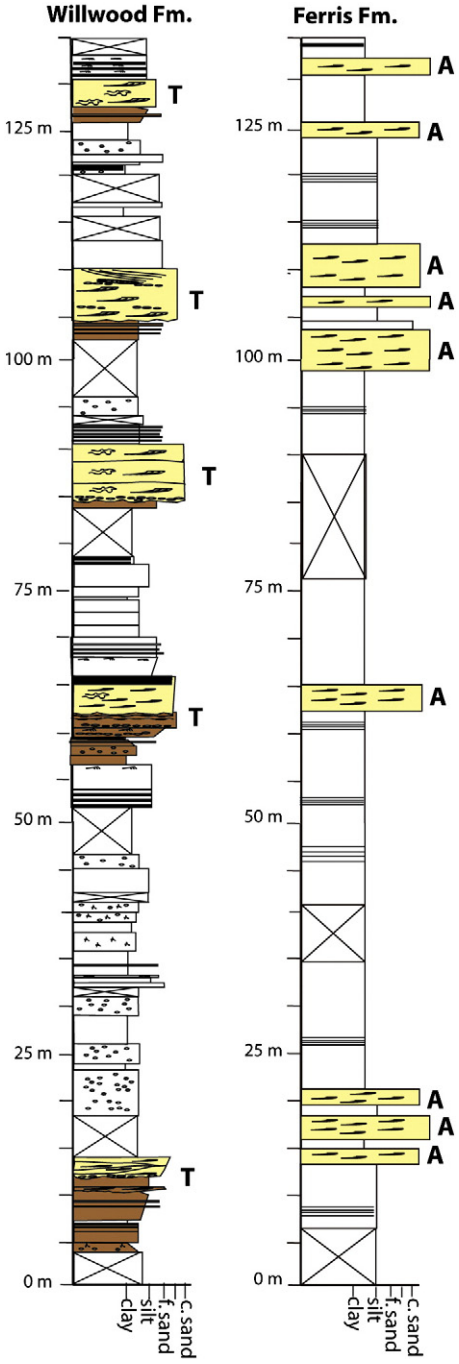

Fig. 15. Flowpath selection & floodplain sedimentation – Stratigraphic records of avulsion deposits. Representative stratigraphic sections from the Willwood and Ferris formations (from Jones and Hajek, 2007). Paleochannels are yellow, heterolithic avulsion deposits are brown, and overbank floodplain mudstones are white. The Willwood Formation is dominated by transitional avulsion stratigraphy (T) and stratigraphically abrupt avulsion deposits (A) dominate the Ferris Formation. Transitional and stratigraphically abrupt avulsion deposits are interpreted as being associated with progradational and incisional avulsions, respectively.

potential influence of local incision and aggradation near bifurcation points and across the floodplain. Beyond these exploratory studies, the extent to which floodplain conditions influence avulsion and alluvial architecture is virtually unconstrained at present.

5. Connecting models to ancient data

Addressing outstanding questions and testing predictions from avulsion models will require targeted, coupled field and modeling efforts. Although not as precisely quantifiable as modern processes or shallow stratigraphy, deposits in the rock record include a broader range of systems (boundary conditions) and offer hundreds of individual paleoavulsions preserved within a given formation. Consequently ancient deposits provide important opportunities for hypothesis testing. Extracting quantitative data from the sedimentary record can be a challenge, and it can be particularly difficult to evaluate the "fit" between simplified process models and data (e.g. Murray, 2003; Bridge, 2008). Fortunately, dimensionless comparisons of model trends and statistical characterizations of alluvial architecture can be used test model predictions in natural basins. Additionally, "paleomorphodynamic" measurements can help determine appropriate model inputs and indicate which models are most suitable for exploring a particular ancient system. Here we review these methods and propose strategies for comparing stratigraphic data to models. Some of these techniques are well established while others are still developing.

5.1. Paleomorphodynamics

As outlined in Section 3.2, morphodynamics provides the process foundation for avulsion models. Alluvial basins contain fossilized information about sedimentary processes in ancient depositional systems, and the resulting landform geometries and landscape evolution, which can be quantitatively constrained by simple measurements in outcrop, core, and well logs. Such paleomorphodynamic data provide a means of estimating model input parameters and appropriately pairing models and field sites. Here we discuss opportunities for measuring channel, floodplain, and avulsion-threshold paleomorphodyamic proxies in the stratigraphic record.

5.1.1. Channel and channel-belt measurements

A substantial amount of information about paleochannel hydraulic geometry can be gleaned from ancient fluvial deposits. Estimates of bankfull paleoflow depth, H, are relatively easy to obtain and can be used as a basis for several paleomorphodynamic calculations (Appendix A). The thickness of fully preserved bar clinoforms (those which show up-dip rollover; see Mohrig et al., 2000), and abandoned channel fills such as mud plugs, are the most reliable approximations of local maximum paleo channel depth (Figs. 17 and 20). Partially preserved or truncated bar clinoforms can provide a lower bound for maximum paleoflow depth, although care should be taken when interpreting and comparing such values because of greater uncertainty associated with these measurements. Paleoflow depth can also be constrained with the thickness of fining-upward packages, identifiable in cores or well logs (e.g. Bridge and Tye, 2000) as well as outcrops in which surface weathering precludes identification of bar clinoforms (Fig. 17). Because dune height scales with flow depth, paleoflow-depth estimates can also be made from the thickness of preserved cross-bed sets (Paola and Borgman, 1991; Leclair and Bridge, 2001); however, the scaling relationship is highly variable (Leclair, 2011). Consequently such paleoflow-depth estimates are more difficult to interpret than those from bar and channel-scale features, and direct comparison to model results is more uncertain.

When combined with proxy bed-material-load samples, readily obtained from trough-cross-bedded channel sandstones, paleoflow-depth estimates H and median bed-material grain size d_{50} can provide insights into paleomorphodynamic characteristics of ancient river systems. For example first-order estimates of paleoslope (e.g. Paola and Mohrig, 1996) can be calculated from relative roughness d/H by combining Eqs. (3) and (12) to give

$$S \approx R\tau^{*}(d/H) \tag{23}$$

Even using the relatively crude approximation of piecewise-constant Shields stress τ^{*} in sand- vs. gravel-bed streams (Fig. 4B), this approach provides surprisingly accurate constraints on paleoslope (Fig. 18). In

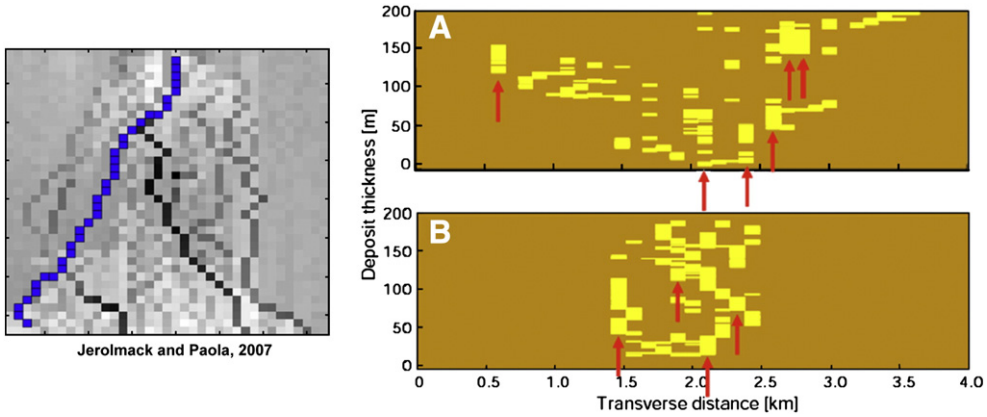

Fig. 16. Floodplain sedimentation – architecture implications. The spatial distribution of floodplain sedimentation can significantly impact avulsion flowpath selection and alluvial architecture, as illustrated by the JP model. Left: Spatially uniform sedimentation preserves floodplain topography (grayscale, black = low, white = high), including relict channels which can act as attractors for avulsions. Active channel shown in blue. Right: The alluvial architecture resulting from different floodplain sedimentation rules shows marked differences in lateral dispersion of channel-belt sandbodies (yellow) within the floodplain "matrix" (brown), and reoccupation (red arrows). Upper Panel: Uniform sedimentation. Lower Panel: Depth-dependent sedimentation. (Adapted from Jerolmack and Paola, 2007).

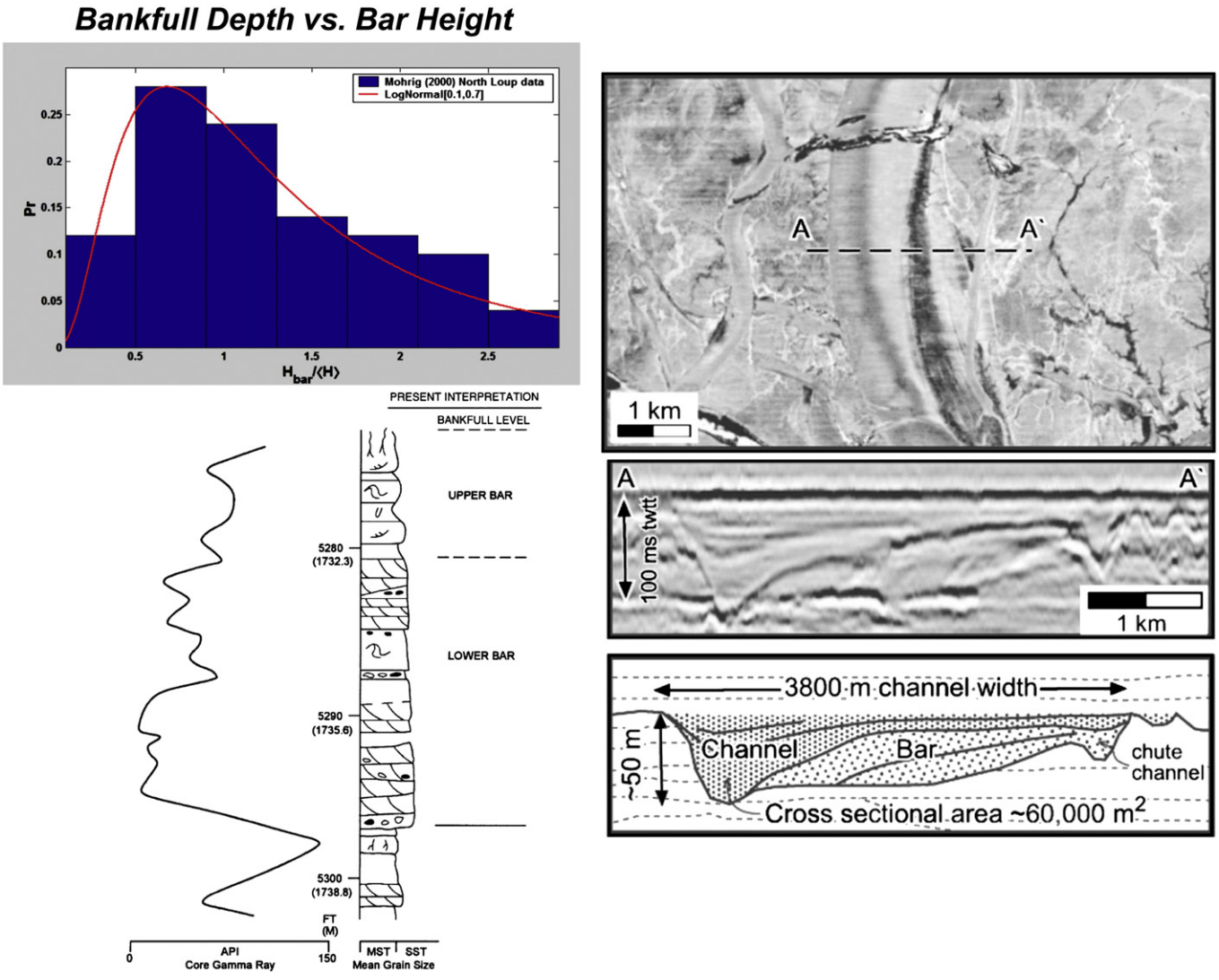

Fig. 17. Paleomorphodynamics – Flow depth and grain size. Upper left: Histogram showing measured local bar height relative to reach-averaged bankfull flow depth in a modern river (after Mohrig et al., 2000). Lower left: Figure from Bridge and Tye (2000) showing fining upward successions (identifiable in wireline logs, core, or outcrop) that can be used to estimate paleoflow depth. Right: Seismic image of a fluvial channel deposit where both channel width and depth can be estimated (from Darmadi et al., 2007).

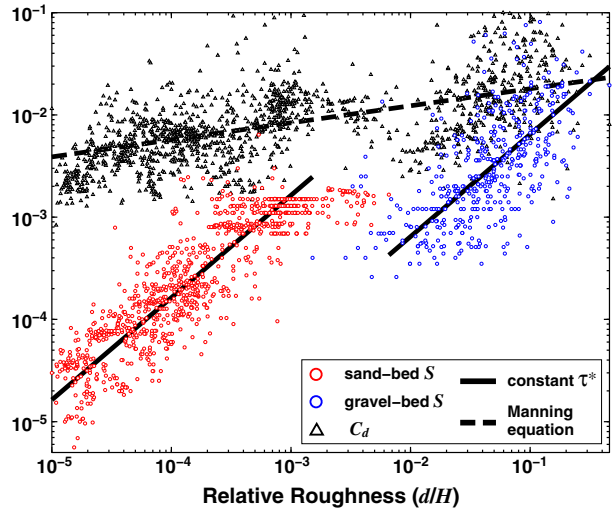

Fig. 18. Paleomorphodynamics – Slope and drag. Estimates of flow depth H and bed-material grain size d_{50} from ancient deposits allow prediction of slope S and drag C_d based on relative roughness d/H. Points are alluvial rivers from modern reach morphodynamics database. Solid lines are slope predictions for gravel- and sand-bed rivers based on Eq. (23) using constant τ^* (black lines in Fig. 4B). Dashed line is best-fit of Manning-style drag relation $C_d \sim (d/H)^{1/6}$ (e.g. Parker, E-book Ch5).

similar fashion, estimates of flow depth and bed-material grain size can yield quantitative constraints on flow velocity and shear stress, bed-material transport mode, backwater effects, and even channel-belt and overbank deposition length scales, via a relatively rigorous "paleomorphodynamics workflow" (Appendix A).

Paleochannel-bankfull width B can be measured from fine-grained abandoned channel fills in outcrop and estimated from cross-sections

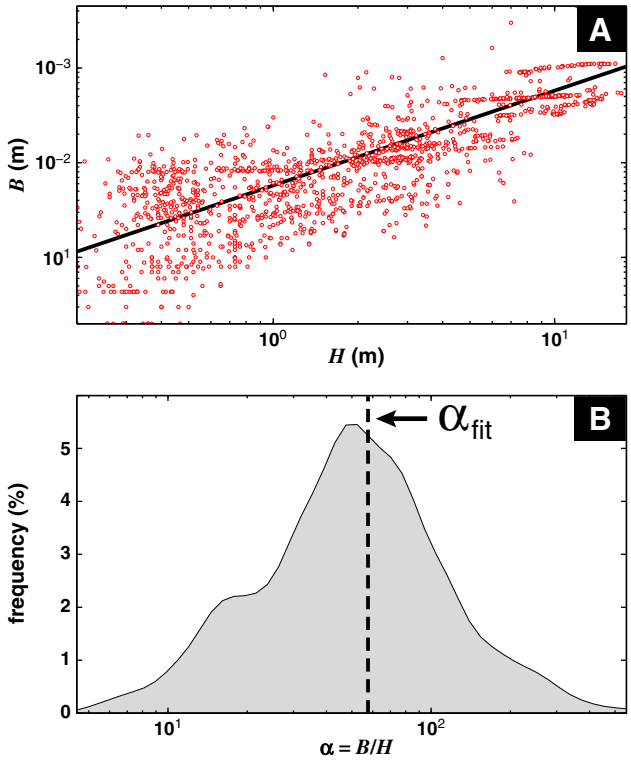

Fig. 19. Paleomorphodynamics – bankfull width. Constraints on bankfull width in modern rivers based on reach database. A) Bankfull width B is correlated to cross-section average bankfull flow depth H. Predictions based on a constant aspect ratio α ($\approx$ 57, black line) provide crude constraints on width for a given flow depth. B) However depth cannot precisely determine width, as there is significant variability in channel x-section aspect ratios.

or horizons in hi-res 3D seismic surveys (e.g. Darmadi et al., 2007; Fig. 17). Although width cannot be directly measured from 1D well data, some constraints on width can be inferred from paleoflow depth measurements using aspect ratios from analogue data (Fig. 19). When available, paleochannel-width measurements also enable estimation of paleochannel sediment and water discharge (Appendix A; see also Davidson and Hartley, 2010), although the uncertainty of these methods remains unquantified. Because it is impossible to discern the number of concurrently active channels for a given time interval in ancient deposits, paleodischarge information should not be over interpreted, particularly with respect to paleoclimate inferences. Proxy estimates of paleochannel dimensions are imprecise, and the paleomorphodynamic relationships presented here are crude, so these approaches are not suitable for detailed comparisons or predictions within ancient deposits. Nonetheless paleomorphodynamic estimates are a valuable tool for discriminating between different types of systems and for constraining model input parameters.

5.1.2. Floodplain observations

As discussed in Section 4.4, floodplain aggradation patterns and the influence of floodplains on avulsion flow-path selection and stabilization are relatively poorly understood. Ancient floodplain deposits record paleo-landscape conditions including floodplain drainage, vegetation, topography, relative overbank-sedimentation rates and styles, and basin temperature and precipitation patterns (e.g. Willis and Beherensmeyer, 1994; Zaleha, 1997; Kraus, 1999; Wright et al., 2000; Retallack, 2001; Wing et al., 2005). While much of this information is difficult to quantify, relative differences within and between systems can be detected through careful study of mudstone sedimentology and paleosol development. For example, the lateral distribution of paleosol development away from channel margins indicates how sedimentation rates vary as a function of distance from channel margins (where higher sedimentation rates are associated with weaker paleosol development; e.g. Bown and Kraus, 1987; Kraus, 1987; Willis and Beherensmeyer, 1994; Zaleha, 1997; Fig. 20). Additionally, lateral changes in floodplain/paleosol character (e.g. Wright et al., 2000) and erosionally truncated paleosol horizons (e.g. Kraus and Middleton, 1987; Kraus and Davies-Vollum, 2004) can be used to characterize paleo-floodplain topography and incision.

Kraus (1996) also differentiates avulsion-related-floodplain deposits from overbank-flooding deposits in the Willwood Formation (Paleocene/Eocene, Bighorn Basin, Wyoming, USA). These differences can be seen in other successions, including the Wasatch Formation (early Paleogene, Piceance Creek Basin, Colorado, USA; Fig. 20). This distinction is helpful for identifying sedimentation patterns associated with progradational-style avulsions. In contrast, the Ferris Formation (Cretaceous/Paleogene, Hanna Basin Wyoming, USA) lacks avulsion-specific deposits (Jones and Hajek, 2007) and instead comprises dominantly overbank mudstones. Better characterization of paleosol and floodplain variability in a wider array of ancient systems will help constrain floodplain-sedimentation patterns over architecture to basin scales.

5.1.3. Avulsion thresholds

Preserved channel-levee deposits record post-avulsion landform configurations and provide an opportunity to collect avulsion-threshold data that is difficult to obtain from extant systems in which avulsion is still ongoing, or occurred so recently that the long-term stability of the avulsion cannot be determined. Paleoslope-ratio measurements (e.g. Stouthamer and Berendsen, 2001) are useful, but require highly constrained elevation measurements from exceptional exposures or subsurface data. Mohrig et al. (2000) provide a basis for collecting superelevation data from ancient deposits (e.g. Fig. 21), and other observations may elucidate additional aspects of avulsion thresholds (e.g. Gibling et al., 2010, estimate channel-blockage ratios associated with avulsion-initiating log jams in Pennsylvanian deposits). These types of measurements need to be repeated in more ancient systems

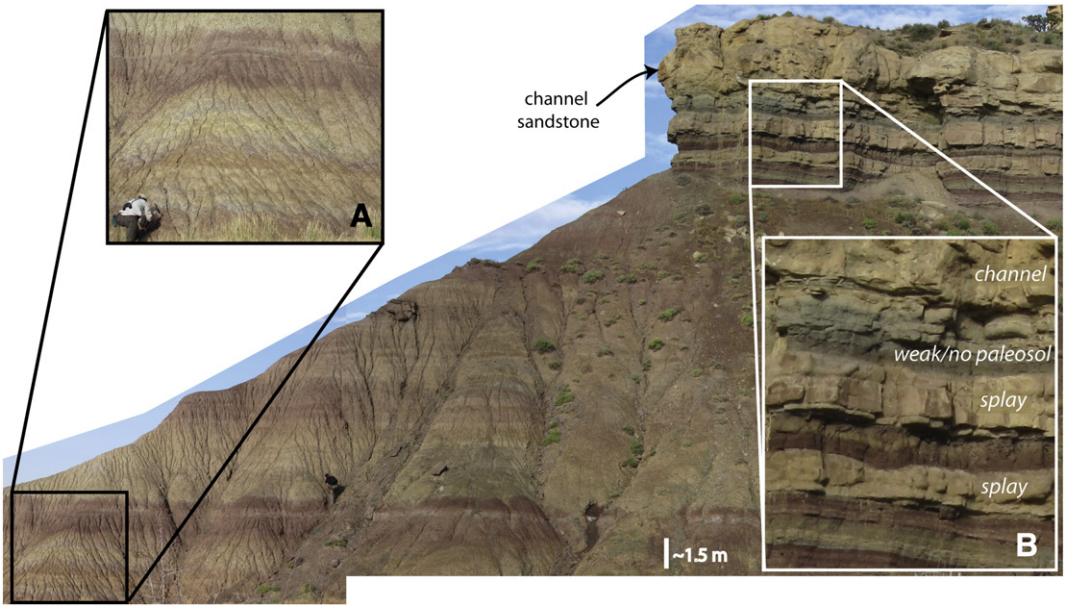

Fig. 20. Paleomorphodynamics – Floodplain observations. Example of floodplain and avulsion deposits in the Wasatch Formation (Paleocene/Eocene, Piceance Creek Basin, CO). This mudstone-dominated succession, capped by a channel-belt sandstone, exhibits distinct color banding resulting from paleosol development. Grain size is dominantly clay with minor amounts of silt. In this interval dark reds tend to be well-developed paleosols (i.e. they exhibit many pronounced pedogenic features), whereas tan intervals generally show only moderate pedogenic modification. Differences between moderate and strong paleosol development may be attributed to changes in sedimentation rate, where soil development is strongest in zones with the lowest sedimentation rates (e.g. Bown and Kraus, 1987). Mapping changes in paleosol character along individual horizons and across a basin can reveal spatial trends in sedimentation rate away from channel margins and overall basin accumulation patterns, respectively. Inset A: Closer view of paleosol color banding; color bands reflect horizons within individual soil profiles and overlapping or amalgamated soil profiles resulting from long timescale floodplain aggradation. Inset B: Just below the channel-belt sandstone, floodplain-deposit character changes; two substantial crevasse-splay sandstones stratigraphically precede the channel and the mudstone deposit just below the channel changes to gray. The gray mudstone has higher silt content and shows virtually no pedogenic modification, indicating that it was deposited relatively rapidly and was buried by the avulsed channel before a soil could develop. This pattern (increasing sedimentation rate, coarsening-upward, and abundant crevasse-splay deposits) is consistent with avulsion deposits formed during progradational avulsion (e.g. Kraus and Wells, 1999).

to further explore variability in avulsion thresholds. Additionally, multistory sandstones, particularly those with overbank deposits preserved between stories, indicate abandonment and reoccupation (e.g. Mohrig et al., 2000; Makaske et al., 2002; Aslan et al., 2005; Stouthamer, 2005). Determining the frequency of reoccupation after a significant period of abandonment may provide constraints on avulsion thresholds and characteristic flowpath selection over basin-filling timescales.

Jerolmack and Mohrig (2007) showed that the relative rate of channel lateral migration vs. superelevation, reflected in a dimensionless "mobility number", strongly influences avulsion behavior and planview channel-network style (and by implication, resulting alluvial architecture) in Holocene fluvial systems. In ancient channel-belt deposits, complementary estimates of channel lateral migration and superelevation (i.e. channel-trajectory slope, Sylvester et al., 2011) may prove to be similarly informative. While planview outcrop exposures or shallow seismic data may directly show channel migration, features such as bar-clinoform continuity or story asymmetry (c.f. Gibling, 2006) may indirectly reflect lateral mobility (where laterally persistent clinoforms and highly asymmetric stories indicate forced bar migration in meandering systems). Relative vertical aggradation can also be determined from story fills using the ratio of lateral to vertical migration of successive bar accretion surfaces (aggradation index of Gibling, 2006). The degree to which individual story fills are preserved in multistory sand bodies can also provide qualitative estimates of paleochannel mobility relative to channel aggradation (Gibling, 2006; Lynds and Hajek, 2006). Collectively these observations may allow a relative mobility number to be estimated in ancient systems.

5.2. Architecture-scale comparisons

Architecture scale ranges from stacking style within individual channel-belt sand bodies to basin-scale stacking of tens to hundreds of sand bodies. Channel-belt internal architecture reflects channel-belt migration processes and avulsion reoccupations. Understanding processes at this scale necessitates channel-resolving models that include dynamics such as channel widening and meandering. Simplified avulsion and architecture models are particularly adept at providing insight into basin-scale stacking patterns that result from the combination of autogenic avulsion dynamics, basin subsidence and sediment supply. Determining the degree to which fluvial systems fill basins randomly or with characteristic structure provides insight into avulsion processes, particularly channel flow-path selection, and statistical characterization of basin-scale stratigraphy can be used to test model hypotheses related to controls on alluvial architecture.

Given the diversity of ancient fluvial successions, it is not difficult to find Holocene or ancient examples that are qualitatively consistent with a given model result. However, quantitative comparisons between field and model results are needed to rigorously test and validate model predictions. Statistical methods for characterizing stratigraphic stacking patterns provide opportunities to pose hypotheses from modeling studies in a manner that can be explored in a wide variety of alluvial successions, even those lacking high-resolution chronostratigraphy.

Hajek et al. (2010) provide an example of how statistical methods can be used to determine the degree to which paleoavulsions were organized or random. Spatial-point-process statistics are used to ascertain whether the distribution of points or objects within a study area is random or organized (Cressie, 1993; Diggle, 2003), and some statistics, including the K function employed by Hajek et al., help determine whether spatial patterns are clustered or evenly spaced at different scales. Fig. 22 (A-D) shows examples of K function curves for hypothetical datasets. Such quantitative measures are essential for discriminating between apparent organization formed by happenstance and statistically significant organization resulting from structured behavior in pattern-forming (e.g. depositional) processes. The K function reveals that channel body distributions in an autogenic physical experiment and a well-exposed fluvial outcrop are nonrandom (Fig. 22). The experimental deposit was generated with

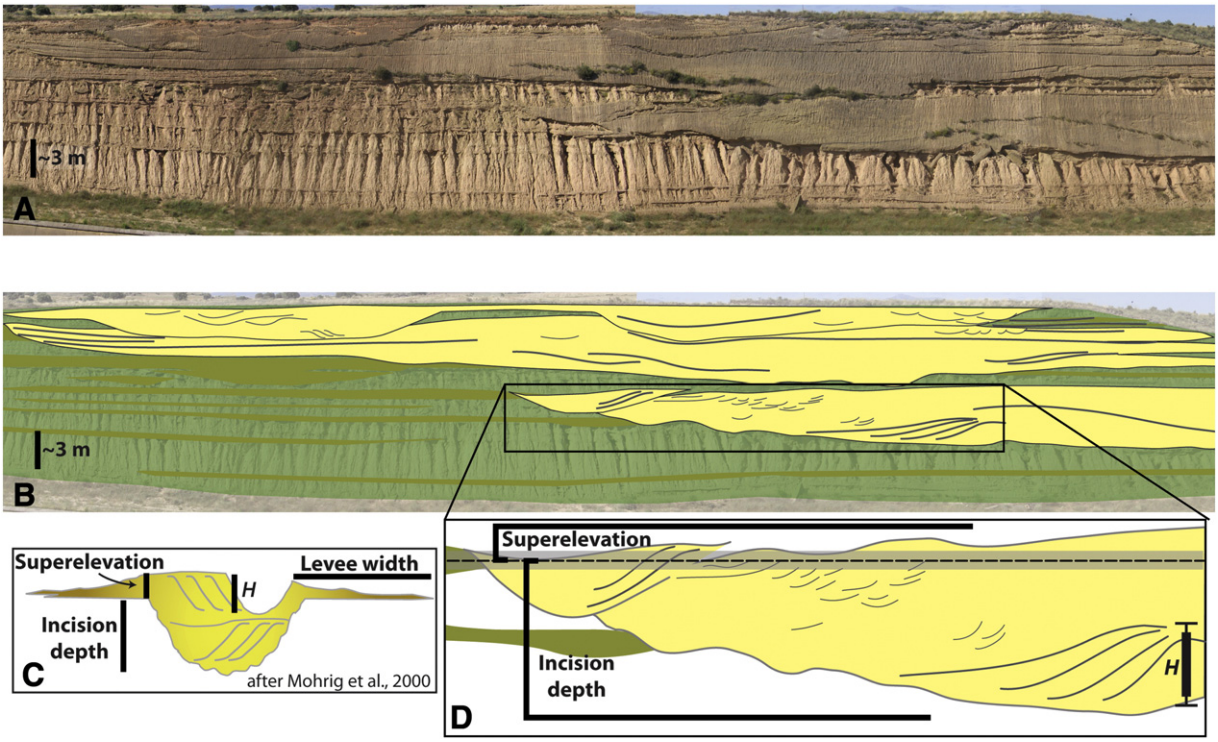

Fig. 21. Paleomorphodynamics – Avulsion thresholds. Example paleomorphodynamic measurements from the Huesca fluvial fan (Miocene, Ebro Basin, Spain; see also Donselaar and Overeem (2008) for another interpreted panel of this outcrop). A: Outcrop photo. B: Panel interpreting major facies and stratigraphic features in A. Yellow = channel-belt sandstone deposits, dark green = proximal overank (e.g. levee and crevasse-splay) deposits, light green = fine-grained floodplain deposits. Heavy lines in channel sandstones indicate major features such as bar clinoform surfaces, scours, or story breaks, and thin lines highlight dune-scale crossbeds. C: Schematic diagram showing the paleomordynamic measurements made by Mohrig et al. (2000), and also levee width. D: Vertically exaggerated example of paleomorphodynamic measurements from panel B, including paleoflow-depth estimate (*H*) from bar clinoforms showing up-dip rollover (indicating full preservation). Superelevation and scour depth are measured from a "distal" floodplain elevation estimated by horizontally projecting the upper-most splay deposit associated with the channel-belt sandstone. Whiskers around paleoflow depth scale and shading around the projected distal floodplain elevation emphasize that there is some degree of uncertainty associated with interpreting and measuring these features in ancient deposits.

a non-cohesive sediment mixture, but nonetheless exhibits spatial organization derived entirely from autogenic channel migration processes (Sheets et al., 2007). (Note that although the K function curve only barely exceeds the random envelope from Monte Carlo simulations, the definition of "random" in this test is relatively strong: significance level of 0.02 for 99 simulations.) The ancient deposit shows stronger spatial patterning where channel-belt sandstones are clustered throughout the basin. Hajek et al. suggest this organization could arise from autogenic avulsion behavior similar to that observed in Jerolmack and Paola (2007).

Straub et al. (2009) quantify stratigraphic architecture with the "compensation index" which determines the degree to which depositional events accumulate randomly or compensationally within a basin. Similar to the K function the compensation index can be used to quantify random, compensational (even), or persistent (~clustered) stratigraphy. Unlike the K function, which utilizes the spatial distribution of sand bodies within a basin, the compensation index is calculated based on chronostratigraphic surfaces and is consequently amenable to reflection seismic datasets. The compensation index is a measure of the standard deviation between two horizons relative to mean basin aggradation rates (Fig. 23). If a basin fills evenly (i.e. each depositional event fills a topographic low over some characteristic timescale), the standard deviation of actual basin topography relative to mean aggradation rate will be low, and the compensation index close to one. Conversely, if depositional events tend to cluster, the standard deviation of topography relative to mean basin aggradation is high and the compensation index close to zero. If depositional events are completely random, the standard deviation of basin topography relative to aggradation decays with exponent 0.5 with increasing sample size (i.e. increasing time steps; compensation index of 0.5).

When Straub et al. (2009) measured compensation indices in several experimental and natural basin-fills, they found stacking patterns which fell somewhere between pure compensation and uniform-random end-members, but were consistent with "noisy diffusion" (Jerolmack and Sadler, 2007). The progradation-backfilling-avulsion cycles observed in Sheets et al. (2002), Edmonds et al. (2009), and Dalman and Weltje (2008) might be examples of deterministic avulsion processes that could produce this pattern of "stochastic" compensation. In these systems correlated patterns of channel deposition during the single-channel phase transition to anti-correlated patterns over the course of multiple avulsions (e.g. Martin et al., 2009).

5.3. Basin scale constraints

Basin-scale boundary conditions and the balance of sediment-supply and accommodation rates determine aggradation/incision and progradation/retrogradation at landscape (architecture) scale (e.g. Jervey, 1988; Paola, 2000). Basin-scale mass balance also moderates timescales of basin filling and system response to allogenic forcing (e.g. Castelltort and Van Den Driessche, 2003; Paola et al., 1992), as well as large-scale autogenic moving-boundary dynamics (i.e. "autostratigraphy", Muto et al., 2007). Mass-conserving architecture models should respond to changes in accommodation and sediment supply in a manner consistent with mass-balance models for shoreline migration (e.g. Wolinsky, 2009). This is particularly important for studies focused on alluvial architecture formed under changing boundary conditions (i.e. variable allogenic forcing). In this case basin-scale mass balance could be included directly into the avulsion model (e.g. DW), or could be incorporated via coupling to basin-scale diffusive or geometric models (e.g. DIONISOS).

The ability to place field data such as outcrop, core, or well logs in a basin-scale and sequence-stratigraphic context can be a useful tool for field-model comparisons. Paleomorphodynamic measurements can help to accomplish this, particularly where estimates of paleodischarge

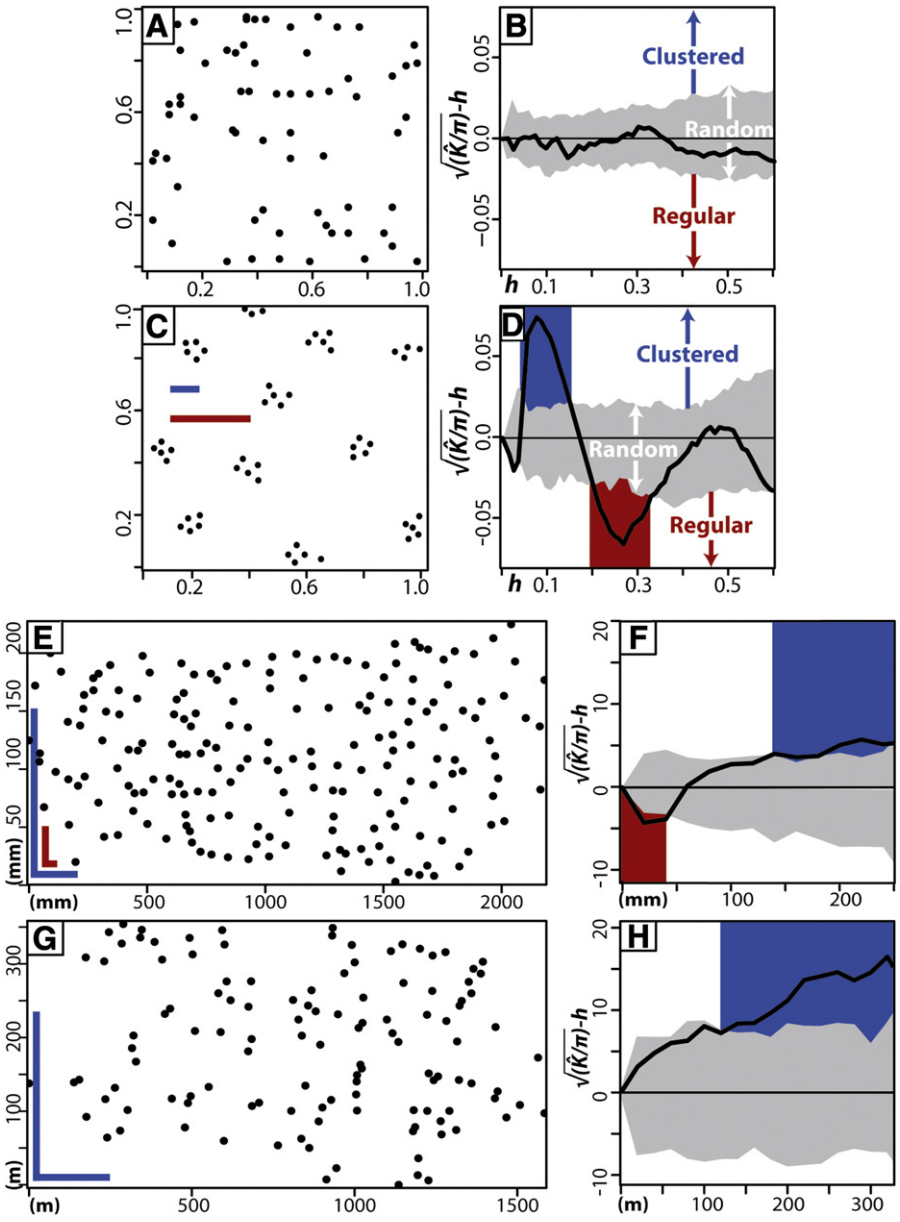

Fig. 22. Architecture-scale metrics – Clustering. Examples of spatial point processes (A, C) with different distributions shown within unit squares and plots of the *K* function for each distribution (B, D, respectively). B: The *K* function for a random distribution (A) plots entirely within the envelope (gray) for 99 Monte Carlo simulations. In contrast, the *K* function for a multiscale pattern with small clusters of points that are regularly spaced across the study area. The *K* function for this pattern shows clustering (blue) over short scales, and regularity (red) at scales approximately the distance between clusters (blue and red lines on C). Pattern in E is the distribution of channel deposits from a physical experiment (NCED, DB03); *K* function for E shown in F. Lines on E indicate peak organization lengths (h) in the vertical and horizontal dimensions (red = regular and blue = clustering). Pattern G shows the distribution of channel bodies in the Upper Cretaceous Ferris Fm (Wyoming, USA); corresponding point process in H. Both the experiment and field locality show statistically clustered alluvial architecture.

can be acquired (Appendix A). For example in the case of deltaic systems, estimates of backwater length L_w may constrain distance from the shoreline (e.g. Fig. 14; Jerolmack and Swenson, 2007). Similarly, estimates of catchment area A from discharge Q_w (e.g. Fig. 24A) can be used to constrain distance from the headwaters, L_{src} (Fig. 24B Hack Law; e.g. Dodds and Rothman, 2000).

In a source-to-sink context, distance from source is a first-order control on bed-material grain size d_{50} (Fig. 24B Sternberg Law; e.g. Frings, 2008), e.g. coarse-grained systems such as fans or fan-deltas tend to occur close to uplifted source areas, while sand-bed rivers occur further downstream, with a gravel-sand transition between (e.g. Marr et al., 2000). Combination of these basin-scale trends with reach-scale S and **Fr** data (Fig. 4A) reveals the characteristic concave long profile associated with discharge accumulation and downstream fining (e.g. Sinha and Parker, 1996), and the downstream transition from normal-to-backwater hydrodynamics (e.g. Lamb et al., 2010) along the profile.

Similarly, paleomorphodynamic measurements can help constrain model boundary conditions such as sediment supply Q_s (Appendix A). Taken together, paleomorphodynamic estimates of sediment supply and landform scales (length, width, relief) can be used to constrain dynamical timescales via (21), e.g. the expected nodal avulsion period on a delta (given by the time to fill a channel-belt volume $T \sim B_{cb} L_w H / Q_s$). Combined estimates of bed-material load and washload may perhaps provide constraints on net-to-gross (sand fraction) at architecture/reservoir scale. The power of reach-scale paleomorphodynamic measurements to constrain architecture-scale landform morphology and basin-scale context and forcing is only beginning to be explored, with many opportunities waiting to be exploited.

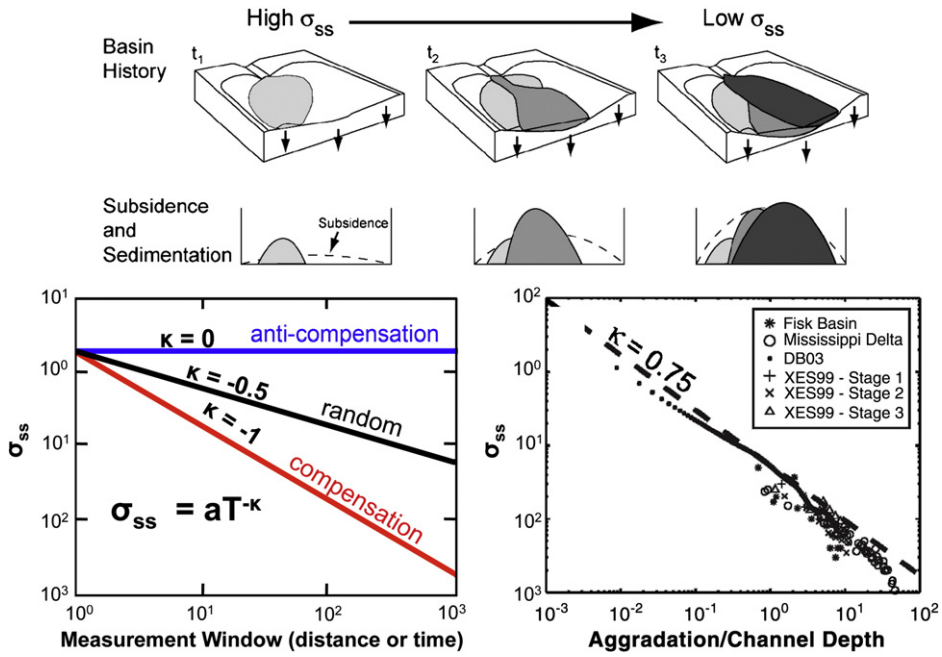

Fig. 23. Architecture-scale metrics – Compensation. Top: schematic diagram of compensational basin filling (from Straub et al., 2009). Lower left: Idealized compensation curves for anti-compensational (channels always stack atop one another), random (channels fill basin randomly), or compensational (channels always fill basin lows) deposition. Lower right: Compensation values for natural and experimental basins normalized by channel depth. Decay value ($\kappa = 0.75$) suggests a mix of random and compensational deposition in each basin. After Straub et al., 2009.

Downstream sediment extraction and fining are also aspects of basin-scale stratigraphy that can be used for validation and comparing model results to field data. Strong et al.'s (2005) mass balance framework for alluvial architecture comparisons helps normalize stratigraphic patterns by downstream position relative to sediment extraction. Their χ value is a measure of cumulative sediment extraction along the length of a basin. Strong et al. found that, for a given χ value, basic alluvial architecture patterns such as sand fraction and channel stacking density were remarkably consistent, even during phases of an experiment with different boundary conditions. This measure provides a way of normalizing stratigraphy within a basin fill thus enabling more robust comparisons between simplified model outputs, ancient strata, and experimental deposits.

6. Moving forward: coupled model-field campaigns

Simplified process models have greatly improved our understanding of avulsion and alluvial architecture. At this point however, exploratory models have generated what might be considered an overabundance of hypotheses. As a result, further exploratory modeling will be of limited use until we can test these hypotheses. Hence a priority moving forward is developing our capability to "winnow the field" by evaluating alternative models with more rigorous comparisons to natural systems. Similarly, the sedimentary record of any particular field site houses a wealth of information on avulsion processes and their influence on paleo-landscape evolution. By providing a common framework of comparison, and helping fill the unpreserved gaps in these imperfect records, process models can be a powerful tool for both inter-site synthesis and for unraveling the history of particular strata.

In advancing our understanding of avulsion processes and the architectures they build, the full potential of process models can only be realized, and the full depths of the sedimentary record tapped, through interdisciplinary approaches that span temporal and spatial scales, drawing on field studies, physical experiments, and numerical modeling. This requires that modelers be aware of the possibilities and limitations of ancient data, that stratigraphers be aware of the possibilities and limitations of simplified process models, and that both communities attempt to frame their hypotheses in a common language which facilitates meaningful comparisons.

In attempting to translate model- and field-based hypotheses into a common framework, the first and perhaps most difficult obstacle is agreeing on how to answer the questions "Are the systems comparable?" and "Do the predictions and/or observations agree?". This review highlights two powerful tools to facilitate passing this hurdle: process-based morphodynamics and process-agnostic morphometrics. As outlined in Sections 3 and 5 (see also Appendix A), the morphodynamic paradigm provides a common reference frame for evaluating process similarity between diverse models and field sites, allowing model input parameters or field observations to be expressed in roughly comparable quantitative terms. Similarly, morphometric measurements allow comparison of predicted or observed landform geometry and stratigraphic-pattern statistics on a relatively even footing. Importantly, both tools allow comparison of systems with widely differing scales via dimensionless measures such as process dominance (e.g. transport-mode in Fig. 4C), channel-normalized landform dimensions (Figs. 5B, 6B, 7D) or superelevation (Fig. 10), and architecture-scale stacking patterns (Figs. 22, 23).

A critical step in connecting models with field data is identifying key questions, using these to generate specific hypotheses, and designing coupled field-modeling campaigns targeted at rigorously testing predictions implied by these hypotheses. This review has highlighted several key unresolved questions, such as the impact of avulsion thresholds, flow-path selection, and floodplain processes on river avulsion and alluvial architecture. One example of a specific hypotheses arising from these questions could be "Backwater and cohesive-sediment effects are a key factor in progradational avulsions". From this hypothesis we might test for a predominance of progradational avulsions in low-slope coastal systems, but a relative absence in steep coarse-grained systems. These predictions might be tested by comparing paleomorphodynamic proxies between outcrops with abundant vs. absent avulsion deposits, and by testing the ability of simplified numerical models to produce progradational avulsions (perhaps via a hierarchical approach, e.g. progressively adding or removing processes).

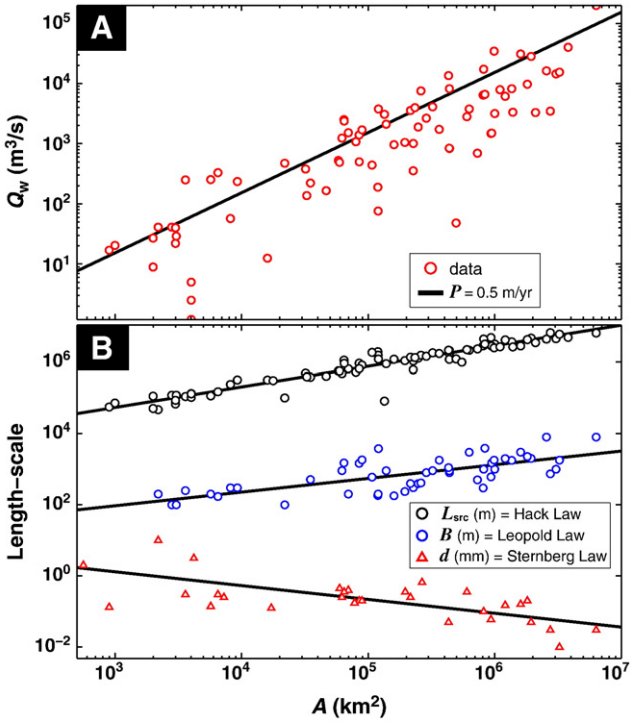

Fig. 24. Paleomorphodynamics – Basin controls. Variations in river systems as a function of drainage area, A (catchment size) from a composite database (Data taken from Orton and Reading, 1993; Coleman and Huh, 2004; Syvitski and Saito, 2007; Sømme et al., 2009b). A) Discharge Q_w is strongly correlated with drainage area. Black curve gives predicted discharge $Q_w \approx PA$ based on constant precipitation (runoff) P. B) Systematic trends (lines) between systems (points) as a function of catchment size echo well-known downstream trends observed along a river profile. Black: distance from source L_{src} , i.e. Hack's Law for drainage basin hydrologic geometry (e.g. Dodds and Rothman, 2000). Blue: bankfull channel width B, i.e. "Leopold's Law" for channel hydraulic geometry (e.g. Leopold and Maddock, 1953). Red: bed-material grain size d, i.e. Sternberg's Law of downstream fining (e.g. Frings, 2008).

Simplified processes models can be used address both generic and relatively specific scenarios, and targeted, fit-for-purpose model design provides an avenue to investigate the interaction of avulsion with other processes (including waves and tides; e.g. Swenson, 2005; Jerolmack and Swenson, 2007; Fagherazzi, 2008; Hood, 2010) and changes in basin boundary conditions, and help link fluvial dynamics to upstream and downstream components of the entire source-to-sink sediment routing system. The field/subsurface measurements presented here offer promise as means of comparing model predictions to ancient and experimental basins. However, significant work is needed to improve stratigraphic data collection and constrain uncertainty associated with identifying measureable paleo-landforms in ancient deposits and understanding preservation bias in the stratigraphic record. Despite these obstacles, the rock record offers important opportunities to understand avulsion dynamics over long timescales and explore fluvial behavior in climatic, tectonic, and eustatic conditions that are difficult to observe in modern or Holocene systems.

Our ability to invert the alluvial record for paleolandscape conditions and ancient climate and tectonic changes requires better understanding of avulsion dynamics under both steady and changing boundary conditions. Practically, this information will also enhance subsurface reservoir modeling and prediction and will improve our ability to manage river and delta environments and mitigate hazards associated with avulsions. Understanding the links between avulsion processes and products, and how each is represented in particular models and datasets, is vital for validating models and making useful predictions. Simplified process models offer a framework for integrating theory and observation from disparate sources and can serve as a basis for interdisciplinary collaborations between geomorphologists and stratigraphers.

Acknowledgements

We thank D. Edmonds, K. Straub, P. Heller, C. Paola, B. Foreman, Z. Sylvester, and Z. Jobe for helpful discussions and are appreciative of conscientious reviews by G. J. Weltje, R. Dalman, and an anonymous reviewer that helped improve the manuscript. Work related to ancient data was partially supported by NSF EAR awards 1024710 and 1124167 to EAH.

Appendix A. Paleomorphodynamics workflow

A.1. "1D" Paleomorphodynamics

1) Estimate average bankfull depth H and bed-material grain size d_{50} from outcrop, core, or well logs (Fig. 17; also see guidelines in Bridge and Tye, 2000; Mohrig et al., 2000).
2) Use grain size d_{50} to estimate settling velocity w_s and bedload-entrainment velocity $U_{c,\mathrm{bedload}}$ (Fig. 4C; also see Ferguson and Church, 2004; Brownlie, 1981), as well as Shields stress τ^* (Fig. 4B) and shear stress τ (Eq. (12)).
3) From relative roughness d_{50}/H and Shields stress τ^* estimate slope S and drag C_d (Fig. 18, Eq. (23)).
4) Estimate depth-averaged velocity U from shear stress τ and drag C_d (Eq. (4)). Combined with step 2 this allows estimation of bed-material transport mode, i.e. bedload vs. suspended load (Fig. 4C).
5) Use depth H, velocity U, and slope S to estimate Froude number **Fr** (Eq. 8b) and backwater length L_w (Eq. 9). This allows the potential influence of backwater and water-surface effects to be constrained.

A.2. "2D" Paleomorphodynamics

6) If bankfull channel width B can be estimated (e.g. from outcrop, Fig. 17, or via depth H and aspect ratio, Fig. 19), then discharge Q_w can be estimated via Eq. (11).
7) Use discharge Q_w and slope S to estimate bed-material load $Q_{s,\mathrm{b}}$ from (14a), using grain-size class to estimate the transport coefficient K_s (e.g. Marr et al., 2000).
8) Discharge Q_w can also be used to estimate drainage area A (Fig. 24A).
9) Use drainage area A to estimate distance from source L_{src} (Fig. 24B).
10) Drainage area A can also be used to estimate suspended load $Q_{s,s}$ (e.g. Syvitski and Milliman, 2007).
11) Total load is given by $Q_s = Q_{s,b} + \mathrm{washload} \le Q_{s,b} + Q_{s,s}$, because bed-material may be partially transported in suspension. However the estimates from step 4 can be used to constrain the relative importance of suspension on bed-material transport (e.g. for gravel-bed rivers typically $U << w_s$ so $Q_{s,s} \approx \mathrm{washload}$).

A.3. "Extended 1D" Paleomorphodynamics

If flow width B is relatively unconstrained by 2D data, an alternative is to use grain size d_{50} to get a crude estimate of drainage area A (Fig. 24B). Then step 8 can be inverted to estimate discharge Q_w from A, and step 6 can be inverted to estimate B from Q_w. Steps 7 and 9–11 can then proceed unaltered.

A.4. Landform Scales

The paleomorphodynamics workflow (steps 1–11) is based on fundamental morphodynamics and system-independent empirical

relationships, so is applicable to any fluvial system. The information from steps 1–4 can also be used to estimate process-dependent landform scales which may or may not apply to a particular system. For unconfined meandering systems, depth H and drag C_d can be used to estimate channel-belt width $B_{cb} \approx 25H/C_d$ (Fig. 5; Camporeale et al., 2005). Similarly, the overbank-deposition decay length λ for a "wide and dry" floodplain (Fig. 8B) can be estimated by the settling length $L_s \approx UH/w_s$[silt], where w_s[silt] is the settling velocity associated with distal-levee deposits, e.g. d_{10} or just "silt" ≈ 50 microns (Fig. 6).

A.5. Uncertainty

In the simplest case the entire workflow can proceed with "best guess" estimates. However paleomorphodynamics inherently involves quite significant uncertainties in both the basic measurements (steps 1 and 6) and the approximations based on modern analogue data (e.g. residual scatter in Figs. 4, 18, 19, 24). In applications where quantifying uncertainty is desirable (e.g. validating a simplified avulsion model, or building a static reservoir model), propagation of uncertainties through the workflow is relatively straightforward using a simple Monte Carlo approach.

References

Aalto, R., Maurice-Bourgoin, L., Dunne, T., Montgomery, D.R., Nittrouer, C.A., Guyot, J.L., 2003. Episodic sediment accumulation on Amazonian flood plains influenced by El Niño/Southern Oscillation. Nature. doi:10.1038/nature02002.

Aalto, R., Lauer, J.W., Dietrich, W.E., 2008. Spatial and temporal dynamics of sediment accumulation and exchange along Strickland River floodplains (Papua New Guinea) over decadal-to-centennial timescales. Journal of Geophysical Research 113, F01S04. doi:10.1029/2006JF000627.

Adams, P.N., Slingerland, R.L., Smith, N.D., 2004. Variations in natural levee morphology in anastomosed channel flood plain complexes. Geomorphology. doi:10.1016/j.geomorph.2003.10.005.

Allen, J.R.L., 1978. Studies in fluviatile sedimentation; an exploratory quantitative model for the architecture of avulsion-controlled alluvial sites. Sedimentary Geology 21 (2), 129–147.

ASCE Task Committee on Hydraulics, Bank Mechanics, and Modeling of River Width Adjustment, 1998a. River width adjustment I: Processes and mechanisms. Journal of Hydraulic Engineering 9 (881). doi:10.1061/(ASCE)0733-9429(1998)124.

ASCE Task Committee on Hydraulics, Bank Mechanics, and Modeling of River Width Adjustment, 1998b. River width adjustment II: Modeling. Journal of Hydraulic Engineering 9 (903). doi:10.1061/(ASCE)0733-9429(1998)124.

Ashmore, P., 1991. Channel morphology and bed load pulses in braided, gravel-bed streams. Geografiska Annaler 73 (1), 37–52.

Aslan, A., Blum, D., 1999. Contrasting styles of Holocene avulsion, Texas Gulf coastal plain, USA: Fluvial Sedimentology VI: Special Publication Number 28 of the International Association of Sedimentologists, p. 193.

Aslan, A., Autin, W.J., 1999. Evolution of the Holocene Mississippi River floodplain, Ferriday, Louisiana: insights on the origin of fine-grained floodplains. Journal of Sedimentary Research 69 (4), 800–815.

Aslan, A., Autin, W.J., Blum, M.D., 2005. Causes of River Avulsion: Insights from the Late Holocene Avulsion History of the Mississippi River, U.S.A. Journal of Sedimentary Research. doi:10.2110/jsr.2005.053.

Aslan, A., Autin, W.J., Blum, M.D., 2006. Causes of River Avulsion: Insights from the Late Holocene Avulsion History of the Mississippi River, U.S.A.—Reply. Journal of Sedimentary Research. doi:10.2110/jsr.2006.077.

Blum, M.D., Törnqvist, T.E., 2000. Fluvial responses to climate and sea-level change: a review and look forward. Sedimentology. doi:10.1046/j.1365-3091.2000.00008.x.

Bown, T.M., Kraus, M.J., 1987. Integration of channel and floodplain suites: I. Development of sequence and lateral relations of alluvial paleosols. Journal of Sedimentary Petrology 57, 587–601.

Box, G.E.P., 1979. Robustness in the Strategy of Scientific Model Building. In: Launer, R.L., Wilkinson, G.N. (Eds.), Robustness in Statistics. Academic Press, New York.

Bratvold, R.B., Begg, S.H., 2008. I would rather be vaguely right than precisely wrong: A new approach to decision making in the petroleum exploration and production industry. AAPG Bulletin. doi:10.1306/06040808070.

Bridge, J.S., 2008. Numerical Modelling of Alluvial Deposits: Recent Developments. IAS Spec. Pub., 40. doi:10.1002/9781444303131.ch4.

Bridge, J.S., Leeder, M.R., 1979. A simulation model of alluvial stratigraphy. Sedimentology 26 (5), 617–644.

Bridge, J.S., Tye, R.S., 2000. Interpreting the Dimensions of Ancient Fluvial Channel Bars, Channels, and Channel Belts from Wireline-Logs and Cores. AAPG Bulletin 84 (8), 1205–1228.

Bristow, C.S., Skelly, R.L., Etheridge, F.G., 1999. Crevasse splays from the rapidly aggrading, sand-bed, braided Niobrara River, Nebraska: effect of base-level rise. Sedimentology. doi:10.1046/j.1365-3091.1999.00263.x.

Brownlie, W.R., 1981. Prediction of flow depth and sediment discharge in open channels. Report KH-R-43A. W.M. Keck Laboratory of Hydraulics and Water Resources, California Institute of Technology (232 pp.).

Bryant, M., Falk, P., Paola, C., 1995. Experimental study of avulsion frequency and rate of deposition. Geology 23 (4), 365–368.

Burgess, P.M., Lammers, H., van Oosterhout, C., Granjeon, D., 2006. Multivariate sequence stratigraphy: Tackling complexity and uncertainty with stratigraphic forward modeling, multiple scenarios, and conditional frequency maps. AAPG Bulletin 90 (12), 1883–1901.

Camporeale, C., Perona, P., Porporato, A., Ridolfi, L., 2005. On the long-term behavior of meandering rivers. Water Resources Research 41, W12403. doi:10.1029/2005WR004109.

Castelltort, S., Van Den Driessche, J., 2003. How plausible are high-frequency sediment supply-driven cycles in the stratigraphic record? Sedimentary Geology 157, 3–13.

Chakraborty, T., Kar, P., Ghosh, P., Basu, S., 2010. Kosi Megafan: Historical records, geomorphology and the recent avulsion of the Kosi River. Quaternary International.

Church, M., Rood, K., 1983. Catalogue of Alluvial River Channel Regime Data. University of British Columbia, Department of Geography, Vancouver.

Coleman, J., Huh, O., 2004. Major deltas of the world: A perspective from Space. NASA Report (74 pp.).

Coulthard, T.J., Macklin, M.G., Kirkby, M.J., 2002. A cellular model of Holocene upland river basin and alluvial fan evolution. Earth Surface Processes and Landforms 27 (3), 269–288.

Coulthard, T.J., Hicks, D.M., Van de Wiel, M.J., 2007. Cellular modelling of river catchments and reaches: Advantages, limitations and prospects. Geomorphology 90, 192–207.

Cressie, N.A.C., 1993. Statistics for Spatial Data, revised edition: Wiley Series in Probability and Mathematical Statistics, John Wiley and Sons, 900 p.

Dalman, R.A.F., Weltje, G.J., 2008. Sub-grid parameterisation of fluvio-deltaic processes and architecture in a basin-scale stratigraphic model. Computers and Geosciences 34, 1370–1380.

Darmadi, Y., Willis, B.J., Dorobek, S.L., 2007. Three-Dimensional Seismic Architecture of Fluvial Sequences on the Low-Gradient Sunda Shelf, Offshore Indonesia. Journal of Sedimentary Research. doi:10.2110/jsr.2007.024.

Davidson, S.K., Hartley, A.J., 2010. Towards a Quantitative Method for Estimating Paleohydrology from Clast Size and Comparison with Modern Rivers. Journal of Sedimentary Research. doi:10.2110/jsr.2010.062.

Day, G., Dietrich, W.E., Rowland, J.C., Marshall, A., 2008. The depositional web on the floodplain of the Fly River, Papua New Guinea. Journal of Geophysical Research 113, F01S02. doi:10.1029/2006JF000622.

Dietrich, W.E., Bellugi, D., Sklar, L.S., Stock, J.D., Heimsath, A.M., Roering, J.J., 2003. Geomorphic transport laws for predicting landscape form and dynamics. In: Iverson, R.M., Wilcock, P. (Eds.), Prediction in Geomorphology. American Geophysical Union, Washington, DC, pp. 103–132.

Diggle, P.J., 2003. Statistical Analysis of Spatial Point Patterns: London, Hodder Arnold, 159 p.

Dodds, P.S., Rothman, D.H., 2000. Scaling, Universality, and Geomorphology. Annual Review of Earth and Planetary Sciences. doi:10.1146/annurev.earth.28.1.571.

Donselaar, M.E., Overeem, I., 2008. Connectivity of fluvial point-bar deposits: An example from the Miocene Huesca fluvial fan, Ebro Basin, Spain. AAPG Bulletin 92 (9), 1109–1129.

Duller, R.A., et al., 2010. From grain size to tectonics. Journal of Geophysical Research 115 (F03022).

Dunne, T., Mertes, L.A.K., Meade, R.H., Richey, J.E., Forsberg, B.R., 1998. Exchanges of sediment between the flood plain and channel of the Amazon River in Brazil. GSA Bulletin 110 (4), 450–467.

Edmonds, D.A., Slingerland, R.L., 2008. Stability of delta distributary networks and their bifurcations. Water Resources Research. doi:10.1029/2008WR006992.

Edmonds, D.A., Slingerland, R.L., 2010. Significant effect of sediment cohesion on delta morphology. Nature Geoscience. doi:10.1038/ngeo730.

Edmonds, D.A., Hoyal, D.C.J.D., Sheets, B.A., Slingerland, R.L., 2009. Predicting delta avulsions: Implications for coastal wetland restoration. Geology. doi:10.1130/G25743A.1.

Fagherazzi, S., 2008. Self-organization of tidal deltas. PNAS. doi:10.1073/pnas.0806668105.

Fedele, J.J., Paola, C., 2007. Similarity solutions for fluvial sediment fining by selective deposition. Journal of Geophysical Research 112 (F02038).

Ferguson, R.I., Church, M., 2004. A simple universal equation for grain settling velocity. Journal of Sedimentary Research. doi:10.1306/051204740933.

Fowler, A.C., 1997. Mathematical models in the applied sciences. Cambridge University Press. (402 pp.).

Freeman, T., 1991. Calculating catchment area with divergent flow based on a regular grid. Computers and Geosciences. doi:10.1016/0098-3004(91)90048-I.

Frings, R.M., 2008. Downstream fining in large sand-bed rivers. Earth-Science Reviews. doi:10.1016/j.earscirev.2007.10.001.

Garcia, M., Parker, G., 1991. Entrainment of bed sediment into suspension. Journal of Hydraulic Engineering 117 (4), 414–435.

Gibling, M.R., 2006. Width and thickness of fluvial channel bodies and valley fills in the geological record: a literature compilation and classification. Journal of Sedimentary Research 76, 731–770.

Gibling, M.R., Bashforth, A.R., Falcon-Lang, H.J., Allen, J.P., Fielding, C.R., 2010. Log jams and flood sediment buildup caused channel abandonment and avulsion in the Pennsylvanian of Atlantic Canada. Journal of Sedimentary Research 80, 268–287. doi:10.2110/jsr.2010.024.

Gouw, M.J.P., Berendsen, H.J.A., 2007. Variability of Channel-Belt Dimensions and the Consequences for Alluvial Architecture: Observations from the Holocene Rhine–Meuse Delta (The Netherlands) and Lower Mississippi Valley (U.S.A.). Journal of Sedimentary Research. doi:10.2110/jsr.2007.013.

Granjeon, D., Joseph, P., 1999. Concepts and applications of a 3D multiple lithology, diffusive model in stratigraphic modelling. In: Harbaugh, J.W., et al. (Ed.), Numerical Experiments in Stratigraphy: SEPM Special Publications, vol. 62, pp. 197–210.

Hajek, E.A., Heller, P.L., Sheets, B.A., 2010. Significance of channel-belt clustering in alluvial basins. Geology 38 (6), 535–538.
Heller, P.L., Paola, C., 1996. Downstream changes in alluvial architecture; an exploration of controls on channel-stacking patterns. Journal of Sedimentary Research 66 (2), 297–306.
Hood, W.G., 2010. Delta distributary dynamics in the Skagit River Delta (Washington, USA): Extending, testing, and applying avulsion theory in a tidal system. Geomorphology. doi:10.1016/j.geomorph.2010.07.007.
Howard, A.D., 1992. Modelling channel migration and floodplain sedimentation in meandering streams. In: Carling, P.A., Petts, G.E. (Eds.), Lowland Floodplain Rivers: Geomorphological Perspectives. Wiley, Chichester, pp. 1–41.
Howard, A.D., 1994. A detachment-limited model of drainage basin evolution. Water Resources Research 30 (7), 2261–2285. doi:10.1029/94WR00757.
Howard, A.D., 1996. Modelling channel evolution and floodplain morphology. In: Anderson, M.G., Walling, D.E., Bates, P.D. (Eds.), Floodplain Processes. Wiley, Chichester, pp. 15–62.
Hoyal, D.C.J.D., Sheets, B.A., 2009. Morphodynamic evolution of experimental cohesive deltas. Journal of Geophysical Research 114, F02009. doi:10.1029/2007JF000882.
Jerolmack, D.J., Mohrig, D., 2007. Conditions for branching in depositional rivers. Geology. doi:10.1130/G23308A.1.
Jerolmack, D.J., Paola, C., 2007. Complexity in a cellular model of river avulsion. Geomorphology 91 (3–4), 259–270.
Jerolmack, D.J., Paola, C., 2010. Shredding of environmental signals by sediment transport. Geophysical Research Letters 37, L19401. doi:10.1029/2010GL044638.
Jerolmack, D.J., Sadler, P., 2007. Transience and persistence in the depositional record of continental margins. Journal of Geophysical Research 112, F03S13. doi:10.1029/2006JF000555.
Jerolmack, D.J., Swenson, J.B., 2007. Scaling relationships and evolution of distributary networks on wave-influenced deltas. Geophysical Research Letters 34, L23402. doi:10.1029/2007GL031823.
Jervey, M.T., 1988. Quantitative geological modeling of siliciclastic rock sequences and their seismic expression. In: Wilgus, C.K., Hastings, B.S., Kendall, C.G.St.C., Posamentier, H.W., Ross, C.A., Van Wagoner, J.C. (Eds.), Sea-Level Changes: An Integrated Approach: SEPM Special Publication, 42, pp. 47–69.
Jones, H.L., Hajek, E.A., 2007. Characterizing avulsion stratigraphy in ancient alluvial deposits. Sedimentary Geology 202 (1–2), 124–137.
Jones, L.S., Schumm, S.A., 1999. Causes of avulsion; an overview. Special Publication of the International Association of Sedimentologists, 28, pp. 171–178.
Kang, S., Lightbody, A., Hill, C., Sotiropoulos, F., 2010. High-resolution numerical simulation of turbulence in natural waterways. Advances in Water Resources. doi:10.1016/j.advwatres.2010.09.018.
Karssenberg, D., Bridge, J.S., 2008. A three-dimensional numerical model of sediment transport, erosion and deposition within a network of channel belts, floodplain and hill slope: extrinsic and intrinsic controls on floodplain dynamics and alluvial architecture. Sedimentology 55 (6), 1717–1745.
Karssenberg, D., Törnqvist, T.E., Bridge, J.S., 2001. Conditioning a Process-Based Model of Sedimentary Architecture to Well Data. Journal of Sedimentary Research. doi:10.1306/051501710868.
Kelly, S., 2006. Scaling and hierarchy in braided rivers and their deposits: examples and implications for reservoir modelling. In: Sambrook Smith, G.H. (Ed.), Braided rivers: process, deposits, ecology and management. Wiley-Blackwell (390 pp.).
Kim, W., Jerolmack, D.J., 2008. The Pulse of Calm Fan Deltas. Journal of Geology. doi:10.1086/588830.
Kim, W., Paola, C., 2007. Long-period cyclic sedimentation with constant tectonic forcing in an experimental relay ramp. Geology 35 (4), 331–334.
Kim, W., Paola, C., Voller, V.R., Swenson, J.B., 2006a. Experimental Measurement of the Relative Importance of Controls on Shoreline Migration. Journal of Sedimentary Research. doi:10.2110/jsr.2006.019.
Kim, W., Paola, C., Swenson, J.B., Voller, V.R., 2006b. Shoreline response to autogenic processes of sediment storage and release in the fluvial system. Journal of Geophysical Research, Earth Surface 111 (F04013).
Kleinhans, M.G., 2010. Sorting out river channel patterns. Progress in Physical Geography. doi:10.1177/0309133310365300.
Koltermann, C.E., Gorelick, S.M., 1996. Heterogeneity in Sedimentary Deposits: A Review of Structure-Imitating, Process-Imitating, and Descriptive Approaches. Water Resources Research 32 (9), 2617–2658. doi:10.1029/96WR00025.
Kraus, M.J., 1987. Integration of channel and floodplain suites: II. Lateral relations of alluvial paleosols. Journal of Sedimentary Petrology 57, 602–612.
Kraus, M.J., 1996. Avulsion deposits in lower Eocene alluvial rocks, Bighorn Basin, Wyoming. Journal of Sedimentary Research 66, 354–363.
Kraus, M.J., 1999. Paleosols in clastic sedimentary rocks: their geologic applications. Earth-Science Reviews 47, 41–70.
Kraus, M.J., Davies-Vollum, K.S., 2004. Mudrock-dominated fills formed in avulsion splay channels: examples from the Willwood Formation, Wyoming. Sedimentology 51, 1127–1144.
Kraus, M.J., Middleton, L.T., 1987. Dissected paleotopography and base-level changes in a Triassic fluvial sequence. Geology 15, 18–21.
Kraus, M.J., Wells, T.M., 1999. Recognizing avulsion deposits in the ancient stratigraphical record. In: Smith, N.D., Rogers, J. (Eds.), Fluvial Sedimentology VI: International Association of Sedimentologists, Special Publication, 28, pp. 251–268.
Lal, A.M.W., 2008. Development of a Robust Diffusion-Kinematic Flow Algorithm for Regional Hydrologic Models Operating with Large Time Steps. Proceedings of the World Environmental & Water Resources Congress. doi:10.1061/40976(316)378.
Lal, A.M.W., Van Zee, R., Belnap, M., 2005. Case Study: Model to Simulate Regional Flow in South Florida. Journal of Hydraulic Engineering 4 (247). doi:10.1061/(ASCE)0733-9429(2005)131.
Lamb, M.P., Nittrouer, J.A., Mohrig, D.C., Shaw, J.B., 2010. Fluvial backwater zones as filters on source to sink sediment transport. American Geophysical Union Fall Meeting 2010, abstract #EP54A-07.
Leclair, S., 2011. Interpreting fluvial hydromorphology from the rock record: large-river peak flows leave no clear signature. In: Davidson, S.K., Leleu, S., North, C.P. (Eds.), From River to Rock Record: The Preservation of Fluvial Sediments and Their Subsequent Interpretation, SEPM Special Publication No. 97, pp. 113–124.
Leclair, S.F., Bridge, J.S., 2001. Quantitative interpretation of sedimentary structures formed by river dunes. Journal of Sedimentary Research 71, 713–716.
Leeder, M.R., 1978. A quantitative stratigraphic model for alluvium, with special reference to channel deposit density and interconnectedness. Memoir - Canadian Society of Petroleum Geologists (5), 587–596.
Leleu, S., Hartley, A., Williams, B.P.J., 2009. Large-scale alluvial architecture and correlation in a Triassic pebbly braided river system, lower Wolfville Formation (Fundy Basin, Nova Scotia, Canada). Journal of Sedimentary Research 79, 265–286.
Leopold, L.B., Maddock, T., 1953. The hydraulic geometry of stream channels and some physiographic implications. U.S. Geological Survey Professional Paper 252 (57 pp.).
Lesser, G.R., Roelvink, J.A., van Kester, J.A.T.M., Stelling, G.S., 2004. Development and validation of a three-dimensional morphological model. Coastal Engineering. doi:10.1016/j.coastaleng.2004.07.014.
Liang, M., Voller, V.R., Paola, C., Edmonds, D., 2009. A CAFE Delta Building Model With Channel Networks. Eos Transactions of AGU 90 (52) (Fall Meet. Suppl., Abstract EP41A-0596).
Lynds, R., Hajek, E., 2006. Conceptual model for predicting mudstone dimensions in sandy braided-river reservoirs. AAPG Bulletin 90, 1273–1288.
Mackey, S.D., Bridge, J.S., 1992. A revised Fortran program to simulate alluvial stratigraphy. Computers and Geosciences 18 (2–3), 119–181.
Mackey, S.D., Bridge, J.S., 1995. Three-dimensional model of alluvial stratigraphy; theory and applications. Journal of Sedimentary Research, Section B: Stratigraphy and Global Studies 65 (1), 7–31.
Makaske, B., 2001. Anastomosing rivers: a review of their classification, origin and sedimentary products. Earth-Science Reviews. doi:10.1016/S0012-8252(00)00038-6.
Makaske, B., Smith, D.G., Berendsen, H.J.A., 2002. Avulsions, channel evolution, and floodplain sedimentation rates of the anastomosing upper Columbia River, British Columbia, Canada. Sedimentology 49, 1049–1071.
Marr, J.G., Swenson, J.B., Paola, C., Voller, V.R., 2000. A two-diffusion model of fluvial stratigraphy in closed depositional basins. Basin Research. doi:10.1111/j.1365-2117.2000.00134.x.
Marriott, S.B., 1999. The use of models in the interpretation of the effects of base-level change on alluvial architecture. Special Publication of the International Association of Sedimentologists, 28, pp. 271–281.
Martin, J., Sheets, B., Paola, C., Hoyal, D., 2009. Influence of steady base-level rise on channel mobility, shoreline migration, and scaling properties of a cohesive experimental delta. Journal of Geophysical Research 114, F03017. doi:10.1029/2008JF001142.
Mertes, L.A.K., 1997. Documentation and significance of the perirheic zone on inundated floodplains. Water Resources Research 33 (7), 1749–1762. doi:10.1029/97WR00658.
Mohrig, D., Heller, P.L., Paola, C., Lyons, W.J., 2000. Interpreting avulsion process from ancient alluvial sequences; Guadalope-Matarranya system (northern Spain) and Wasatch Formation (western Colorado). Geological Society of America Bulletin 112 (12), 1787–1803.
Montgomery, D.R., Dietrich, W.E., 1992. Channel Initiation and the Problem of Landscape Scale. Science. doi:10.1126/science.255.5046.826.
Murray, A.B., 2003. Contrasting the goals, strategies, and predictions associated with simplified numerical models and detailed simulations. In: Iverson, R.M., Wilcock, P.R. (Eds.), Prediction in Geomorphology: American Geophysical Union, Geophysical Monograph No. 135, pp. 151–165.
Murray, A.B., 2007. Reducing model complexity for explanation and prediction. Geomorphology. doi:10.1016/j.geomorph.2006.10.020.
Murray, A.B., Paola, C., 1994. A cellular model of braided rivers. Nature 371 (6492), 54–57.
Murray, A.B., Paola, C., 2003. Modelling the effect of vegetation on channel pattern in bedload rivers. Earth Surface Processes and Landforms. doi:10.1002/esp. 428.
Muto, T., Steel, R.J., 2000. The accommodation concept in sequence stratigraphy: some dimensional problems and possible redefinition. Sedimentary Geology 130 (1–2), 1–10.
Muto, T., Steel, R.J., Swenson, J.B., 2007. Autostratigraphy: A Framework Norm for Genetic Stratigraphy. Journal of Sedimentary Research 77 (1), 2–12. doi:10.2110/jsr.2007.005.
NCED (DB03), a. Delta Basin experiment DB03-1https://repository.nced.umn.edu/browse.php?folder=259037.
NCED (XES99), a. Jurassic Tank experiment XES99 https://repository.nced.umn.edu/browse.php?folder=291725.
Nicoll, T.J., Hickin, E.J., 2010. Planform geometry and channel migration of confined meandering rivers on the Canadian prairies. Geomorphology. doi:10.1016/j.geomorph.2009.10.005.
Orton, G.J., Reading, H.G., 1993. Variability of deltaic processes in terms of sediment supply, with particular emphasis on grain size. Sedimentology. doi:10.1111/j.1365-3091.1993.tb01347.x.
Paola, C., 2000. Quantitative models of sedimentary basin filling. Sedimentology 47 (Suppl. 1), 121–178.
Paola, C., Borgman, L.E., 1991. Reconstructing random topography from preserved stratification. Sedimentology 38, 553–565.
Paola, C., Mohrig, D., 1996. Palaeohydraulics revisited: palaeoslope estimation in coarse-grained braided rivers. Basin Research. doi:10.1046/j.1365-2117.1996.00253.x.

Paola, C., Voller, V.R., 2005. A generalized Exner equation for sediment mass balance. Journal of Geophysical Research 110, F04014. doi:10.1029/2004JF000274.
Paola, C., Heller, P.L., Angevine, C.L., 1992. The large-scale dynamics of grain-size variation in alluvial basins; 1, Theory. Basin Research 4, 73–90.
Paola, C., Straub, K.M., Mohrig, D., Reinhardt, L., 2009. The "unreasonable effectiveness" of stratigraphic and geomorphic experiments. Earth-Science Reviews 97 (1–4), 1–43.
Parker, G. (E-book) 1D sediment transport morphodynamics with applications to rivers and turbidity currents. University of Illinois, http://vtchl.uiuc.edu/people/parkerg/morphodynamics_e-book.htm. (Accessed in November, 2011).
Perez-Arlucea, M., Smith, N.D., 1999. Depositional patterns following the 1870s avulsion of the Saskatchewan River (Cumberland Marshes, Saskatchewan, Canada). Journal of Sedimentary Research 69, 62–73.
Phillips, J.D., 2011. Universal and local controls of avulsions in southeast Texas Rivers. Geomorphology 130, 17–28.
Pizzuto, J.E., 1987. Sediment diffusion during overbank flows. Sedimentology 34, 301–317.
Posamentier, H.W., Vail, P.R., 1988. Eustatic controls on clastic deposition II — sequence and systems tracts models. In: Wilgus, C.K., Hastings, B.S., Kendall, C.G.St.C., Posamentier, H.W., Ross, C.A., Van Wagoner, J.C. (Eds.), Sea-Level Changes: An Integrated Approach: SEPM Special Publication, 42, pp. 125–154.
Reitz, M.D., Jerolmack, D.J., Swenson, J.B., 2010. Flooding and flow path selection on alluvial fans and deltas. Geophysical Research Letters 37 (L06401).
Retallack, G.J., 2001. Soils of the Past: an Introduction to Paleopedology, Second edition. Blackwell, Oxford. (600 pp.).
Rogers, R.R., 1998. Sequence analysis of the Upper Cretaceous Two Medicine and Judith River formations, Montana; nonmarine response to the Claggett and Bearpaw marine cycles. Journal of Sedimentary Research 68 (4), 615–631.
Rowland, J.C., Dietrich, W.E., Day, G., Parker, G., 2009. Formation and maintenance of single-thread tie channels entering floodplain lakes: Observations from three diverse river systems. Journal of Geophysical Research 114, F02013. doi:10.1029/2008JF001073.
Sadler, P.M., 1981. Sediment accumulation rates and the completeness of stratigraphic sections. Journal of Geology 89, 569–584.
Sammis, C., Smith, S., 1999. Seismic cycles and the evolution of stress correlation in cellular automaton models of finite fault networks. Pure and Appllied Geophysics. doi:10.1007/s000240050267.
Sanford, L.P., Maa, J.P.-Y., 2001. A unified erosion formulation for fine sediments. Marine Geology. doi:10.1016/S0025-3227(01)00201-8.
Schlager, W., 2010. Ordered hierarchy versus scale invariance in sequence stratigraphy. International Journal of Earth Sciences. doi:10.1007/s00531-009-0491-8.
Segel, L.A., Slemrod, M., 1989. The quasi-steady-state assumption: A case study in perturbation. SIAM Review. doi:10.1137/1031091.
Seybold, H.J., et al., 2009. Simulation of birdfoot delta formation with application to the Mississippi Delta. Journal of Geophysical Research 114 (F03012).
Shanley, K.W., McCabe, P.J., 1993. Alluvial architecture in a sequence stratigraphic framework; a case history from the Upper Cretaceous of southern Utah, USA. Special Publication of the International Association of Sedimentologists, 15, pp. 21–55.
Shanley, K.W., McCabe, P.J., 1994. Perspectives on the sequence stratigraphy of continental strata. AAPG Bulletin 78, 544–568.
Sheets, B.A., Hickson, T.A., Paola, C., 2002. Assembling the stratigraphic record; depositional patterns and time-scales in an experimental alluvial basin. Basin Research 14 (3), 287–301.
Sheets, B.A., Paola, C., Kelberer, J.M., 2007. Creation and preservation of channel-form sand bodies in an experimental alluvial system. In: Nichols, G.J., Williams, E., Paola, C. (Eds.), Sedimentary Processes, Environments and Basins: Special Publication, 38. Blackwell, Oxford, pp. 555–567.
Sinha, R., 2009. The Great avulsion of Kosi on 18 August 2008. Current Science 97 (3), 429–433.
Sinha, S.K., Parker, G., 1996. Causes of Concavity in Longitudinal Profiles of Rivers. Water Resources Research 32 (5), 1417–1428. doi:10.1029/95WR03819.
Slingerland, R.L., Smith, N.D., 1998. Necessary conditions for a meandering-river avulsion. Geology 26, 435–438.
Slingerland, R.L., Smith, N.D., 2004. River Avulsions and Their Deposits. Annual Review of Earth and Planetary Sciences. doi:10.1146/annurev.earth.32.101802.120201.
Soar, P.J., Thorne, C.R., 2001. Channel restoration design for meandering rivers. Report ERDC/CHL CR-01-1. U.S. Army Engineer Research and Development Center, Vicksburg, Miss.
Sømme, T.O., Helland-Hansen, W., Didier Granjeon, D., 2009a. Impact of eustatic amplitude variations on shelf morphology, sediment dispersal, and sequence stratigraphic interpretation: Icehouse versus greenhouse systems. Geology. doi:10.1130/G25511A.1.
Sømme, T.O., Helland-Hansen, W., Martinsen, O.J., Thurmond, J.B., 2009b. Relationships between morphological and sedimentological parameters in source-to-sink systems: a basis for predicting semi-quantitative characteristics in subsurface systems. Basin Research. doi:10.1111/j.1365-2117.2009.00397.x.
Stouthamer, E., 2005. Reoccupation of channel belts and its influence on alluvial architecture in the Holocene Rhine-Meuse Delta, The Netherlands. Special Publication - Society for Sedimentary Geology 83, 319–339.
Stouthamer, E., Berendsen, H.J.A., 2001. Avulsion frequency, avulsion duration, and interavulsion period of Holocene channel belts in the Rhine-Meuse Delta, the Netherlands. Journal of Sedimentary Research 71 (4), 589–598.
Straub, K.M., Paola, C., Mohrig, D., Wolinsky, M.A., George, T., 2009. Compensational stacking of channelized sedimentary deposits. Journal of Sedimentary Research 79 (9), 673–688.
Strong, N., Sheets, B.A., Hickson, T.A., Paola, C., 2005. A mass balance framework for quantifying down-system changes in fluvial architecture. In: Blum, M.D. (Ed.), Fluvial Sedimentology VII: IAS Special Publication, pp. 242–252.
Sun, T., Meakin, P., Jøssang, T., Schwarz, K., 1996. A simulation model for meandering rivers. Water Resources Research. doi:10.1029/96WR00998.
Sun, T., Paola, C., Parker, G., Meakin, P., 2002. Fluvial fan deltas; linking channel processes with large-scale morphodynamics. Water Resources Research 38 (8), 10.
Swanson, K.M., Watson, E., Aalto, R., Lauer, J.W., Bera, M.T., Marshall, A., Taylor, M.P., Apte, S.C., Dietrich, W.E., 2008. Sediment load and floodplain deposition rates: Comparison of the Fly and Strickland rivers, Papua New Guinea. Journal of Geophysical Research 113, F01S03. doi:10.1029/2006JF000623.
Swenson, J.B., 2005. Relative importance of fluvial input and wave energy in controlling the timescale for distributary-channel avulsion. Geophysical Research Letters 32, L23404. doi:10.1029/2005GL024758.
Sylvester, Z., Pirmez, C., Cantelli, A., 2011. A model of submarine channel-levee evolution based on channel trajectories: Implications for stratigraphic architecture. Marine and Petroleum Geology. doi:10.1016/j.marpetgeo.2010.05.012.
Syvitski, J.P.M., 2010. Community Surface Dynamics Modeling System and its CSDMS Modeling Tool to couple models and data. Abstract IN23C-01 presented at 2010 Fall Meeting, AGU, San Francisco, CA.
Syvitski, J.P.M., Milliman, J.D., 2007. Geology, Geography, and Humans Battle for Dominance over the Delivery of Fluvial Sediment to the Coastal Ocean. Journal of Geology. doi:10.1086/509246.
Syvitski, J.P.M., Saito, Y., 2007. Morphodynamics of deltas under the influence of humans. Global and Planetary Change 57 (3–4), 261–282.
Tal, M., Paola, C., 2007. Dynamic single-thread channels maintained by the interaction of flow and vegetation. Geology. doi:10.1130/G23260A.1.
Tooth, S., et al., 2007. Chronology and controls of avulsion along a mixed bedrock-alluvial river. Geological Society of America Bulletin 119 (3/4), 452–461.
Törnqvist, T.E., 1994. Middle and late Holocene avulsion history of the River Rhine (Rhine-Meuse Delta, Netherlands). Geology 22 (8), 711–714.
Törnqvist, T.E., Bridge, J.S., 2002. Spatial variation of overbank aggradation rate and its influence on avulsion frequency. Sedimentology. doi:10.1046/j.1365-3091.2002.00478.x.
Törnqvist, T.E., Bridge, J.S., 2006. Causes of River Avulsion: Insights from the Late Holocene Avulsion History of the Mississippi River, U.S.A.—Discussion. Journal of Sedimentary Research. doi:10.2110/jsr.2006.076.
Tversky, A., Kahneman, D., 1983. Extensional versus intuitive reasoning: The conjunction fallacy in probability judgment. Psychological Review 90 (4), 293–315.
Van de Wiel, M.J., Couthard, T.J., 2010. Self-organized criticality in river basins: Challenging sedimentary records of environmental change. Geology 38 (1), 87–90.
Van De Wiel, M.J., Coulthard, T.J., Macklin, M.G., Lewin, J., 2007. Embedding reach-scale fluvial dynamics within the CAESAR cellular automaton landscape evolution model. Geomorphology. doi:10.1016/j.geomorph.2006.10.024.
van der Wegen, M., Wang, Z.B., Savenije, H.H.G., Roelvink, J.A., 2008. Long-term morphodynamic evolution and energy dissipation in a coastal plain, tidal embayment. Journal of Geophysical Research 113, F03001. doi:10.1029/2007JF000898.
Walling, D.E., He, Q., 1998. The spatial variability of overbank sedimentation on river floodplains. Geomorphology. doi:10.1016/S0169-555X(98)00017-8.
Wang, Y., Straub, K.M., Hajek, E.A., 2011. Scale dependent compensational stacking: an estimate of autogenic timescales in sedimentary deposits. Geology 39, 811–814.
Welsh, M.B., Bratvold, R.B., Begg, S.H., 2005. Cognitive Biases in the Petroleum Industry: Impact and Remediation. SPE Annual Technical Conference and Exhibition. doi:10.2118/96423-MS.
Werner, B.T., 1999. Complexity in Natural Landform Patterns. Science. doi:10.1126/science.284.5411.102.
Werner, B.T., 2003. Modeling landforms as self-organized, hierarchical dynamical systems. In: Wilcock, P.R., Iverson, R.M. (Eds.), Prediction in Geomorphology. Geophysical Monograph. American Geophysical Union, Washington, DC, pp. 133–150.
Wilcock, P., 2009. StreamLab: Full-scale Experiments in River Science. Eos Transactions of AGU 90 (52) (Fall Meet. Suppl., Abstract EP31D-01).
Willis, B.J., 1993. Evolution of Miocene fluvial systems in the Himalayan fordeep through a two kilometer thick succession in northern Pakistan. Sedimentary Geology 88, 77–121.
Willis, B.J., Beherensmeyer, A.K., 1994. Architecture of Miocene overbank deposits in northern Pakistan. Journal of Sedimentary Research B64, 60–67.
Wing, S.L., Harrington, G.J., Smith, F.A., Bloch, J.I., Boyer, D.M., Freeman, K.H., 2005. Transient floral change and rapid global warming at the Paleocene-Eocene boundary. Science 310, 993–995.
Wolinsky, M.A., 2009. A unifying framework for shoreline migration: 1. Multiscale shoreline evolution on sedimentary coasts. Journal of Geophysical Research 114, F01008. doi:10.1029/2007JF000855.
Wolinsky, M.A., Edmonds, D.A., Martin, J., Paola, C., 2010a. Delta allometry: Growth laws for river deltas. Geophysical Research Letters 37, L21403. doi:10.1029/2010GL044592.
Wolinsky, M.A., Swenson, J.B., Litchfield, N., McNinch, J.E., 2010b. Coastal progradation and sediment partitioning in the Holocene Waipaoa Sedimentary System, New Zealand. Marine Geology 270 (1–4), 94–107.
Wright, V.P., Marriott, S.B., 1993. The sequence stratigraphy of fluvial depositional systems: the role of floodplain sediment storage. Sedimentary Geology 86, 203–210.
Wright, V.P., Taylor, K.G., Beck, V.H., 2000. The paleohydrology of Lower Cretaceous seasonal wetlands, Isle of Wight, Southern England. Journal of Sedimentary Research 70, 619–632.
Zaleha, M.J., 1997. Siwalik paleosols (Miocene, Northern Pakistan): Genesis and controls on their formation. Journal of Sedimentary Research 67, 821–839.